

SELECTIVE REMOVAL OF AS(V) FROM WATER BY POLYMERIC LIGAND
EXCHANGE AND ENGINEERED TREATMENT OF SPENT REGENERANT

Except where reference is made to the work of others, the work described in this thesis is my own or was done in collaboration with my advisory committee. This thesis does not include proprietary or classified information.

Byungryul An

Certificate of Approval:

T. Prabhakar Clement
Associate Professor
Civil Engineering

Dongye Zhao, Chair
Associate Professor
Civil Engineering

Willie F. Harper, Jr
Assistant Professor
Civil Engineering

Stephen L. McFarland
Acting Dean
Graduate School

SELECTIVE REMOVAL OF AS(V) FROM WATER BY POLYMERIC LIGAND
EXCHANGE AND ENGINEERED TREATMENT OF SPENT REGENERANT

Byungryul An

A Thesis

Submitted to

the Graduate Faculty of

Auburn University

in Partial Fulfillment of the

Requirements for the

Degree of

Master of Science

Auburn, AL
August 7, 2006

SELECTIVE REMOVAL OF AS(V) FROM WATER BY POLYMERIC LIGAND
EXCHANGE AND ENGINEERED TREATMENT OF SPENT REGENERANT

Byungryul An

Permission is granted to Auburn University to make copies of this thesis at its discretion,
upon request of individuals or institutions at their expense. The author reserves all
publication rights.

Signature of Author

Date of Graduation

THESIS ABSTRACT

SELECTIVE REMOVAL OF AS(V) FROM WATER BY POLYMERIC LIGAND EXCHANGE AND ENGINEERED TREATMENT OF SPENT REGENERANT

Byungryul An

Master of Science, August 7, 2006
(B.S., Pukyong National University, 1997)

122 Typed Pages

Directed by Dongye Zhao

Arsenic introduced by natural or human activities into drinking water sources has been a challenging issue around the world. In the western United States, high arsenic concentrations in drinking water have caused serious health threats. The U.S. Environmental Protection Agency (U.S. EPA) has recently implemented a Maximum Contaminant Level (MCL) for arsenic of 10 $\mu\text{g/L}$. To comply with the MCL, development of new technologies or modification of conventional treatment is needed. This study developed a new technology, polymeric ligand exchange (PLE) for selective removal of arsenic from drinking water in the presence of strong competing anions (e.g. sulfate). Compared to Strong Base Anion Exchanges (SBA), which is currently recommended by the U.S. EPA, PLE resins exhibited much improved arsenic selectivity. Equilibrium isotherm tests also demonstrate 60 ~ 120 times orders of magnitude greater

selectivity for arsenic by the PLE. The relative affinity of the anions observed for the PLE and IRA 900 (SBA) resins are shown respectively: $\text{HAsO}_4^{2-} \gg \text{HCO}_3^- > \text{SO}_4^{2-} > \text{Cl}^-$; and $\text{SO}_4^{2-} > \text{HAsO}_4^{2-} > \text{Cl}^-$. The arsenic selectivity of two best PLE resins, XUS 3N-Cu and DOW 3N-Cu, is 12 and 17 times greater, respectively than that of SBA. Although the PLE has a strong affinity for arsenic, 96% of sorbed arsenic could be removed during regeneration using 4% NaCl at pH 9.1 within 20 BV. Furthermore, it can be reused for four consecutive runs with only pH adjustment.

It has been reported that millions of tons As-bearing sludge are annually produced as waste residuals from water treatment process. It is imperative to reduce waste volume and to yield the most stable process waste residuals. Aluminum chloride (AlCl_3) was investigated to treat the spent regenerant brine containing concentrated arsenic. At an Al/As molar ratio of 5 or greater and at pH 5-8, nearly 100% of As in the spent brine can be removed. The U.S. EPA TCLP and California WET leaching tests, both with a limit of 5 mg/L as arsenic, were followed to determine the leachability of arsenic from the brine treatment residuals. When the Al/As molar ratio was increased from 5 to 20, the arsenic leachability was reduced from 200 mg/L to 50 mg/L according to the WET test. In the pH range 5 – 10, the extractable arsenic was at a minimum at pH 5. Also, the extracted arsenic concentration increased by 30% as the dry aging time increased from 20 to 40 days.

ACKNOWLEDEMENTS

The author would like to thank his advisor Dr. Dongye Zhao for his kind guidance throughout this study. The author also thanks Dr. T. Prabhakar Clement and Dr. Willie F. Harper, Jr for their service on his advisory committee. Thanks are due to Dr. Fu and Mr. Zhong Xiong for preparing the XAD resin.

The author would like to thank his parents and mother in law. Finally the author deeply thanks his wife Bukyung Son for her loving support.

Style manual or journal followed: Auburn University Graduate School: Guide to Preparation and Submission of Theses and Dissertations.

Computer software used: Microsoft Office XP: Excel, PowerPoint, Word, SigmaPlot8.0.

TABLE OF CONTENTS

LIST OF TABLES.....	xi
LIST OF FIGURES.....	xii
I. INTRODUCTION.....	1
1.1 ARSENIC ORIGINS.....	1
1.2 ARSENIC CHEMISTRY.....	1
1.3 BACKGROUND OF REGULATION.....	4
1.4 ARSENIC REMOVAL TECHNOLOGY.....	5
1.5 CONCEPTION OF POLYMERIC LIGAND EXCHANGE.....	6
1.6 ENGINEERED TREATMENT OF SPENT REGENERATION BRINE.....	11
1.7 OBJECTIVES.....	11
II. SYNTHESIS OF POLYMERIC LIGAND EXCHANGE.....	13
2.1 PREPARATION OF DOW 3N-Cu and XUS 3N-Cu.....	13
2.2 SYNTHESIS OF PLES BASED ON NON-FUNCTIONALIZED POLYMERIC SORBENTS (XAD).....	15
2.2.1 MATERIALS	15
2.2.2 FUNCTIONALIZATION OF XAD COPOLYMERS.....	17
2.2.3 COPPER LOADING AND COPPER CAPACITY MEASUREMENT	21
III. MATERIALS AND EXPERIMENTAL PROCEDURES.....	26
3.1 MATERIALS.....	26

3.2 EXPERIMENTAL METHODS.....	26
3.2.1 EQUILIBRIUM SORPTION TESTS.....	26
3.2.2 FIXED-BED COLUMN TESTS.....	28
3.2.3 pH EFFECT.....	28
3.2.4 KINETIC TESTS.....	31
3.2.5 RESIN REGENERATION AND REUSE.....	31
3.3 TREATMENT OF SPENT BRINE.....	32
3.3.1 PREPARATION OF SIMULATED SPENT BRINE.....	32
3.3.2 TREATMENT OF SPENT BRINE.....	32
3.3.3 PREPARATION OF ARSENIC- LADEN SOLID WASTE/SLUDGE	33
3.3.4 ARSENIC-LEACHING TESTS.....	33
3.4 CHEMICAL ANALYSIS.....	34
IV. RESULTS AND DISSCUSION.....	35
4.1 EQUILIBRIUM ISOTHERMS AND ARSENATE ADSORPTION.....	35
4.1.1 ARSENIC-SULFATE ISOTHERMS FOR PLEs.....	35
4.1.2 ARSENIC-PHOSPHATE ISOTHERM FOR DOW 3N-Cu AND	
XUS 3N-Cu.....	41
4.2 BREAKTHROUGH BEHAVIORS.....	44
4.3 EFFECT OF pH.....	60
4.4 KINETIC TEST.....	64
4.5 REGENERATION AND REUSE OF PLES.....	71
4.6 ARSENIC REMOVAL FROM SPENT BRINE.....	83
4.7 STABILIZATION OF ARSENIC-LADEN PROCESS WASTE SLUDGE	88

V. CONCLUSIONS.....	98
REFERENCES.....	101

LIST OF TABLES

TABLE 1.1	Identified arsenic removal technology.....	7
TABLE 2.1	Properties of parent polymer matrices.....	16
TABLE 2.2	Maximum copper loading of the chelating resins.....	24
TABLE 2.3	Effect of chloromethylation time on maximum copper loading capacity of di(2-picoly)amine-functionalized XAD1180.....	25
TABLE 3.1	Salient properties of various ion exchange resins used in this study..	27
TABLE 3.2	Major compositions in the influent water and hydrodynamic condition for each column run.....	30
TABLE 4.1	The model-fitted Langmuir parameters (b, Q), and experimentally determined arsenate/sulfate binary separation factor ($\alpha_{As/S}$).....	36

LIST OF FIGURES

FIGURE 1.1	Speciation of arsenite (above) as a function of pH.....	3
FIGURE 1.2	Speciation of arsenate as a function of pH.....	3
FIGURE 1.3	A conceptualized illustration of the functional group of PLE.....	9
FIGURE 2.1	XUS 3N-Cu, a highly As- selective PLE based on commercial resin XUS43578 (Total capacity > 3 meq/g; Bead size: 0.41 mm of uniform particles; Shelf life = 8-10 years).....	14
FIGURE 2.2	DOW 3N-Cu, a PLE based on a commercial resin, DOW 3N (Total capacity = 2.98 meq/g; Surface area = 139 m ² /g; Bead size = 0.2-1.2 mm; Shelf life = 8-10 years).....	14
FIGURE 2.3	Schematic and key reactions in synthesizing PLEs based on polystyrene-DVB XAD polymers.....	20
FIGURE 2.4	Schematic and key reactions in synthesizing PLEs based on acrylic polymers.....	22
FIGURE 3.1	Fixed-bed Column Test Set-up.....	29
FIGURE 4.1	Arsenate sorption isotherms for DOW 3N-Cu, XUS 3N-Cu and two conventional SBA resins (IRA 900 and IRA 958) in the presence of competing sulfate ions. (Symbols: observed data; lines: Langmuir model fits).....	38
FIGURE 4.2	Arsenate sorption isotherms for XAD1180-3N-Cu, XAD16-3N-Cu	

	and XAD7HP-3N-Cu in the presence of competing sulfate ions. (Symbols: observed data; lines: Langmuir model fits).....	39
FIGURE 4.3	Arsenate sorption isotherms for DOW 3N-Cu and XUS 3N-Cu in the presence of competing phosphate ions. (Symbols: observed data; lines: Langmuir model fits).....	42
FIGURE 4.4	Arsenic isotherms for DOW 3N-Cu at four different background concentrations of sulfate.....	43
FIGURE 4.5	Breakthrough histories of arsenate and sulfate in a simulated multi-component system using a standard SBA resin, IRA 900.....	45
FIGURE 4.6	Breakthrough histories of arsenate and sulfate in a simulated multi-component system using a standard SBA resin, IRA 958.....	46
FIGURE 4.7	Breakthrough histories of arsenate and competing anions in a simulated multi-component system using a polymeric ligand exchange, DOW 3N-Cu.....	47
FIGURE 4.8	Breakthrough histories of arsenate and competing anions in a multi-component a system using a polymeric ligand exchange, DOW 3N-Cu.....	48
FIGURE 4.9	Breakthrough histories of arsenate and other competing anions in a fixed-bed run with XUS 3N-Cu in the presence of an unusually high concentration (0.5 mg/L as P) of phosphate.....	50
FIGURE 4.10	Breakthrough histories of arsenate and competing anions in a multi-component system using a polymeric ligand exchange, XUS 3N-Cu.....	53

FIGURE 4.11	Breakthrough histories of arsenate and competing anions in a multi-component system using a polymeric ligand exchange, XAD1180-3N-Cu.....	54
FIGURE 4.12	Breakthrough histories of arsenate and competing anions in a multi-component system using a polymeric ligand exchange, XAD16-3N-Cu.....	55
FIGURE 4.13	Breakthrough histories of arsenate and competing anions in a multi-component system using a polymeric ligand exchange, XAD7HP-3N-Cu.....	56
FIGURE 4.14	Breakthrough histories of arsenite in the present of sulfate using a polymeric ligand exchange, DOW 3N-Cu.....	57
FIGURE 4.15	Breakthrough histories of arsenate in a multi-component system using a polymeric ligand exchange, XUS 3N-Cu at pH 6.7.....	58
FIGURE 4.16	Breakthrough histories of arsenate in a multi-component system using a polymeric ligand exchange, XUS 3N-Cu at pH 8.5.....	59
FIGURE 4.17	Arsenate uptake by DOW 3N-Cu as a function of solution pH.....	61
FIGURE 4.18	Arsenite uptake by DOW 3N-Cu as a function of solution pH.....	63
FIGURE 4.19	Experimental and model-simulated arsenate sorption kinetics of DOW 3N-Cu. (Symbols: observed data; line: model simulation)...	66
FIGURE 4.20	Experimental and model-simulated arsenate sorption kinetics of XAD16-3N-Cu. (Symbols: observed data; line: model simulation).	67
FIGURE 4.21	Experimental arsenate sorption kinetics of the commercial ion exchange, IRA 958.....	68

FIGURE 4.22	Experimental arsenate sorption kinetics of the commercial ion exchange, IRA 900.....	69
FIGURE 4.23	Arsenic elution profile during regeneration of saturated DOW 3N-Cu using 4% NaCl (w/w) at pH 4.1, 7.0, and 9.1, respectively.....	72
FIGURE 4.24	Arsenic elution profile during regeneration of saturated XAD1180-3N-Cu using 4%, 6%, and 8% NaCl (w/w), respectively.....	73
FIGURE 4.25	Arsenic elution profile during regeneration of saturated XAD16-3N-Cu using 4%, 6%, and 8% NaCl (w/w), respectively.....	74
FIGURE 4.26	Arsenic elution profile during regeneration of saturated XAD7HP-3N-Cu using, 6%, and 8% NaCl (w/w), respectively.....	75
FIGURE 4.27	Arsenic elution profile during regeneration of saturated XUS 3N-Cu using, 4% NaCl (w/w) at pH 10.....	76
FIGURE 4.28	Reuse of brine for multiple regeneration cycles for DOW 3N-Cu...	79
FIGURE 4.29	Reuse of brine for multiple regeneration cycles for XUS 3N-Cu....	80
FIGURE 4.30	Comparing the equilibrium arsenate sorption (q_e) of fresh and regenerated DOW 3N-Cu under otherwise identical conditions. (Note: a. One cycle consists of one saturation run and subsequent regeneration run; b. each point represents the mean of duplicates; the maximum standard deviation was 1.60).....	81
FIGURE 4.31	Comparing the equilibrium arsenate sorption (q_e) of fresh and regenerated XUS 3N-Cu under otherwise identical conditions. (Note: a. One cycle consists of one saturation run and subsequent regeneration run; b. each point represents the mean of duplicates;	

	the maximum standard deviation was 1.60).....	82
FIGURE 4.32	Percentage arsenic removed from a simulated regenerant brine as a function of the Al/As molar ratio.....	85
FIGURE 4.33	Percent of arsenic removed from a simulated regenerant brine as a function of the pH Al/As molar ratio of 5 and 10.....	86
FIGURE 4.34	Percentage removal of As as a function of calcium dosage.....	87
FIGURE 4.35	Extractable As concentration in TCLP or WET extraction fluid as a function of Al addition. Note: arsenic is in $\mu\text{g/L}$ in TCLP fluid, but in mg/L in WET fluid.....	92
FIGURE 4.36	Extractable As concentration based on WET method as a function of treatment temperature and wet aging time. All samples were air-dried for 20 days before the extraction tests.....	93
FIGURE 4.37	Effect of wet aging on extractable As.....	94
FIGURE 4.38	Extractable As concentration based on TCLP method as a function of treatment temperature and wet aging time. All samples were air-dried for 20 days before the extraction tests.....	95
FIGURE 4.39	Extractable As concentration based on WET method as a function of drying time and temperatures. Tests were carried out at two Al/As molar ratios (10 and 20).....	96
FIGURE 4.40	Extractable As concentration based on WET method as a function of brine treatment pH and dry aging times.....	97

I. INTRODUCTION

1.1 ARSENIC ORIGINS

Arsenic, the 20th most abundant element in the earth's crust, is a naturally occurring contaminant widely present in the environment (Cullen and Reimer, 1989). Arsenic in drinking water can originate either from natural or human activities. The major natural source of arsenic is weathering, biological activity, volcanic activity, forest fires, and erosion of arsenic-containing rocks and soil (EPA, 2001). Anthropogenic sources of *As* are widespread and can be categorized as follow: industry, mining, agriculture, and other sources (Smith et al. 1998). Manufacture of ceramics, glass, electronics, pigments, cosmetics, fireworks, and steel are some of the major constituents of industrial *As* use. Mining and smelting of Pb, Zn, Cu, and Au ores also act as a source of *As*. From the 19th century until recently, inorganic arsenic compounds have been a major component of pesticides and herbicides used in agriculture. However, the most anthropogenic arsenic input today is due to smelting operations and fossil-fuel combustion. Some estimates have placed the ratio of natural to anthropogenic inputs at 6:4 (Lantzy and Peterson, 1987).

1.2 ARSENIC CHEMISTRY

Arsenic, classified as a semi-metallic, is the 33rd element on the periodic table and has an atomic weight of 72.9. Arsenic is commonly found in the natural environment as an inorganic form as an oxyanion in two valence states, *As(V)* (arsenate) or *As(III)*

(arsenite) (Baughan, 1993), and in seafood in organic form, which is less harmful to health and is readily eliminated by the body. Generally, the trivalent form, $As(III)$, is found in reduced condition (assuming anaerobic conditions) and the pentavalent form, $As(V)$, is found in oxidic conditions (assuming aerobic conditions). Usually, the ratio of $As(V)$ to $As(III)$ is a function of the pH and redox conditions of the system. However, both forms have been found together in the same water source. Arsenate is less toxic and less mobile than arsenite (Smith et al., 1998).

The equilibria for both $As(V)$ and $As(III)$ is given in equations (1)-(6) along with their respective acid disassociation constants (O'Neill, 1990).

Arsenic acid, $As(V)$



Arsenous Acid, $As(III)$



Figures 1.1 and 1.2 show $As(V)$ and $As(III)$ speciation as a function of the pH, respectively. As shown in Figure 1.1, in the typical pH range (6-8) of natural waters, the most thermodynamically stable compounds of $As(V)$ is present as $H_2AsO_4^-$ and $HAsO_4^{2-}$, and $As(III)$ is found mostly as the uncharged species, H_3AsO_3 , while AsO_4^{3-} , $HAsO_3^{2-}$, and $H_2AsO_3^-$ are the predominant ionic forms in alkaline pH (Figure 1.1).

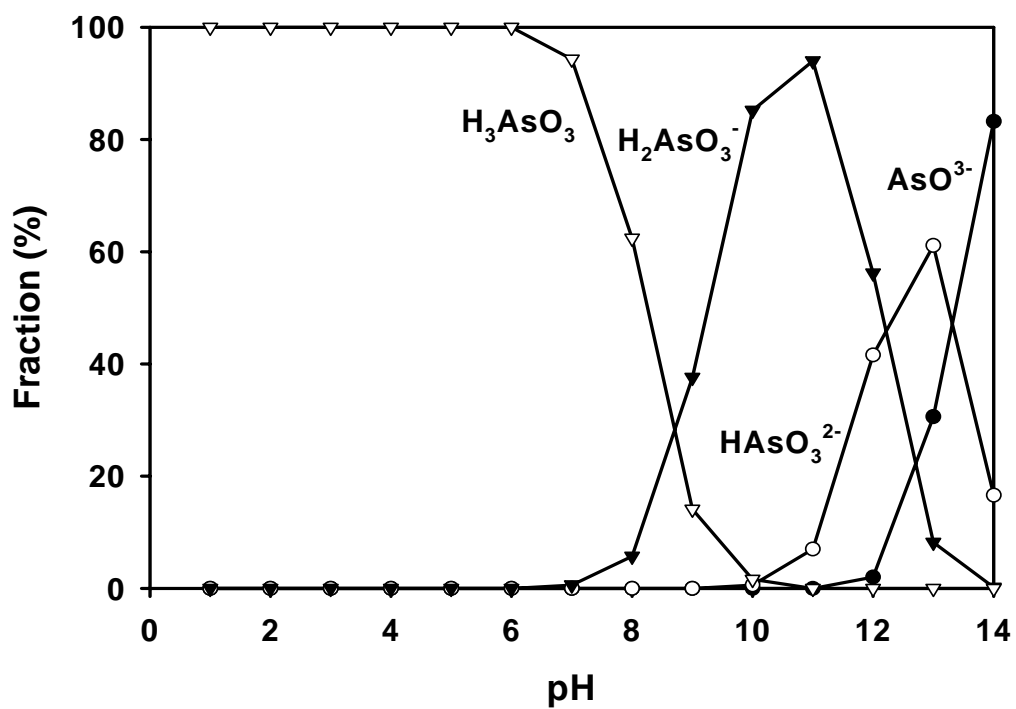


Figure 1.1. Speciation of arsenite as a function of pH.

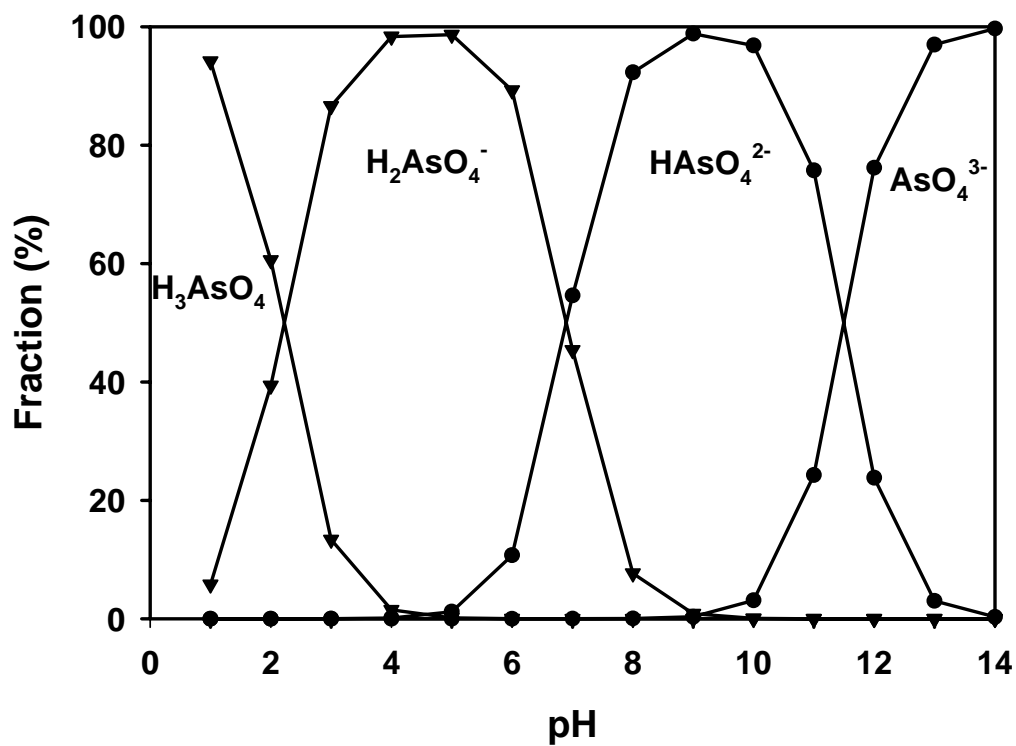


Figure 1.2. Speciation of arsenate as a function of pH.

1.3 BACKGROUND OF REGULATION

Exposure to arsenic has been known to cause severe adverse health effects in humans. Two major exposure pathways are ingestion of *As*-containing food and consumption of *As*-contaminated drinking water (ATSDR, 2000). Cancer of kidneys, lungs, skin, bladder, nasal passages, liver, and prostate have been linked to long-term exposure to arsenic in drinking water (EPA, 2001). In 1999, the National Research Council (NRC) released a report concluding that consumption of drinking water contaminated with *As* (even at low concentrations) has harmful cardiovascular, neurological, reproductive, respiratory, hepatic, hematological, diabetic, and dermal effects (NRC, 1999). Even at *As* levels of 3 µg/L the risk of death due to lung and bladder cancer is 4 to 7 deaths per 10,000 people. At 10 µ/L, the risk increases to between 12 and 23 deaths per 10,000 people (NRC, 2001).

The United States Geological Survey (USGS) has estimated that 14% of groundwater sources exceed 5 µg/L (Focazio et al., 1999), while the EPA states that approximately 2% of the US population receives drinking water containing >10 µ/L *As* (Holm, 2002). The Natural Resources Defense Council (NRDC) also estimates that 56 million people in the United States are exposed to unsafe levels of *As* in drinking water (Mushak, 2000).

The first legislative effort to minimize the harmful effects of water pollution occurred in 1972 with the passage of the Federal Water Pollution Control Act Amendments which later became known as the Clean Water Act. In 1975, U.S. EPA issued the standard of 50 µg/L set by the U.S. Public Health Service in 1942. The Safe Drinking Water Act, as amended in 1996, required U.S. EPA to issue a new drinking

water standard for arsenic, and in 1999, the National Academy of Sciences (NAS) concluded that the current standard, 50 µg/L, did not achieve EPA's goals for public health protection and suggested that it should be reduced. The U.S. EPA proposed a maximum contaminant level (MCL) for arsenic of 5 µg/L on June 22, 2000. Finally, the final rule, 10µg/L, was set in October 2001 by the U.S.EPA. All of the water utilities must meet this standard by January 22, 2006. This enforced ruling poses tremendous economic consequences for water utilities. Approximately 4100 water utilities serving ~13 million people are affected by the law (EPA, 2001 b). The compliance cost has been estimated to be ~\$600 million per year using current treatment technologies (Frey et al., 2000). For instance, almost half of the wells in Albuquerque, NM, will require additional treatment to meet the new standard (German, 2001). In the state of Maine, 12% of community water systems will need additional treatment.

1.4 ARSENIC REMOVAL TECHNOLOGY

In 1999, the U.S. EPA has identified several kinds of treatment options to reduce or essentially eliminate arsenic contamination of tap water: modifying existing coagulation and filtration, water softening with lime, activated alumina, ion exchange, electro dialysis reversal, reverse osmosis and nanofiltration membranes. Currently, three kinds of treatment technologies are commonly cited for As removal: 1) modified conventional treatment (MCT) (Chwirka et al., 2004; Ghurye et al., 2004; Clifford et al., 2003; Fan et al., 2003; Brandhuber and Amy, 1998; McNeill and Edwards, 1997; Hering and Elimelech, 1996; Scott et al., 1995), 2) sorption using activated alumina (AA) (Wang et al., 2002), standard ion exchange resins (IX) (Clifford, 1999), granular ferric hydroxide (GFH) (Sperlich et al., 2005; Badruzzaman et al., 2004; Driehaus et al., 1998),

or granular ferric oxide (GFO) (Westerhoff et al., 2005; Manna et al., 2003), or iron-coated sand (Benjamin et al., 1996), 3) reverse osmosis (RO) (EPA, 2002). Table 1.1 describes the characteristics of those treatments in more detail. To meet the urgent demands for better technology, a number of other technologies were also explored, including electro-coagulation (Kumar et al., 2004), polymer inclusion membrane process (Ballinas et al., 2004), mesoporous alumina sorption (Kim et al., 2004), activated mud (Genc-Fuhrman et al., 2004) and ferrihydrite crystallization process (Richmond et al., 2004). However, these new techniques are in the developmental stage. Consequently, innovative cost-effective treatment processes are urgently needed (Han et al., 2003)

1.5 CONCEPTION OF POLYMERIC LIGAND EXCHANGE

The concept of ligand-exchange-based separation was first introduced by Helfferich (1962). Generally, a PLE is composed of a) a cross-linked hosting resin that can firmly bind with a transition metal such as copper and iron, and b) metal ions that are immobilized to the functional groups of the hosting resin. While sharing many common features with standard ion exchanges, a ligand exchange employs transition metal ions as its terminal functional groups. As a result, ligand exchange involves concurrent Lewis acid-base (LAB) interactions (metal-ligand complexation) and electrostatic interactions between the fixed metal ions and target anionic ligands. While conventional anion exchanges' selectivity for various anions is only governed by electrostatic interactions, the affinity of a PLE is determined by both the ligand strength and ionic charge of the ligands. In his pioneering work, Helfferich (1962) prepared some of the very first PLEs by loading a transition metal (Ni or Cu) onto commercial cation exchange resins. Because the charges of the loaded metal ions are neutralized by the negative charges of the resins'

Table 1.1 Identified arsenic removal technologies.

	Strong	Weak
MCT	-Take simple steps to modify -80-95 % removal efficiency - Inexpensive	- Hard to meet the new MCL - Needs additional treatment process
WS	-60-90 % removal - Inexpensive	- Hard to meet the new MCL
AA	- Works well for most waters	- Not effective if the source water has high levels of selenium, fluoride, or sulfate
IX	- Can remove effectively in most water	- Needs to pretreatment if a certain contaminant is too high
ER	- The charge of particles	-80 % removal efficiency
RO, NM	- 90-95 removal efficiency	- Increase the cost if arsenic level is high

MCT: Modified conventional treatment

WS: Water softening with lime

AA: Activated alumina

IX: Ion exchange

ER: Electrodialysis reversal

RO: Reverse osmosis

NM: Nanofiltration membranes

functional groups, the PLEs could only sorb some neutral ligands such as ammonia and diamine (Helfferich, 1962). Later, Chanda et al. (1988) prepared a new PLE for selective removal of arsenic by loading ferric ions onto a weak base chelating resin (known as DOW 3N) with di(2-picolyl)amine groups. They observed that this PLE was able to remove ~140 bed volumes (BVs) of arsenate-laden water and that the saturated PLE can be regenerated using 1 M of NaOH. However, because of the weak Lewis acid characteristics of ferric ions, the amount of Fe^{3+} loaded was low. As a result, the PLE's capacity for arsenate was very limited. Moreover, the loaded iron was nearly completely stripped off the hosting resin during regeneration, and reloading of Fe^{3+} was necessary after each cycle of operation. Realizing the critical drawbacks of Fe^{3+} ions, Ramana and SenGupta (1992) prepared a PLE by loading Cu^{2+} onto a weak base chelating resin (known as DOW 2N) with 2-picolylamine groups. Since Cu^{2+} is a much stronger Lewis acid than Fe^{3+} , which is in accord with the Irving and Williams order, a much greater metal-loading capacity was observed. The copper loaded DOW 2N showed orders of magnitude of greater selectivity for arsenate and selenate in the presence of competing sulfate ions than commercial SBA resins.

To achieve selective removal of phosphate, Zhao and SenGupta (1997) developed and characterized a model PLE, referred to as DOW 3N-Cu, by loading Cu^{2+} ions onto the chelating resin DOW 3N resin. Compared to DOW 2N, DOW 3N contains one more (2-picolyl)amine group per functional group. As a result, the copper capacity for DOW 3N nearly doubles that for DOW 2N (Henry et al., 2004). DOW 3N-Cu showed unusually high selectivity for phosphate in the presence of high concentrations of sulfate, chloride, nitrate, and bicarbonate (Zhao and SenGupta, 1998). Figure 1.3 depicts the

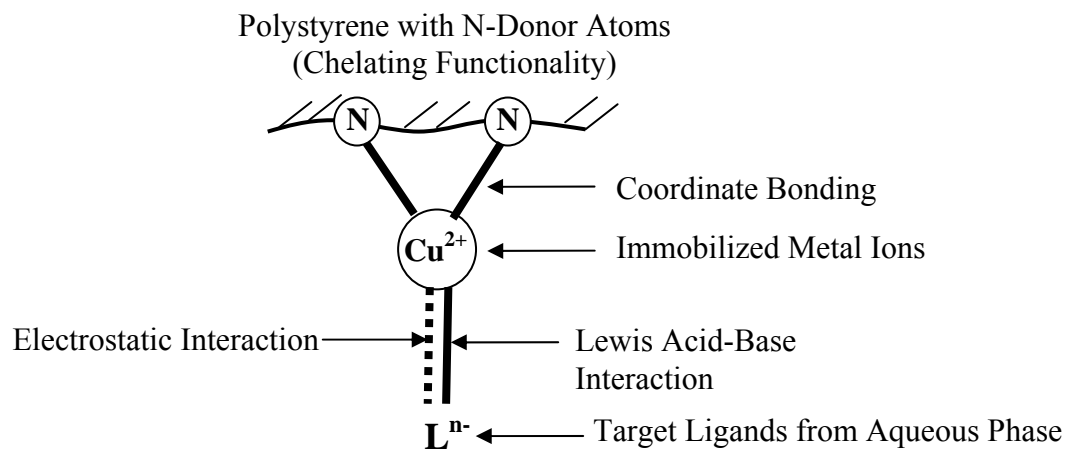


Figure 1.3. A conceptualized illustration of the functional group of PLE.

functional group of such a PLE (designated as DOW 3N-Cu), where a chelating resin containing nitrogen as electron donor atoms is employed as the metal hosting polymer. Metal ions (Cu^{2+}) are firmly immobilized on the polymer surface by covalently bonding with the N donor atoms. Since the nitrogen atoms are predominately in their free base form at $\text{pH} > 3$ (Zhao, 1997), the positive charges of loaded Cu^{2+} ions remain available to interact with anions in the aqueous phase. Moreover, since only a fraction of the copper's 6 coordination bonding sites are consumed for binding copper onto the polymer surface, the immobilized Cu^{2+} ions remain capable of complexing with target ligands from the aqueous phase. Consequently, the Cu^{2+} -tailored PLE can interact with anionic ligands, such as arsenate, in the aqueous phase through concurrent Lewis acid-base interaction (metal-ligand complexation) and electrostatic interactions. Compared to conventional strong base anion exchanges where electrostatic interaction governs the resins' selectivity, PLE's selectivity sequence is strongly controlled by the ligand characteristics of anions due to the additional Lewis-acid-base interaction.

The PLE's unusually high selectivity toward strong ligands is due to strong interactions between the resins' metal functional groups (Lewis acid) and the target ligand's electron donor atoms (Lewis base) (Zhao and SenGupta, 2000; 1998a; 1998b; Zhao, 1997). Strong ligands, such as phosphate and arsenate, will be preferred by a PLE over sulfate, which virtually reverses the selectivity sequence of commercial SBA resins.

The arsenate/sulfate exchange reaction can be depicted by eqn (1)



where R is the resin matrix carrying the immobilized Cu^{2+} ion as its functional group. Due to the extremely strong metal-ligand interactions between Cu^{2+} and nitrogen donor

atoms in the host polymer, DOW 3N-Cu exhibited very low copper bleeding when used for phosphate removal from both drinking water and municipal wastewater.

1.6 ENGINEERED TREATMENT OF SPENT REGENERATION BRINE

The high arsenic capacity and efficient regenerability of PLEs results in a much reduced volume of spent brine. Consequently, engineered manipulation of the arsenic removal becomes much more feasible both technically and economically. Significant As removal has been observed at water treatment plants that generate residuals containing Fe or Al oxyhydroxides (e.g., from coagulation or Fe and Mn oxidation) (McNeill and Edwards, 1997). Iron and aluminum were also employed to treat spent brine (Clifford, 1999). The predominant As-removal mechanism is the sorption of arsenate by precipitates of Fe and Al resulting from coagulation or oxidation. For example, when AlCl₃ is applied to arsenate-laden solution, the following reaction takes place (Clifford, 1999):



Based on this reaction using AlCl₃, all solid produced from brine treatment process must be conducted to determine their suitability for land disposal using two kinds of leaching tests: the Toxicity Characteristic Leaching Procedure (TCLP) and California Waste Extraction Test (WET) procedures. In both procedures, acceptable concentration of As is limited to 5 mg/L.

1.7 OBJECTIVES

The overall goal of this research is to develop an innovative, selective ion exchange (IX) process that 1) removes As(V) highly selectively and 2) minimizes the volume and As-leachability of process waste residuals. The specific research objectives were to

- 1). Prepare and characterize a new class of IX materials, referred to as polymeric ligand exchanges (PLEs), for highly selective removal of As(V) under normal drinking water conditions
- 2). Determine arsenic removal capacity and kinetic using batch and column experimental methods
- 3). Test the regenerability of the PLEs and reusability of the spent regenerant
- 4). Investigate the optimal conditions for treatment of spent regeneration brine using AlCl_3
- 5). Develop an engineered approach to treat the spent regenerant and to minimize the volume and As-leachability of process waste residuals.

II. SYNTHESIS OF POLYMERIC LIGAND EXCHANGES

2.1 PREPARATION OF DOW 3N-Cu AND XUS 3N-Cu

DOW 3N purchased from Aldrich, and XUS 3N, which was obtained from Dowex company. Accordingly, DOW 3N-Cu and XUS 3N-Cu were prepared by loading Cu^{2+} ions onto their commercial chelating ion exchange resin. The copper loading procedures used by Zhao and SenGupta (1998) were slightly modified. In brief, both DOW 3N and XUS 3N were first conditioned through cyclic acid and base washing using 1N HCl and 1N NaOH, respectively. Upon rinsing using DI water, the resin was equilibrated with 0.1% (w/w) copper solution at pH 3.5-4.0 for two weeks. Analytical grade $\text{CuCl}_2 \cdot 2\text{H}_2\text{O}$ (Aldrich, Milwaukee, WI, USA) was used for preparing the copper solution. The resin-to-solution ratio was approximately 1:200 (w/w). To enhance copper loading, the resin-solution mixture was intermittently heated at 70 °C for ~4 hours every other day and then placed back at ambient temperature (~21 °C). (Note: mild heating can cause resin swelling and enhance aging, thereby enhancing copper loading kinetics and stability). To avoid oxidation of the resin matrix, nitrogen gas was blown in the solution during heating. Upon completion, the copper-loaded resin was thoroughly rinsed using DI water and air dried for use. Figures 2.1 and 2.2 represent the two copper-loaded PLEs, XUS 3N-Cu, and DOW 3N-Cu, respectively.



Figure 2.1. XUS 3N-Cu, a highly As- selective PLE based on commercial resin

XUS43578 (Total capacity > 3 meq/g; Bead size: 0.41 mm of uniform particles; Shelf life = 8-10 years).

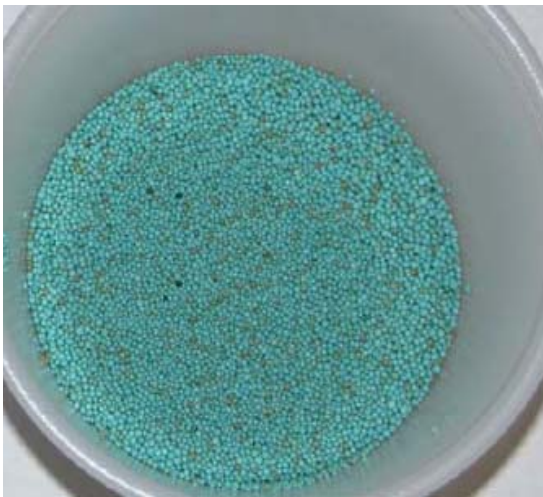


Figure 2.2. DOW 3N-Cu, a PLE based on a commercial resin, DOW 3N (Total capacity =

2.98 meq/g; Surface area = 139 m²/g; Bead size = 0.2-1.2 mm; Shelf life = 8-10 years).

2.2 Synthesis of PLEs based on non-functionalized polymeric sorbents (XAD)

A total of six additional PLEs based on three representative XAD matrices (XAD1180, XAD16, and XAD7HP) were prepared to explore the effect of matrix properties on the selective removal of arsenate. To facilitate copper loading, the XAD resins were first functionalized with two functional monomers (2-picolylamine and di(2-picolyl)amine), respectively, as illustrated below.

2.2.1 MATERIALS

Non-functionalized, macroporous polymer beads, Amberlite® XAD 1180, XAD 16, and XAD 7HP, were purchased from Sigma Aldrich (Milwaukee, WI) and were used as the starting polymeric matrices for making the new PLEs. Table 2.1 summarizes the key physical properties of these polymeric sorbents. XAD1180 and XAD16 are composed of polystyrene copolymers crosslinked with divinylbenzene (DVB), whereas XAD7 HP is a crosslinked poly(methyl methacrylate), i.e. a polyacrylic polymer. Because of the different matrices, XAD 7HP behaves much more like a hydrophilic than XAD1180. Three XAD sorbents have relatively large pore sizes compared to other currently available macroporous resins. Two nitrogen-rich monomers (di(2-picolyl)amine and 2-picolylamine) were used to functionalize the XAD resins for their known high affinity toward copper ions. Di(2-picolyl)amine was purchased from Richman Chemicals (Lower Gwynedd, PA), and 2-picolylamine from Sigma Aldrich. All solvents and other chemicals were also purchased from Sigma Aldrich.

The XAD resins contained moisture and small amounts of sodium carbonate. Before functionalization, the resins were conditioned through the following successive procedure: 1) rinse the resins with DI water, 2) rinse for ~4 hours using 0.5 N HCl, 3)

Table 2.1 Properties of parent polymer matrices.

Matrix	Polymer Type	Particle Size(mm)	Surface Area (m ² /g)	Porosity (ml/ml)	Medium Pore Size(nm)/ Distribution
XAD1180 (macroporous beads)	PS/DVB	0.35-0.60	≥500	≥0.60	45/narrow
XAD16 (macroporous beads)	PS/DVB	0.56-0.71	≥800	≥0.55	n/a
XAD7HP (macroporous beads)	Arcrylic	0.56-0.71	≥380	≥0.50	35/narrow
DOW 3N (macroporous beads)	PS/DVB	0.2-1.2	139	n/a	n/a
XUS 3N (macroporous beads)	PS/DVB	0.41	n/a	n/a	n/a

rinse three more times with DI water, 4) rinse with methanol, and 5) air dry and then oven dry at 70 °C until the weight no longer changes.

2.2.2 FUNCTIONALIZATION OF XAD COPOLYMERS

Functionalization of styrene-divinylbenzene copolymers, XAD1180 and XAD16, involved two steps of reactions: 1) chloromethylation of available aromatic rings in the copolymer, and 2) the immobilization of pyridine-containing functional groups through reactions between the chloromethyl groups on the polymer and the amine groups of the ligand compounds.

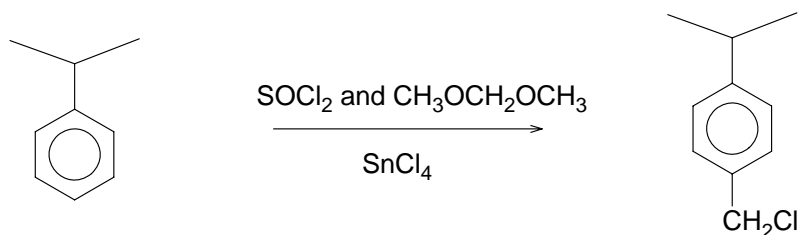
Chloromethylation of XAD1180 (XAD16) was carried out via two methods. In Method A, the polymer beads were soaked in chloromethyl methyl ether (5 mL per gram of resin) at room temperature for 30 minutes. Anhydrous SnCl₄ (0.2 mL per gram of resin) was then added as a catalyst while stirring. The reaction flask was then set in an oil bath with the temperature set between 35 to 55 °C. The reaction mixture was stirred for 1 to 5 hours. At the end of the reaction, the mixture was quenched by dropwise addition of methanol under stirring until the mixture was cooled to room temperature. The liquid was then separated from the resin, and the resin was washed successively with acetone, DI water, and methanol.

In Method B, a mixture of thionyl chloride and dimethoxymethane (5:6 v/v) was used as the reagent for *in-situ* generation of chloromethyl methyl ether, and anhydrous SnCl₄ was also used as the catalyst. The reagent mixture and catalyst amounts were kept at 8 mL and 0.2 mL per gram of resin, respectively. The resin was first soaked with reagent mixture for 20 minutes, and then SnCl₄ was added dropwise while the resin and reagent mixture was under stirring and cooling. The reaction temperature was controlled

below 40 °C. When all the catalyst was added, the reaction vessel was placed into a 35 °C or 40 °C oil bath, allowing for reaction (under stirring) to continue for predetermined times (0.5 to 5 hours). Then the mixture was quenched by dropwise addition of methanol under stirring until the mixture was cooled. The liquid was then separated from the resin, and the resin was successively washed with acetone, DI water, and methanol.

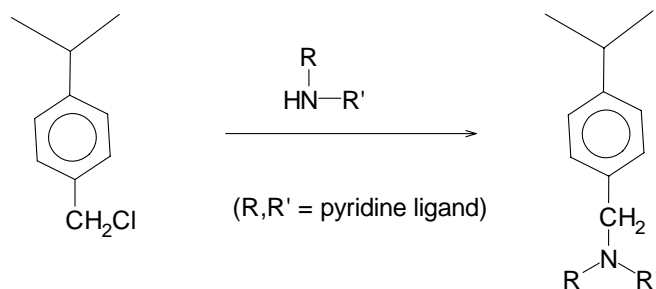
In both methods, the chloromethylated resins were rinsed with DI-water, air-dried, and oven-dried at 70 °C. The resin weight gain was measured to determine the degree of chloromethylation. Based on chloromethylation measurements and the subsequent ligand functionalization tests, Methods A and B showed similar results. However, because Method B avoids the direct use of chloromethyl methyl ether, which is a carcinogen, Method B was used in all subsequent chloromethylation tests in this study.

The general chloromethylation reaction is depicted as follows:



Immobilization of the chelating functional groups was carried out by reacting the chloromethylated polymer beads with the functional ligands 2-picolylamine or di(2-picolyl)amine. The amination was carried out in the presence of a mixture of toluene and dimethylformamide (DMF) (2:1 v/v) as the solvent. The molar ratio of a ligand and the chloromethyl group was kept at 2:1. The resin, ligand, and solvents were mixed in a dry Erlenmeyer flask connected with a condenser, and all the reactions were carried out in a 95 °C oil bath for 24 hours under gentle stirring. Upon completion, the functionalized

resins were thoroughly washed with acetone and methanol and then air-dried. The reaction scheme is shown below:



The ligand-grafted beads were then washed using DI water, and copper loading was then performed in the same manner as for DOW 3N. The resultant chelating resins were designated as XAD1180-3N (XAD16-3N) and XAD1180-2N (XAD16-2N), respectively, where 3N indicates the di(2-picoly)amine functional groups (three nitrogen atoms per functional group), whereas 2N refers to the 2-picolyamine groups (two nitrogen atoms per functional group). Cu(II) was then loaded to the functionalized XAD sorbents to yield the corresponding PLEs, XAD1180-3N-Cu (XAD16-3N-Cu) and XAD1180-2N-Cu (XAD16-2N-Cu), respectively. Figure 2.3 shows the schematic and key reactions in synthesizing PLEs based on PS/DVB polymers. Note that the product before copper loading is also a valuable chelating resin, which is of value for removal of heavy metals from water.

Functionalization of acrylic copolymer, XAD7HP, was carried out through the aminolysis of the ester groups in the polymer matrix through the amine group of 2-(picoly)amine or di(2-picoly)amine. Dimethyl sulfoxide (DMSO) was used as the solvent. The ligand to polymer ratio was 1:1 (w/w), and 5 ml of DMSO was used per gram of polymer. The resin, ligand, and solvent were loaded in a dry Erlenmeyer flask, which was then heated in an oil bath while stirring and under nitrogen purging. The bath

⌘ XAD1180 2N-Cu

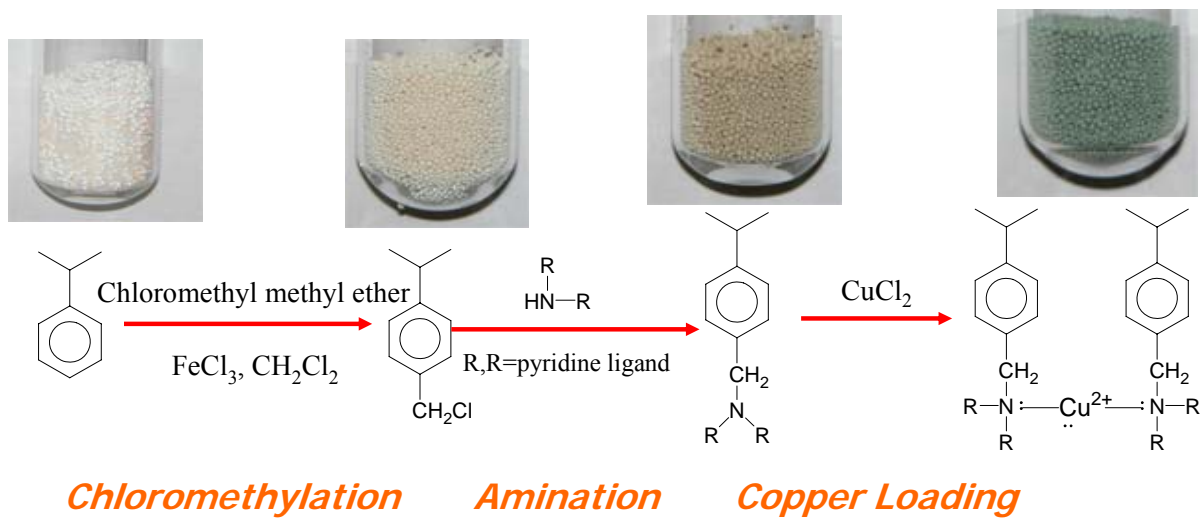
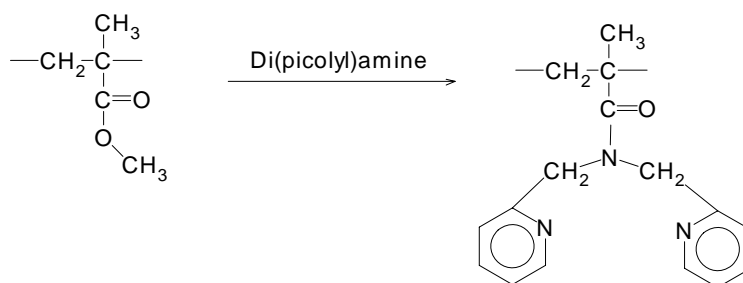


Figure 2.3. Schematic and key reactions in synthesizing PLEs based on polystyrene-DVB XAD polymers.

temperature was gradually raised from room temperature to 170 °C during the first hour of the reaction. Then the reaction was kept at 170 °C for 4 hours. The reaction was then cooled down, and the resin was successively washed with DI water, 0.1N HCl aqueous solution, and DI water. The reaction scheme is depicted as follows:



The resultant chelating resins are designated as XAD7HP-3N and XAD7HP-2N, respectively. Cu(II) was then loaded on the resins to yield the corresponding PLEs, XAD7HP-3N-Cu and XAD7HP-2N-Cu. Figure 2.4 shows the schematic and key reactions in synthesizing PLEs based on polyacrylic polymers. Note that PLEs based on PA-polymers are expected to show better resistance to organic fouling.

2.2.3 COPPER LOADING AND COPPER CAPACITY MEASUREMENT

All the functionalized resin samples were conditioned according to the following procedure: 4 hours of equilibration with 0.1 N HCl aqueous solution, washing with DI water, 4 hours of equilibration with 0.1 N NaOH aqueous solution, and washing with DI water. The resins were then loaded with copper by equilibrating with CuCl₂ solution (1% w/w of Cu, 30 mL solution per gram of resin) under shaking for 2 days. The resin color turned to blue-green upon copper loading. The copper-loaded resins were then thoroughly washed with DI water and air-dried for uses.

To measure the maximum copper loading capacity, ~0.12 gram of a copper-loaded resin was mixed with 15 mL of ammonium hydroxide solution (4 wt.% of NH₃),

⌘ XAD7HP 2N-Cu

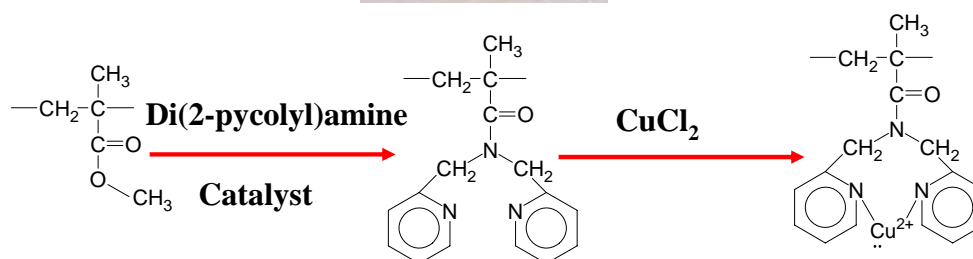


Figure 2.4. Schematic and key reactions in synthesizing PLEs based on acrylic polymers.

and the mixture was shaken for one day to strip off the copper from the resin. The amount of copper in the stripping solution was then measured by the absorbance at 630 nm using UV-Vis spectrometer (Hewlett Packer UV-Vis 8453), and copper uptake was calculated.

Table 2.2 lists the copper uptake capacity for the six XAD-based chelating resins and for the commercial chelating resin, DOW 3N and XUS 3N. The copper capacity for five of the XAD based on PLEs (except XAD7HP-3N) ranged between 1.2 and 1.4 meq/g. Despite considerable differences in the properties (polymer type and surface area) of the parent polymers (Table 2.1), the resultant chelating resins do not differ significantly in their copper capacity. This observation suggests that the sorption capacity of the XAD-based chelating resins may be limited by the extremely high crosslinkage (~40%) of these polymers. Although the high crosslinkage greatly increases the surface area of the resins, it reduces the size of the pores. The pore size may be further reduced during the functionalization of the resins. As a result, the final copper uptake capacity of the XAD-based chelating resins was lower than that for DOW 3N-Cu (Note: DOW 3N has a much smaller surface area (~139 m²/g), but larger mean pore size (~250 Å) (Zhao, 1997).

In addition, the optimal reaction time in chloromethylation should be controlled at ~1.5 hours, in order to provide for the greatest copper capacity, as shown in Table 2.3.

Table 2.2 Maximum copper loading of the chelating resins.

Chelating Resin	Functional group	Maximum Cu-Loading Capacity (mg/g)
XAD1180-2N	2-Picolylamine	40
XAD1180-3N	Di(2-picolyl)amine	39
XAD16-2N	2-Picolylamine	41
XAD16-3N	Di(2-picolyl)amine	40
XAD7HP-2N	2-Picolylamine	44
XAD7HP-3N	Di(2-picolyl)amine	26
DOW 3N	Di(2-picolyl)amine	90
XUS 3N	Di(2-picolyl)amine	95

Table 2.3 Effect of chloromethylation time on maximum copper loading capacity of di(2-picolyl)amine-functionalized XAD1180.

Chloromethylation Time	35 °C, 0.5 hour	35 °C, 1 hour	35 °C, 1.5 hours	35 °C, 2 hours	40 °C, 5 hours
Weight Gain after Chloromethylation (%)	18	20	21	22	24
Max. Cu-Loading Capacity (mg/g resin)	30	35	39	33	26

III. MATERIALS AND EXPERIMENTAL PROCEDURES

3.1 MATERIALS

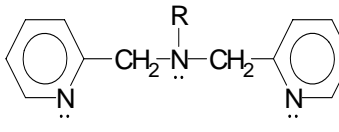
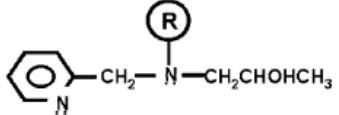
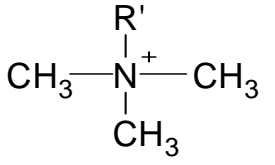
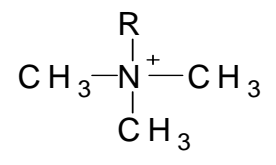
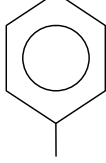
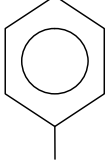
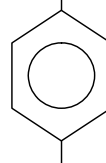
A total of nine sorbents were tested for arsenate removal, including DOW 3N-Cu, XUS 3N-Cu, the five XAD-based PLEs, and two commercial SBA resins (IRA 900 and IRA 958). Table 3.1 summarizes the salient properties of these sorbents. Before use, the resins were conditioned following the standard acid-base washing procedures with 1N HCl and 1N NaOH. All resins were initially in the chloride form.

3.2 Experimental methods

3.2.1 EQUILIBRIUM SORPTION TESTS

Batch isotherm tests were carried out for various PLEs as well as for the commercial SBA resins. In all cases, 60 mL glass vials with Teflon-lined screw caps were used for the equilibrium tests. The tests were initiated by adding known masses (0.004 g to 0.15 g) of a resin to 50 mL of a solution containing an initial concentration of 10 mg/L as *As* and 100 mg/L sulfate or 0.5 mg/L phosphate as *P*. The mixture was then shaken on a rotating tumbler for 7 days, which was sufficient to reach equilibrium as confirmed through separate kinetic tests. The initial pH of the solution was ~7.5, and pH during equilibration was kept in the range of 7.0-7.5 through intermittent adjusting using dilute NaOH or HCl until final equilibrium was reached. At equilibrium, water samples were taken from each vial and analyzed for *As* and sulfate remaining in water.

Table 3.1 Salient properties of various ion exchange resins used in this study.

Sorbent	XUS 3N and XAD16 3N	XAD1180 2N and XAD16 2N	IRA 958	IRA 900
Manufacturer	DOW Chemical Midland, MI, USA	Auburn University (based on XAD resins from Rohm and Haas, Philadelphia, PA)	Rohm and Haas Philadelphia, PA, USA	Rohm and Haas Philadelphia, PA, USA
Functional Group				
Matrix (R or R')	- CH ₂ - CH - CH ₂ -  Polystyrene, Macroporous	- CH ₂ - CH - CH ₂ -  Polystyrene, Macroporous	- CH ₂ - CH - CH ₂ - C = O HN - CH ₂ - CH ₂ Polyacrylic, Macroporous	- CH ₂ - CH - CH ₂ -  Polystyrene, Macroporous
Capacity (meq/g)	>3.0 and 1.26	3.6 and 1.26	3.4	3.6

Arsenic or sulfate uptake was then calculated based on the mass balance equation,

$$q_e = \frac{V(C_o - C_e)}{M} \quad (3-1)$$

where q_e is the equilibrium mass uptake of As by a sorbent (mg/g), V is the solution volume (L), C_o and C_e are the initial and final concentration of arsenic or sulfate in solution, respectively (mg/L), and M is the mass of a sorbent added (g). All tests were carried out at room temperature (~21 °C).

3.2.2 FIXED-BED COLUMN TESTS

The breakthrough behaviors of arsenate as well as various competing anions were tested for DOW 3N-Cu, XUS 3N-Cu, IRA 900, XAD1180-3N-Cu, and XAD7HP-3N-Cu, respectively, in a fixed-bed configuration and in the down-flow mode. The experimental set-up (Figure 3.1) included a Plexiglass column (11 mm in diameter and 25 cm in length), an Accuflow Series II high-pressure liquid chromatography stainless steel pump, and an Eldex automatic fraction collector. Simulated contaminated water was introduced in the resin bed in a down-flow mode. Samples were collected in 22 mL tubes using a fraction collector and then analyzed within 24 hours. There are major compositions in the influent water and hydrodynamic condition for each column run in Table 3.2.

3.2.3 pH EFFECT

The pH effect on equilibrium uptake of arsenate was tested for DOW 3N-Cu in a similar fashion to that in the isotherm tests. However, the final solution pH was adjusted to span from 2.8 to 11 (each vial had a different pH). Each testing vial contained 50 mL solution with an initial As of 8.3 mg/L and SO_4^{2-} of 86 mg/L. The sorption was initiated upon the addition of ~0.020 g of air-dried DOW 3N-Cu to each vial.



Figure 3.1. Fixed-bed column test set-up.

Table 3.2 Major compositions in the influent water and hydrodynamic condition for each column run.

	IRA900	IRA958	XAD	DOW 3N-Cu	XUS 3N-Cu	XUS 3N-Cu
Resin Amount(mL)	5	5	3	5	2.5	2.5
pH	8.3	8.3	7.9	8.6	8.4	7.7
Cl ⁻ (mg/L)	84	68	74	46	33	33
SO ₄ ²⁻ (mg/L)	92	86	46	40	44	44
HCO ₃ ⁻ (mg/L)			35	31	28	28
As(μg/L)	75	112	97	94	99	95
P* (mg/L)					0.5	0.1
EBCT*(min)	4.1	4.1	2.5	4.1	2.0	2.0
SLV*(m/hr)	3.0	3.0	3.0	3.0	3.0	3.0

* P: Phosphate as P

* EBCT: Empty Bed Contact Time (min)

* SLV: Superficial Liquid Velocity (m/hr)

3.2.4 KINETIC TEST

Batch kinetic tests were conducted to test the arsenic sorption rate and determine the effective intraparticle diffusivity for PLEs (DOW 3N-Cu, XUS 3N-Cu, XAD1180-3N-Cu, XAD16 3N-Cu, and XAD7HP-3N-Cu). The experiment was initiated by adding ~0.95 g of the sorbent into 2 L of a solution containing ~1.0 mg/L As and ~100 mg/L sulfate and at an initial pH of 8.0. More detail experimental conditions are described in each result figures. The solution pH was adjusted intermittently by adding small amounts of dilute NaOH to keep the solution pH within 7.0-7.5, where pH effect on the PLE's uptake was minimal. During the experiment, the resin-solution mixture was intensively agitated on a shaker to eliminate the possible film diffusion limitation on the mass transfer process. At predetermined time intervals, water samples (~2 mL/each) were taken and analyzed for As. The As uptake at various times was then determined through mass balance calculations.

3.2.5 RESIN REGENERATION AND REUSE

Regeneration of arsenic loaded DOW 3N-Cu, IRA 900, XAD1180-3N-Cu, XAD16 3N-Cu, and XAD7HP-3N-Cu were carried out in the same fixed-bed column configuration and in the co-current flow mode. In search for an optimal regenerant recipe, a 4% (w/w) NaCl solution at pH 4.1, 7.0, and 9.1 was tested in separate column runs.

Sorption capacity of DOW 3N-Cu that was subjected to up to 8 saturation-regeneration cycles was compared to that of the virgin DOW 3N-Cu. The equilibrium sorption of As was tested in the same manner as described in the isotherm tests with the following conditions: initial As = ~10 mg/L, initial SO₄²⁻ = 100 mg/L, resin weight = 0.01

g, solution volume = 50 mL, final pH = 7.0-7.5. The optimum regenerant (i.e. 4% NaCl at pH = 9.1) was employed to regenerate the resin after each use.

3.3 TREATMENT OF SPENT BRINE

3.3.1 PREPARATION OF SIMULATED SPENT BRINE

Spent regeneration brine (SRB) was prepared based on analysis of the spent brine collected from column tests performed on a PLE resin to conduct brine treatment experiments. The brine was directly reused for regeneration of up to four times until it finally reached its capacity. The initial composition of simulated spent brine was $As = 300$ mg/L, $SO_4^{2-} = 600$ mg/L, $HCO_3^- = 305$ mg/L and $NaCl = 4\%$ (w/w) (or 24 g/L as Cl^-). Each 1 L bottles of SRB were prepared. All compounds were purchased from Fisher Scientific (Pittsburgh, PA, USA) except the sodium arsenate, which was purchased from Sigma-Aldrich (Milwaukee, WI, USA).

3.3.2 TREATMENT OF SPENT BRINE

By adding aluminum salt addition, co-precipitation/sorption was occurred in SRB. Aluminum chloride ($AlCl_3$) was used for the SRB treatment. Batch experiments were carried out to determine the optimal conditions, such as the effect of aluminum chloride addition at the Al/As molar ratio of 2.5, 5, 10, 15, and 20, respectively and the effect of pH of solutions using 4 to 11. After adding $AlCl_3$ into SRB, each bottle was placed on a gang mixer operated at 200 rpm for ~2hours. Treated SRB was allowed to equilibrate for ~24 hours. Supernatant samples were taken, centrifuged, and filtered with 0.45 μ m syringe filter. All analysis for arsenic was duplicated.

3.3.3 PREPARATION OF ARSENIC-LADEN SOLID WASTER/SLUDGE

SRB samples were prepared in larger (1 L) bottle before test in the same manner previously described. The batch samples were then centrifuged and the supernatant took out from solution. Solid precipitates were then air dried in our lab, pulverized with a mortar and pestle, and then leaching tests were carried out to determine extractable As. Treatment conditions, such as solution pH, aging temperature, and aging time, were varied to determine their effect on As leachability.

3.3.4 ARSENIC-LEACHING TESTS

Two widely used standard leaching tests (TCLP and WET) were followed to determine As leachability.

- 1) TCLP: TCLP was performed according to EPA method 1311. In brief, 1 g of solid sample and 20 mL of TCLP fluid #1 were placed into scintillation vials. TCLP fluid #1 was made by adding 5.7 mL glacial $\text{CH}_3\text{CH}_2\text{OOH}$ and 64.3 mL of 1N NaOH to 500 mL DI water and diluting to 1L with DI water. The final pH of the solution was 4.93 ± 0.05 (EPA, 1992). The vials were placed on an end-over-end mixer and mixed for 18 ± 1 hours to allow for extraction equilibrium.
- 2) WET: WET was performed following the method prescribed by the California Department of Health Services (SOP No. 910). In brief, a citrate buffer extraction solution was prepared and purged with nitrogen gas. The 0.2M citrate solution was prepared by dissolving 42.0 g monohydrate citric acid in 950 mL of DI water. The solution was titrated to pH 5 with 50% NaOH and diluted to 1 L with DI water (California Department of Health Services, 1990). Dry As-laden sludge samples were placed in 25 mL scintillation vials. All samples were prepared by

the same procedure with duplicates and an extraction period of 40 hours. Some headspace was left in the scintillation vials.

All tests were duplicated to ensure data precision.

3.4 CHEMICAL ANALYSIS

Arsenic and copper were analyzed using a Perkin Elmer Atomic Adsorption Spectrophotometer in the graphite mode, which has a detection limit of 3 µg/L as *As*. Solution pH was measured using an Orion pH meter (model 520A). Sulfate and chloride ions were analyzed using a Dionex Ion Chromatograph (Model DX-120). Bicarbonate was analyzed with a UV- Persulfate TOC Analyzer (Phoenix 8000).

IV. RESULTS AND DISCUSSION

4.1 EQUILIBRIUM ISOTHERMS AND ARSENATE ADSORPTION

4.1.1 ARSENIC-SULFATE ISOTHERMS FOR PLES

As mentioned before, one of the critical limitations for current SBA resins is its lack of selectivity and low sorption capacity for arsenate, especially in the presence of some omnipresent anions such as sulfate. To probe the PLEs' sorption capacity, arsenate sorption isotherms were constructed for DOW 3N-Cu, XUS 3N-Cu, XAD1180-3N-Cu, XAD16-3N-Cu, and XAD7HP-3N-Cu, respectively, in the presence of an initial sulfate concentration of 100 mg/L or 0.5 mg/L as P. For comparison, arsenic isotherms were also measured for the two commercial SBA resins (IRA 900 and IRA 958) under otherwise identical conditions. The equilibrium pH was maintained at 7.0-7.5 in all cases to minimize the pH effect on the uptake. Figures 4.1, 4.2, and 4.3 show the observed (symbols) and simulated (lines) isotherms for these sorbents.

The classical Langmuir model was employed for fitting the experimental data (Zhao et al., 1995),

$$q_e = \frac{bQC_e}{1+bC_e} \quad (4-1)$$

where q_e is the equilibrium As uptake (mg/g), C_e is the equilibrium concentration of As in water (mg/L), and b and Q are the Langmuir affinity and capacity coefficients, respectively. The non-linear fitting was performed using the SigmaPlot8.0. Table 4.1 lists

Table 4.1 The model-fitted Langmuir parameters (b, Q) and experimentally determined arsenate/sulfate binary separation factor ($\alpha_{As/S}$).

Resin	Q(Standard Error) (mg/g)	b (Standard Error) (L/mg)	$\alpha_{As/S}$ (Standard deviation)
DOW 3N-Cu	92(8.2)	0.20(0.028)	12(0.73)
XUS 3N-Cu	63(0.57)	4.7(0.10)	12(4.3)
IRA 958	5.5(0.36)	6.1(1.5)	0.10(0.026)
IRA 900	4.5(0.51)	4.1(2.1)	0.20(0.057)
XAD1180-3N-Cu	24(8)	0.13(0.078)	7.4(0.54)
XAD1180 2N-Cu	22(2.7)	0.31(0.10)	7.6(0.75)
XAD16-3N-Cu	31(20)	0.081(0.080)	10(0.66)
XAD16 3N-Cu	16(2.5)	0.37(0.20)	10(2.1)
XAD7HP-3N-Cu	18(4.4)	0.15(0.077)	4.9(0.84)

the model-fitted b and Q values. Table 4.1 reveals that all PLEs showed much greater arsenate sorption capacity than the commercial SBA resins. Among the PLEs, DOW 3N-Cu and XUS 3N-Cu offer the greatest sorption capacity. It is especially noteworthy that the Langmuir capacity (Q) for DOW 3N-Cu is almost 17 times greater than for the standard SBA resins. Although the total reported capacity of the SBA resins is greater than the PLEs, very little of the fraction of the capacity is used for arsenate uptake due to the fierce competition of sulfate, i.e. lack of arsenate selectivity for the SBA resins.

The binary separation factor has been commonly used to compare the relative affinity of a sorbent for various competing sorbates. In a binary system, the arsenic/sulfate separation factor ($\alpha_{As/S}$) is defined as

$$\alpha_{As/S} = \frac{q_{As} C_S}{C_{As} q_S} \quad (4-2)$$

where q and C represent the concentration of As in the polymer phase and in the aqueous phase, respectively; As and S in the subscripts denote arsenic and sulfate, respectively. In general, a value of $\alpha_{As/S}$ of greater than unity indicates the resin's preference toward arsenic over sulfate, while the opposite is true if $\alpha_{As/S}$ is less than unity. The greater the $\alpha_{As/S}$ value, the more selective is the resin for arsenate. Based on the experimental equilibrium sorption data in Figures 4.1 and 4.2, the average separation factor was calculated for the resins and is given in Table 4.1. The mean $\alpha_{As/S}$ value of DOW 3N-Cu and XUS 3N-Cu are ~ 12 , which is more than two orders of magnitude greater than that for the SBA resins and clearly indicates the resin's high selectivity toward arsenate over sulfate. The unusually high selectivity for arsenic was also true for the XAD-based PLEs, although the total capacity was not as great as for DOW 3N-Cu between arsenate and the

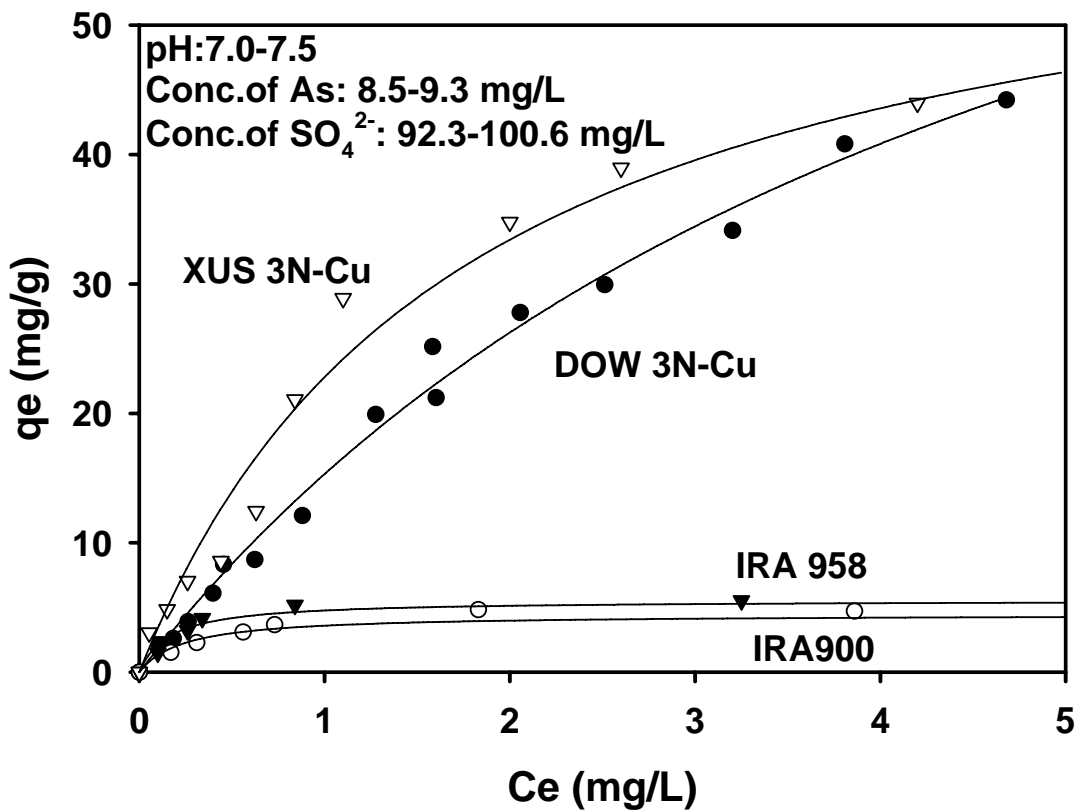


Figure 4.1. Arsenate sorption isotherms for DOW 3N-Cu, XUS 3N-Cu and two conventional SBA resins (IRA 900 and IRA 958) in the presence of competing sulfate ions (symbols: observed data; lines: Langmuir model fits).

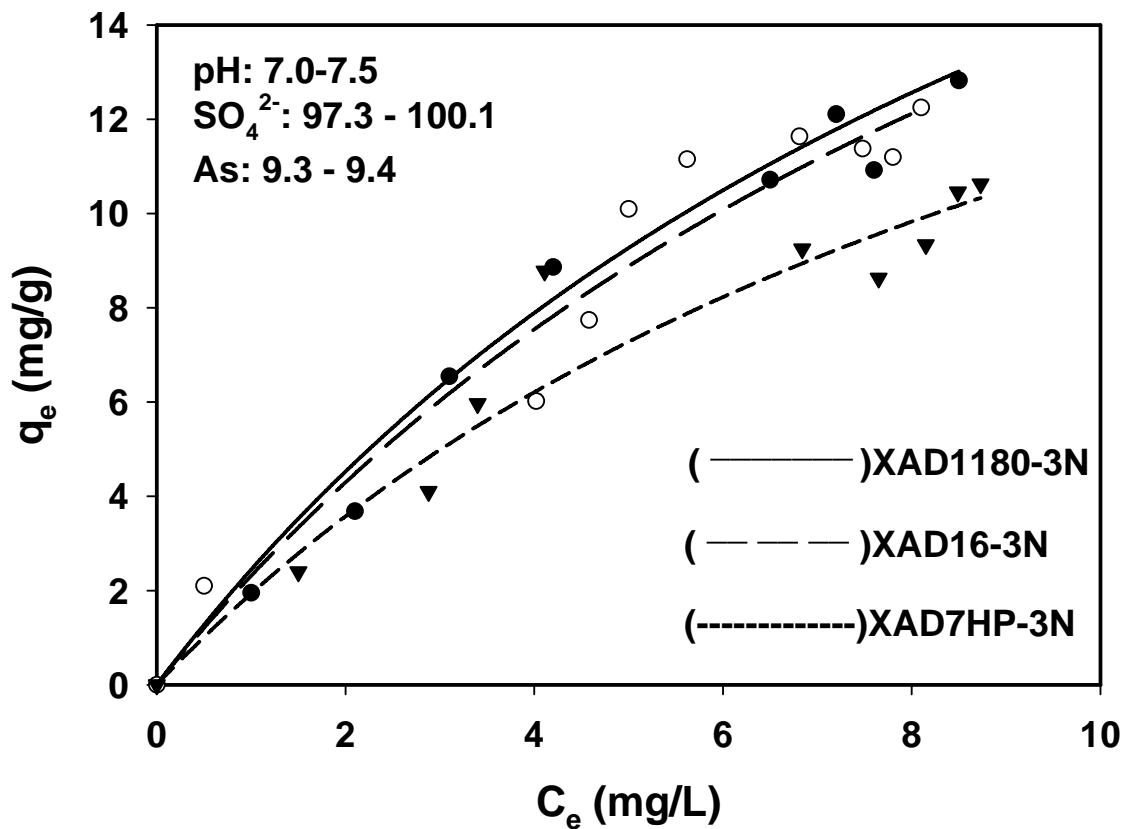


Figure 4.2. Arsenate sorption isotherms for XAD1180-3N-Cu, XAD16-3N-Cu and XAD7HP-3N-Cu in the presence of competing sulfate ions (symbols: observed data; lines: Langmuir model fits).

immobilized Cu^{2+} ions at the sorbent-sorbate interface. Under the experimental conditions, mono-hydrogen arsenate (HAsO_4^{2-}) is considered the predominant arsenate species. HAsO_4^{2-} is a divalently charged, bidentate ligand, and a strong Lewis base (donor of electron lone pairs). The competing sulfate is also a divalently charged ligand, but it is a much weaker Lewis base. Consequently, interactions between arsenate and the immobilized Cu^{2+} ions involve both Lewis acid-base interaction (or inner-sphere complexation) and ion pairing (or electrostatic interactions), while interactions between sulfate and the Cu^{2+} ions is predominantly ion pairing. It is noteworthy that Lewis acid-base interaction also enhances the electrostatic interactions between arsenate and the loaded Cu^{2+} ions. This is because the inner-sphere complexation occurs over a much shorter distance than outer sphere complexation, and the electrostatic interactions within the much shortened distance are much stronger in accord with Coulomb's law. Consequently, DOW 3N-Cu and XUS 3N-Cu offer much greater affinity for arsenate over sulfate. For the commercial SBA resins, the quaternary amine functionalities ($\text{RN}^+(\text{CH}_3)_3$) take up anions predominately through electrostatic interactions, i.e., the ligand strength of an anion does not play a role in sorption affinity. Therefore, SBA resins are not selective for arsenate.

The underlying mechanism for the enhanced arsenate sorption by DOW 3N-Cu can also be revealed by inspecting the fundamental thermodynamic driving forces, i.e., the overall standard free energy change (ΔG^o). For arsenate sorption by DOW 3N-Cu, ΔG^o is composed of two synergistic terms as shown in eqn (4)

$$\Delta G^o = \Delta G_{EL}^o + \Delta G_{LAB}^o \quad (4-3)$$

where ΔG_{EL}° is due to electrostatic interactions and ΔG_{LAB}° is due to the Lewis acid-base interaction (i.e. metal-ligand complexation). Compared to arsenate, other anions such as sulfate, nitrate and chloride are much weaker ligands; only ΔG_{EL}° in eqn (4) is operative, thus the resultant driving force (ΔG_{o}°) for these anions is much smaller than that for arsenate. Commercial SBA resins interact with anions only through electrostatic interactions (i.e., $\Delta G_{LAB}^{\circ} \approx 0$). Therefore, DOW 3N-Cu and XUS 3N-Cu are able to take advantage of the strong ligand characteristics of arsenate over other competing anions and to achieve highly selective removal of arsenate.

4.1.2 ARSENIC-PHOSPHATE ISOTHERM FOR DOW 3N-Cu AND XUS 3N-Cu

Binary isotherm tests between arsenic and phosphate were conducted to determine the relative arsenic uptake for different sorbents because the phosphate is well known for having high affinity for PLEs. Zhao (1997) revealed that phosphate-sulfate isotherm with a competing sulfate concentration of 2 meq/L (100 mg/L) for DOW 3N-Cu showed a significantly greater phosphate sorption capacity. In other words, phosphate can be adsorbed selectively into PLEs in the presence of a strong competing anion, sulfate. Figure 4.3 is the result of isotherm test carried out with 8.4 mg/L as As and 0.5 mg/L as P at pH 7.0-7.5. Although phosphate is a strong competing anion, there was 5 mg/g difference in the maximum capacity of arsenic for XUS 3N-Cu and DOW 3N-Cu is not big difference compared to the arsenic-sulfate isotherm test. To find out the competing effects of sulfate on DOW 3N-Cu's arsenic uptake at varying concentrations of sulfate, isotherm tests were conducted at two initial different sulfate concentrations, 50 mg/L and 100 mg/L, respectively, with other conditions remaining identical. Figure 4.4 shows the arsenic uptakes for these two separate isotherm tests. When 50 mg/L and 100

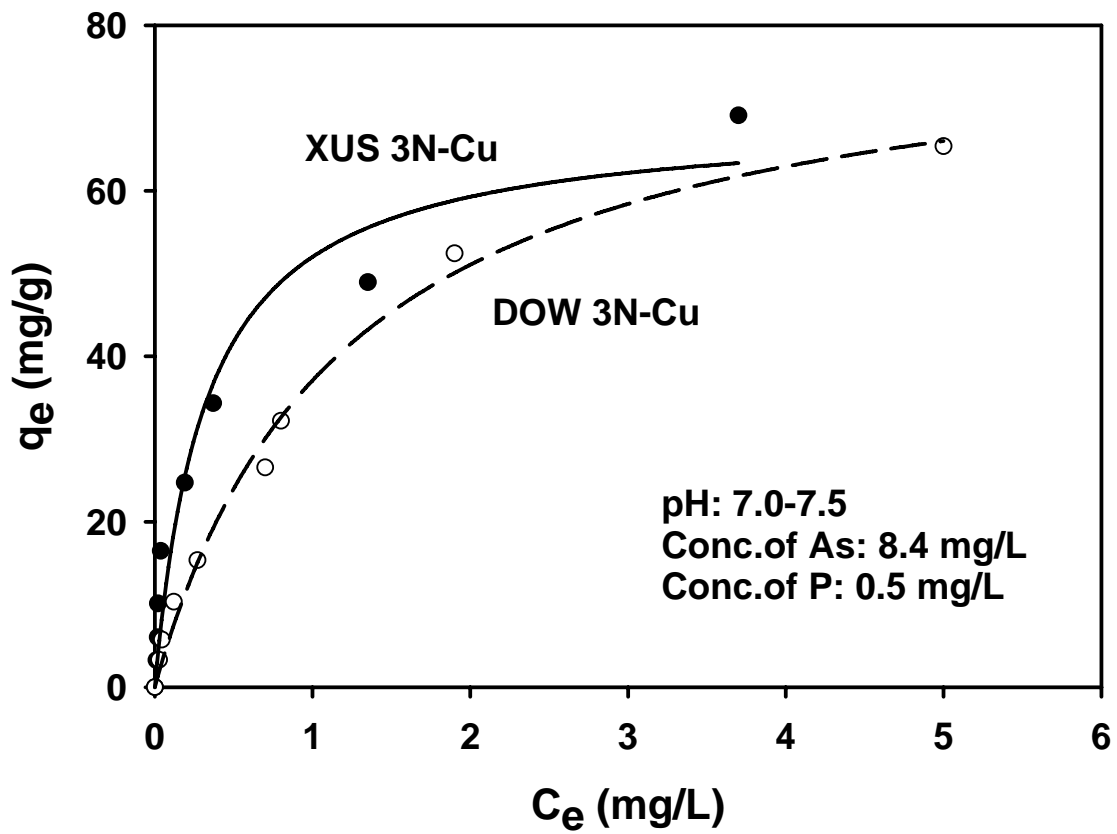


Figure 4.3. Arsenate sorption isotherms for DOW 3N-Cu and XUS 3N-Cu in the presence of competing phosphate ions. (Symbols: observed data; lines: Langmuir model fits)

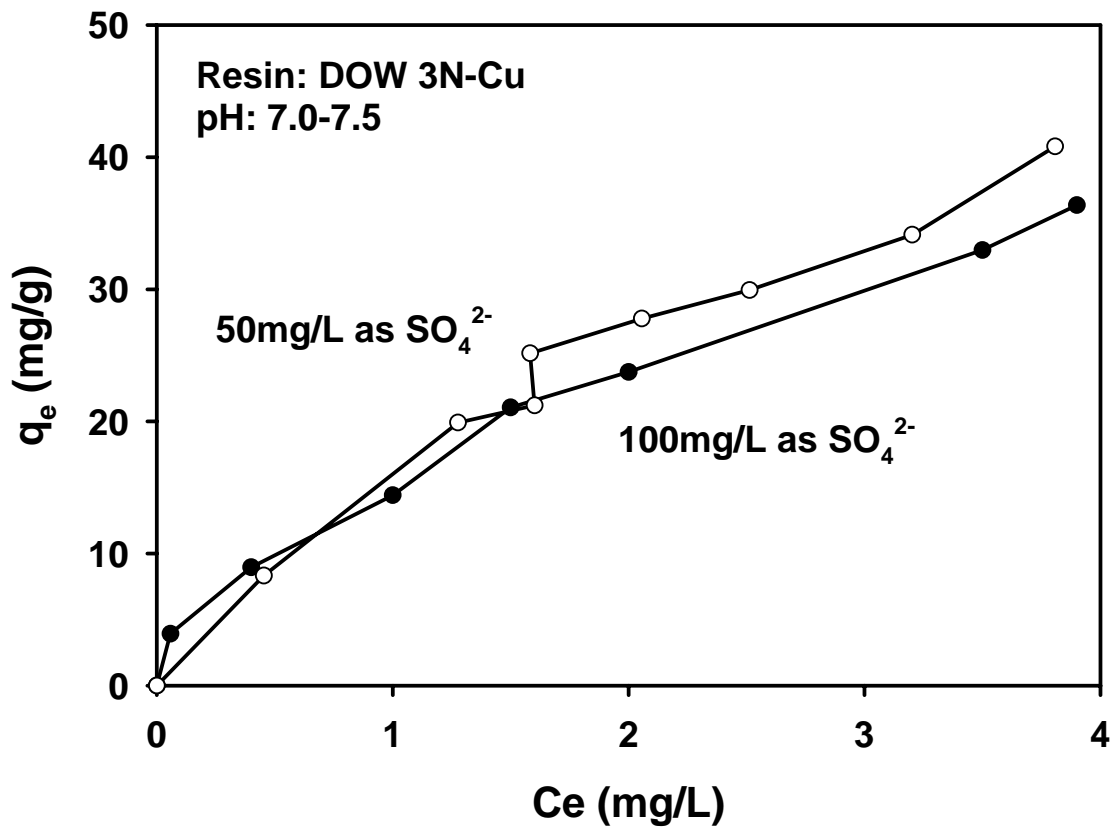


Figure 4.4. Arsenic isotherms for DOW 3N-Cu at two different background concentration of sulfate.

mg/L of sulfate are added into a solution, doubling sulfate concentration reduced the arsenic uptake of DOW 3N-Cu only slightly. Namely, the arsenic removal capacity of DOW 3N-Cu is not vary much dependant on the concentration of sulfate.

4.2 BREAKTHROUGH BEHAVIORS

Figures 4.5, 4.6, and 4.7 show the breakthrough histories of arsenate and other competing anions during the fixed-bed column experiments using IRA 900, IRA 958, and DOW 3N-Cu, respectively. In all cases, lab-simulated water was used in the influent. Compositions and hydrodynamic conditions are provided in each figure. Figure 4.5 and 4.6 show that for IRA 900 and IRA958, the sulfate breakthrough occurred ~100 bed volumes (BVs) later than the arsenate breakthrough, confirming the resin's greater affinity for sulfate over arsenate. Figure 4.5 and 4.6 also reveal a sharp chromatographic peaking of the arsenate breakthrough curve, which again indicates that this commercial SAB resin favors sulfate much more than arsenate. Due to the strong competition from sulfate, IRA 900 can treat only ~600 BVs of contaminated water per operation cycle (a cycle = saturation run + regeneration run). The breakthrough sequence of the anions reveals the following selectivity order for IRA 900:



Field data from Albuquerque, NM, USA, showed that As breakthrough took place typically within ~450 BVs using SBA commercial resins (Clifford, 1999).

In contrast, a completely different breakthrough behavior was observed when DOW 3N-Cu was used. Figure 4.7 and Figure 4.8 show that all three competing anions broke through before 500 BVs. Based on the new MCL value of 10 µg/L for As, arsenate breakthrough

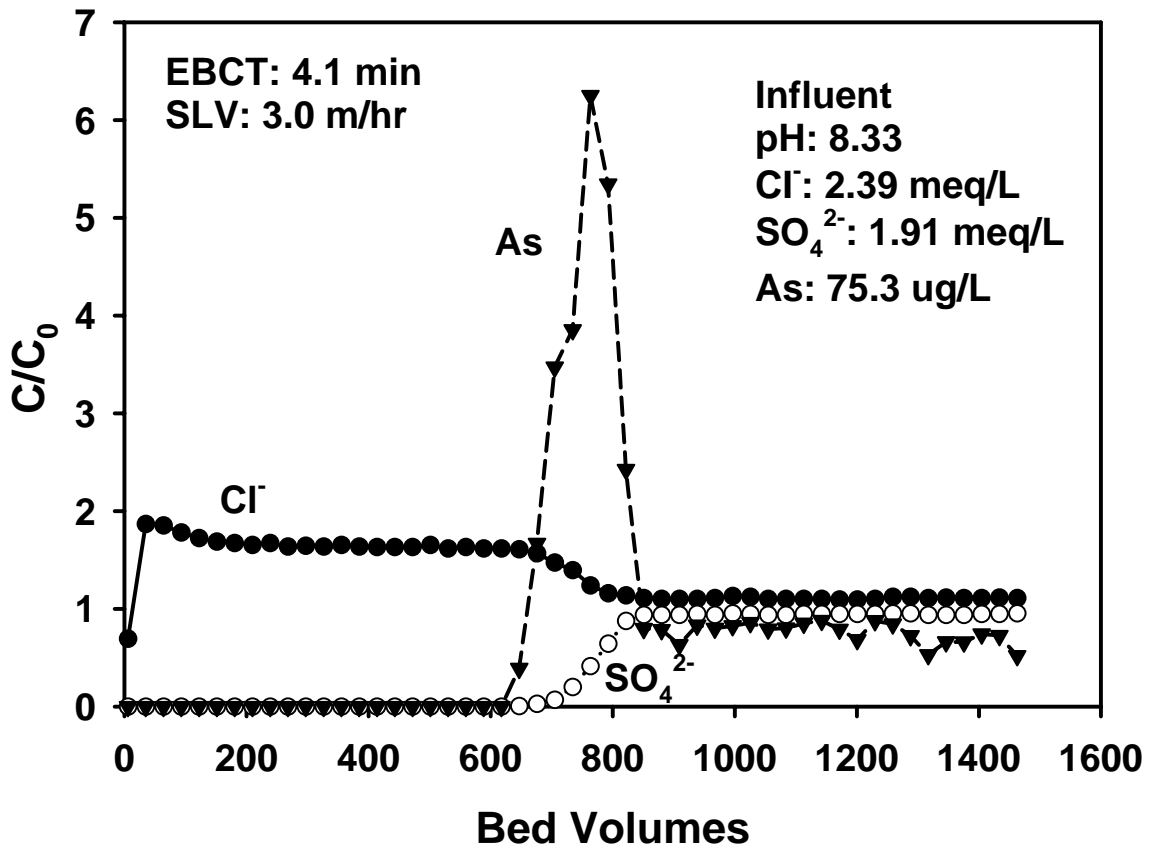


Figure 4.5. Breakthrough histories of arsenate and sulfate in a simulated multi-component system using a standard SBA resin, IRA 900.

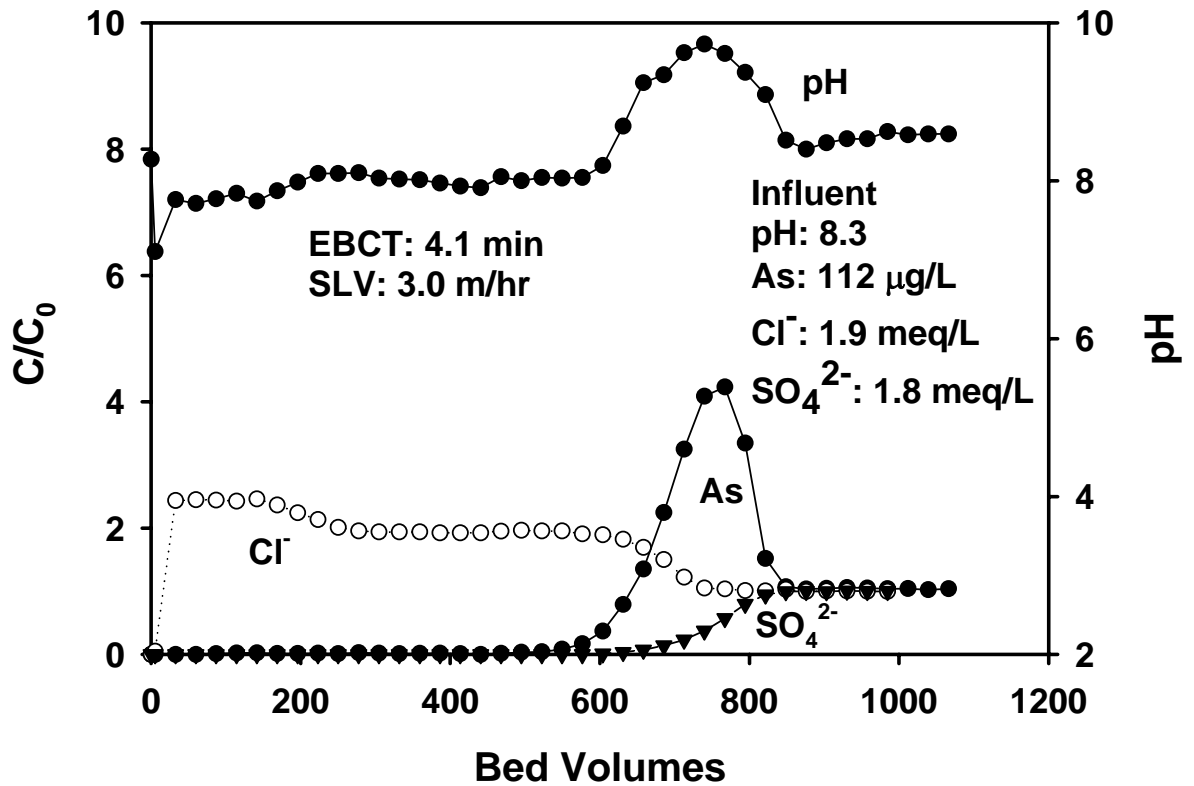


Figure 4.6. Breakthrough histories of arsenate and sulfate in a simulated multi-component system using a standard SBA resin, IRA 958.

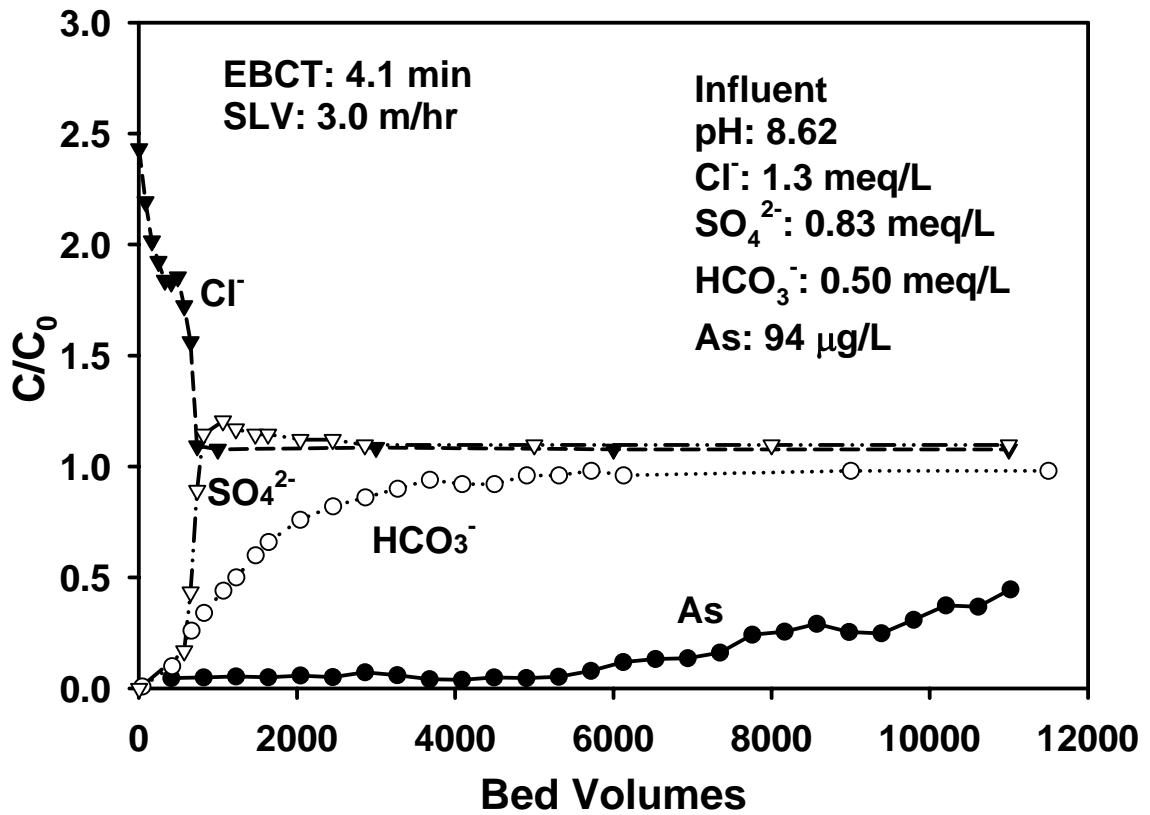


Figure 4.7. Breakthrough histories of arsenate and competing anions in a simulated multi-component system using a polymeric ligand exchange, DOW 3N-Cu.

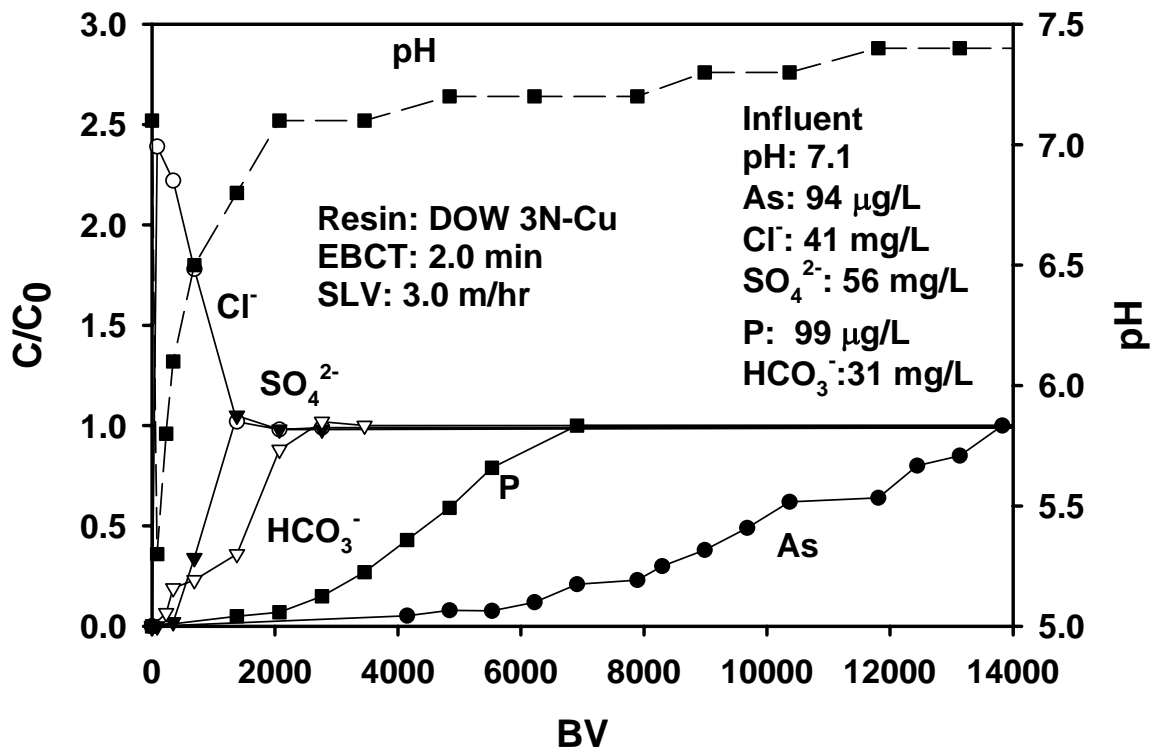
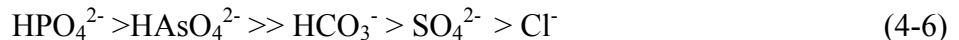


Figure 4.8. Breakthrough histories of arsenate and competing anions in a multi-component a system using a polymeric ligand exchange, DOW 3N-Cu.

did not occur until after 6,000 BVs, i.e. the PLE can treat over 10 times more water than IRA 900 before arsenate breakthrough occurs. A minor chromatographic peaking of sulfate was observed. The breakthrough sequence indicates the following selectivity sequence:



It is noteworthy that the monovalent bicarbonate displayed slightly greater affinity over the divalent sulfate, which is not surprising given that bicarbonate is a stronger ligand than sulfate. However, when phosphate is added into solution as 0.5 mg/L, a significant breakthrough for As and phosphate has occurred. Figure 4.9, which was carried out with the same condition adding 0.5 mg/L as P for XUS 3N-Cu, indicates that the breakthrough histories of all three kinds of anions (Cl^- , SO_4^{2-} , HCO_3^-) is similar to DOW 3N-Cu, but the relation between arsenate and phosphate is definitely different. The breakthrough of arsenate takes place around 3800 BV earlier than the phosphate breakthrough, and, additionally, the sharp chromatographic peak of arsenic is shown when phosphate breakthrough begins. According to these breakthrough histories for XUS 3N-Cu column test, which was conducted with the same conditions, except the addition of P (0.5 mg/L), the following selectivity sequence can be observed:



Eqn. 4-6 indicates that although arsenic has a strong affinity for PLEs, the presence of phosphate can reduce the arsenic adsorption capacity and interrupt the breakthrough of arsenic. Although the influent pH was maintained constant (=8.4), the effluent pH profiled that pH dropped to pH 6.0 at initial BV. Then it recovered and was kept at pH 7.5. Two kinds of factors contribute to the drop in initial pH, as suggested by Zhao

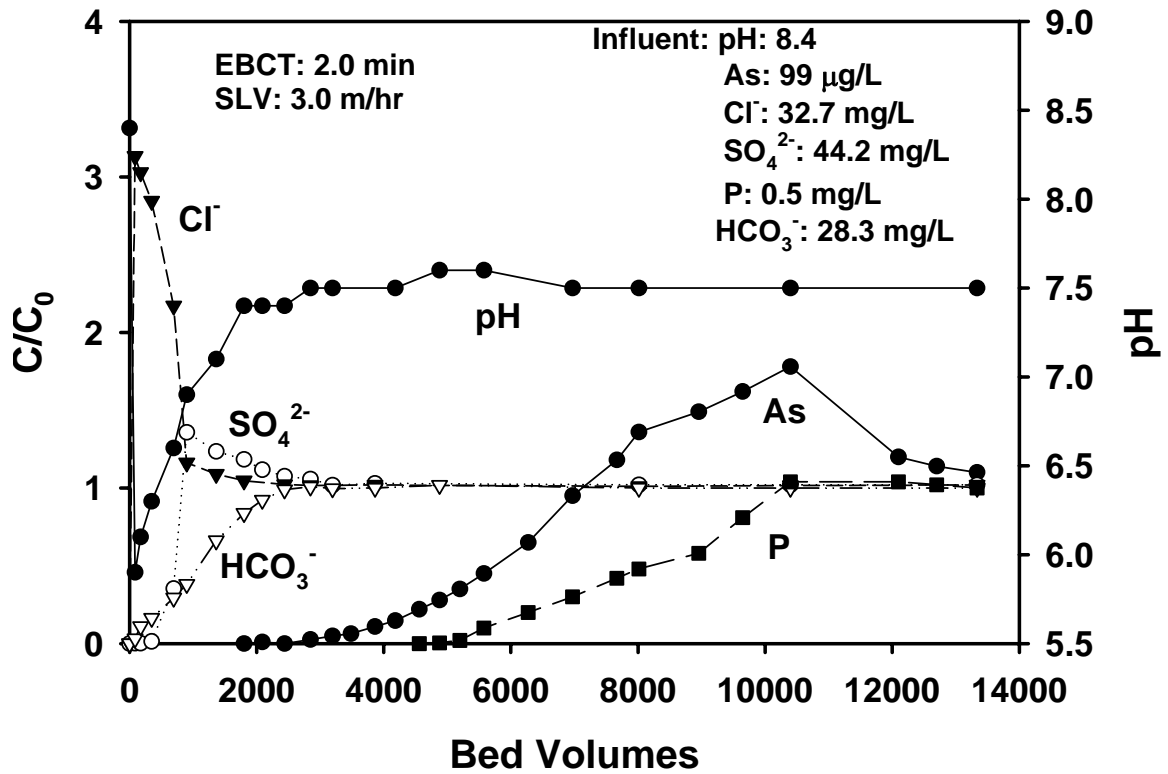


Figure 4.9. Breakthrough histories of arsenate and other competing anions in a fixed-bed run with XUS 3N-Cu in the presence of an unusually high concentration (0.5 mg/L as P) of phosphate.

(1997). The first factor is the release of hydrogen ions from bicarbonate. HCO_3^- is the predominant species at $\text{pH} = 8.4$. However, the fraction of HCO_3^- can be appreciably higher at the positively charged ion exchange site due to the Donnan co-ion exclusion effect. As a result, the following reaction takes place:



As CO_3^{2-} is preferentially taken up by the resin, hydrogen ions are released into the bulk solution. The second factor is the direct uptake of OH^- by PLE or SBA. Another column test for XUS 3N-Cu was carried out to determine the effect of phosphate in the same condition, except to the concentration of phosphate, 0.1 mg/L as P. Figure 4.10 shows in the arsenic breakthrough curve the presence of competing anion phosphate, 0.1 mg/L as P. Compared with using 0.5 mg/L as P, arsenic breakthrough takes place at 8500 BV, which is two times longer than that of using 0.5 mg/L as P and which is much longer for DOW 3N-Cu column test conducted without a strong competing anion, phosphate. The breakthrough sequence is reversed between arsenate and phosphate.

Other experiments were conducted using different PLE resins developed in our laboratory. Figures 4.11, 4.12 and 4.13 show the breakthrough curves with three XAD-based PLEs. In all cases, competing anions (chloride, sulfate, bicarbonate) broke through within ~50 bed volumes (BV), whereas the breakthrough of arsenic occurred at about 800-900 which is more than that for the SBA resins. Although the selective sequence tendency is the same with DOW 3N-Cu, and a minor chromatographic peaking of sulfate was also detected, the BV of breakthrough of arsenic took place so much earlier than that of DOW 3N-Cu because the total capacity of copper for these PLEs is much lower than that for DOW 3N-Cu.

It is also needed to find out the breakthrough of arsenite, As(III), in the presence of competing anion using new PLE, DOW 3N-Cu. Figure 4-14 is the arsenite breakthrough when the test carried out with 46.7 $\mu\text{g/L}$ as As, 100 mg/L as sulfate, and initial pH of 8.40. The arsenite immediately came out after column test ran and the concentration of arsenite reached to 130 $\mu\text{g/L}$ which is much higher than initial arsenite concentration, 46.7 $\mu\text{g/L}$. This result is because the arsenite selectivity for PLE. As mentioned in Figure 1.1, the predominant specie of arsenit in this pH range is H_3AsO_3 . Therefore, there is no ion-pair interaction between Cu^{2+} and arsenite.

To determine the pH effect during the fixed column test, two column tests were carried out with the same condition and different pH , 6.7 and 8.5 in figure 4. 15 and 4.16 Even though the initial concentrations and hydrodynamic conditions are the same, the arsenate breakthrough for using pH 6.7 and pH 8.5 occurred in ~ 8000 BVs and ~ 6000 BVs, respectively. This is because the optimal pH range on arsenate uptake is ~ 7 by An et al (2005).

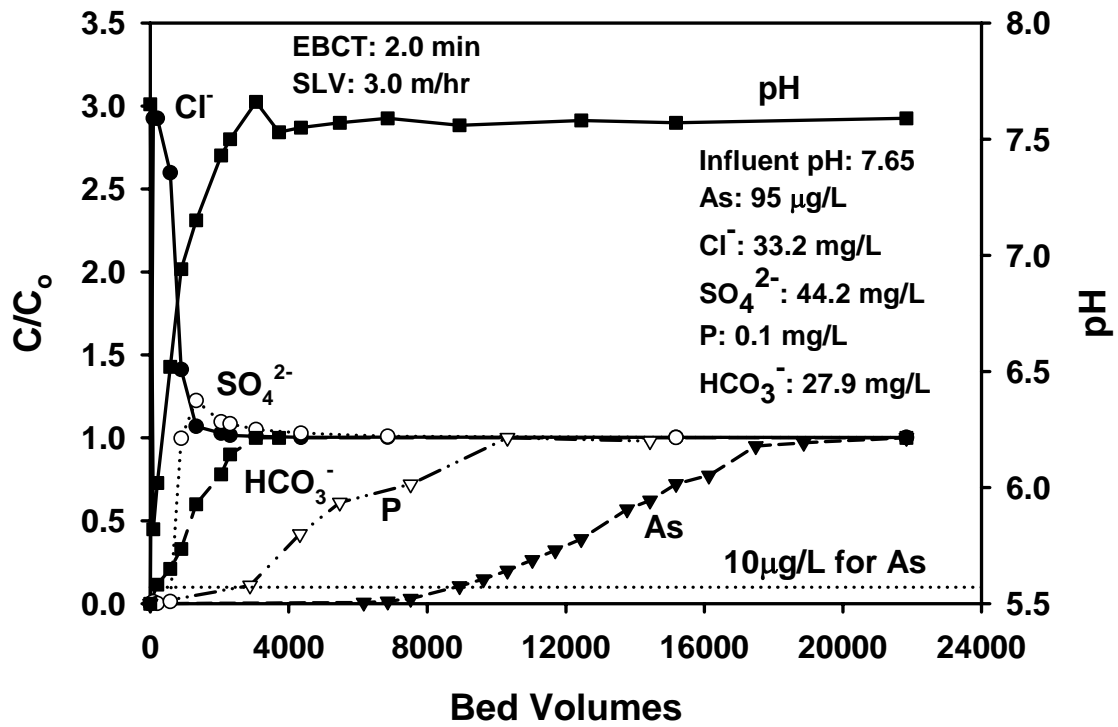


Figure 4.10. Breakthrough histories of arsenate and competing anions in a multi-component system using a polymeric ligand exchange, XUS 3N-Cu.

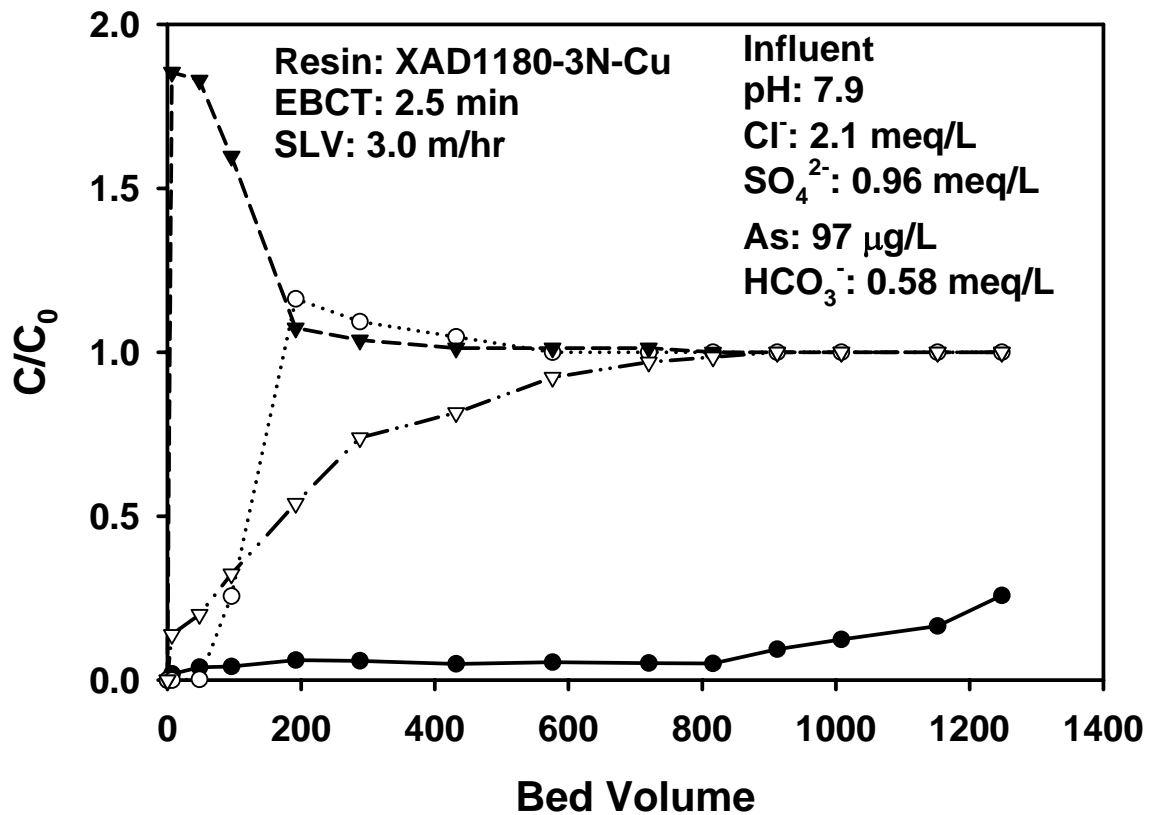


Figure 4.11. Breakthrough histories of arsenate and competing anions in a multi-component system using a polymeric ligand exchange, XAD1180-3N-Cu.

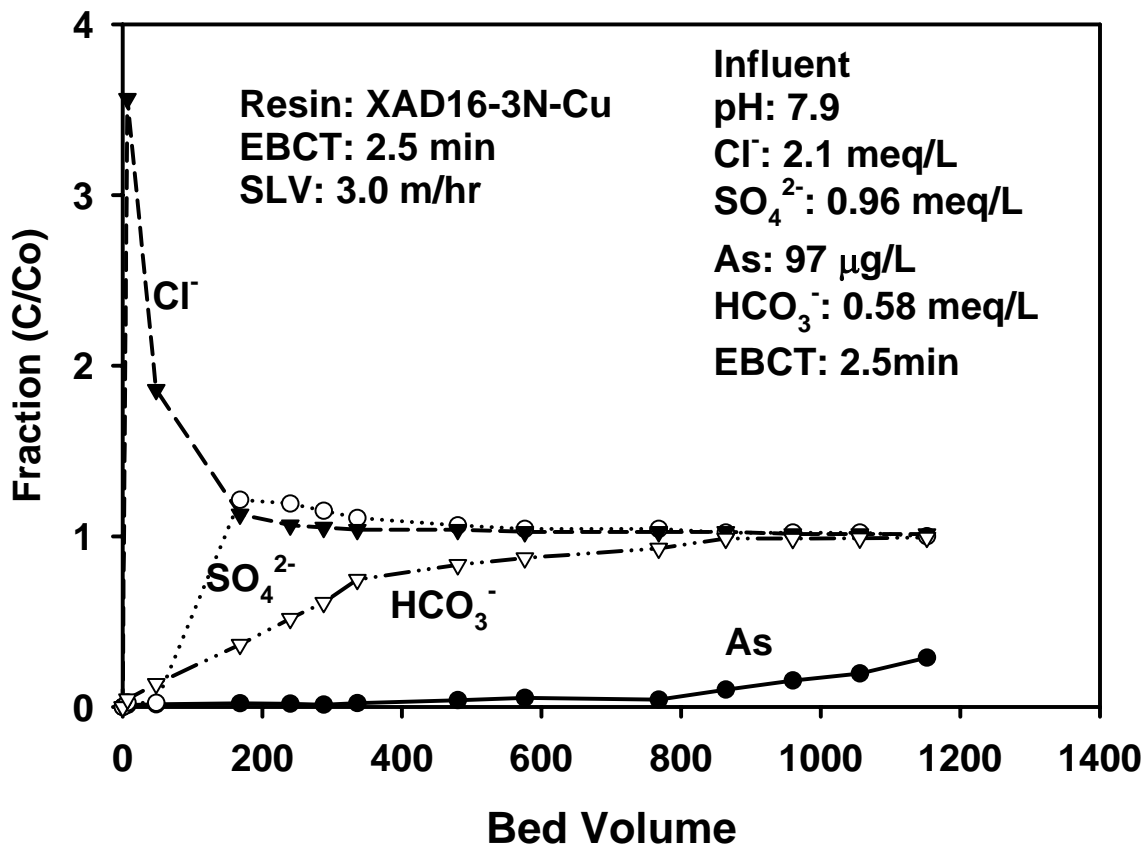


Figure 4.12. Breakthrough histories of arsenate and competing anions in a multi-component system using a polymeric ligand exchange, XAD16-3N-Cu.

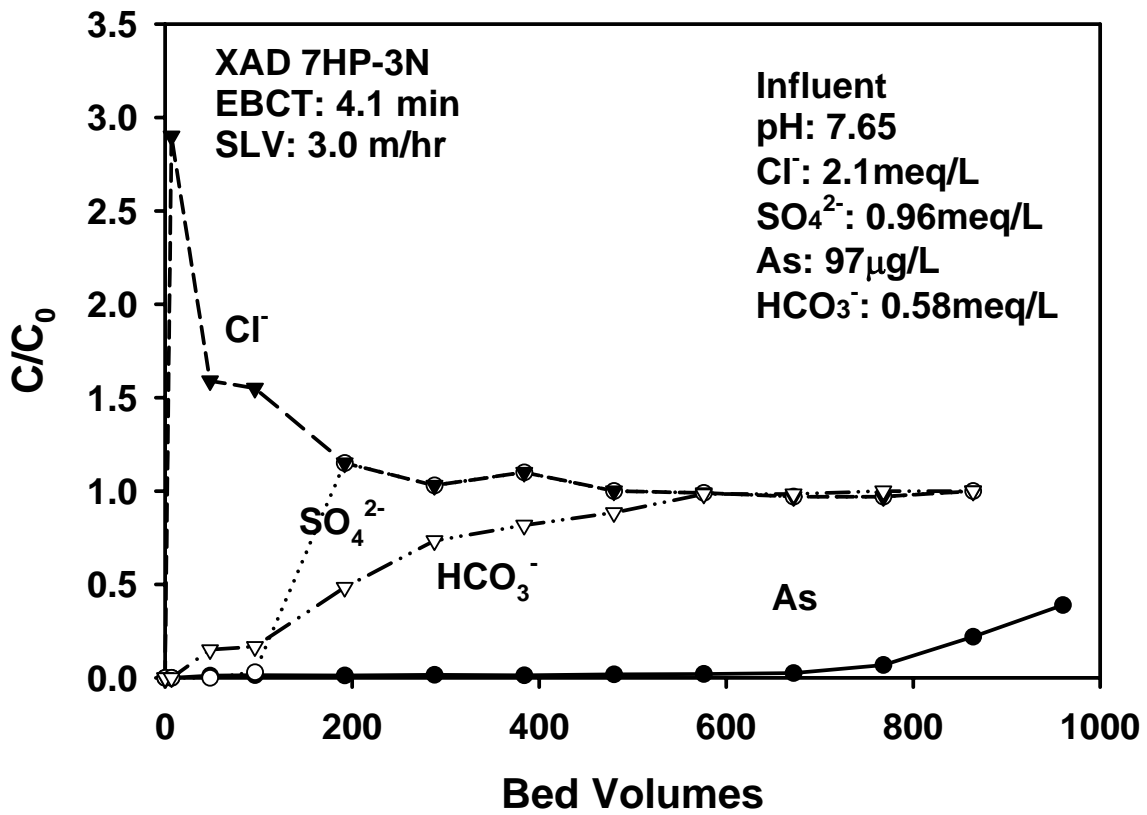


Figure 4.13. Breakthrough histories of arsenate and competing anions in a multi-component system using a polymeric ligand exchange, XAD7HP-3N-Cu.

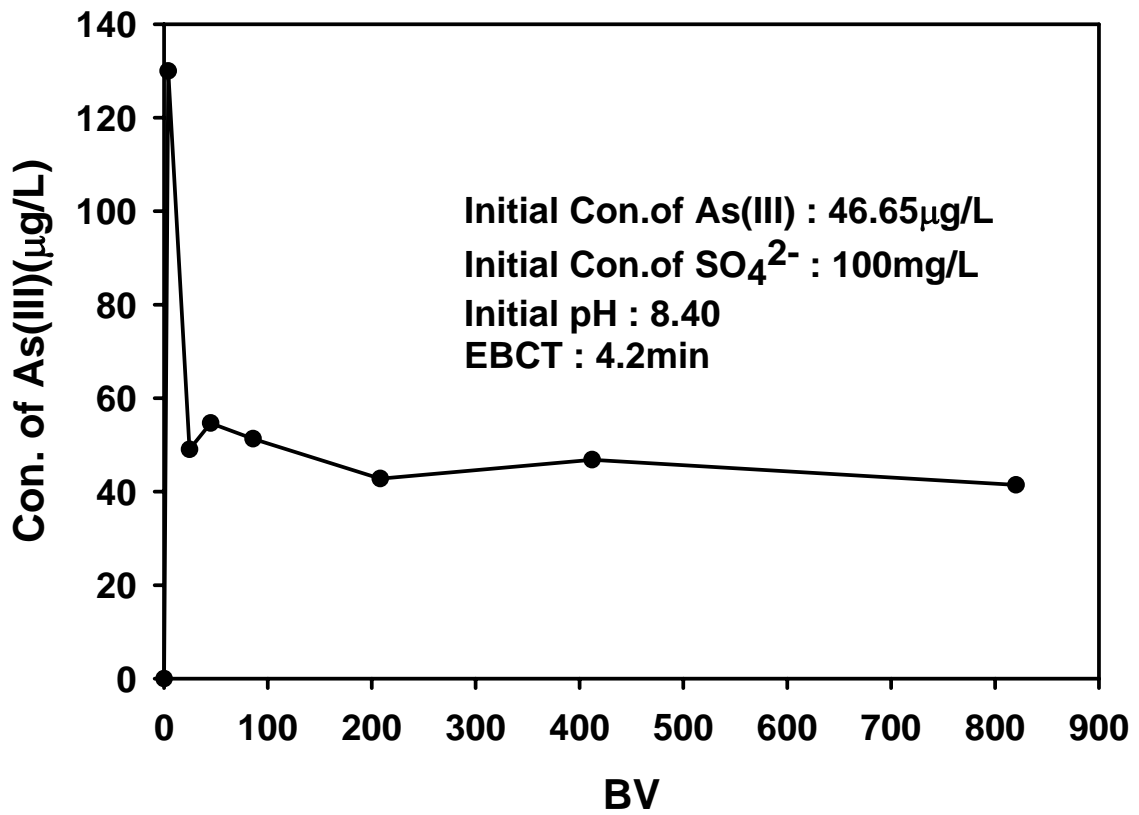


Figure 4.14. Breakthrough histories of arsenite in a multi-component system using a polymeric ligand exchange, DOW 3N-Cu.

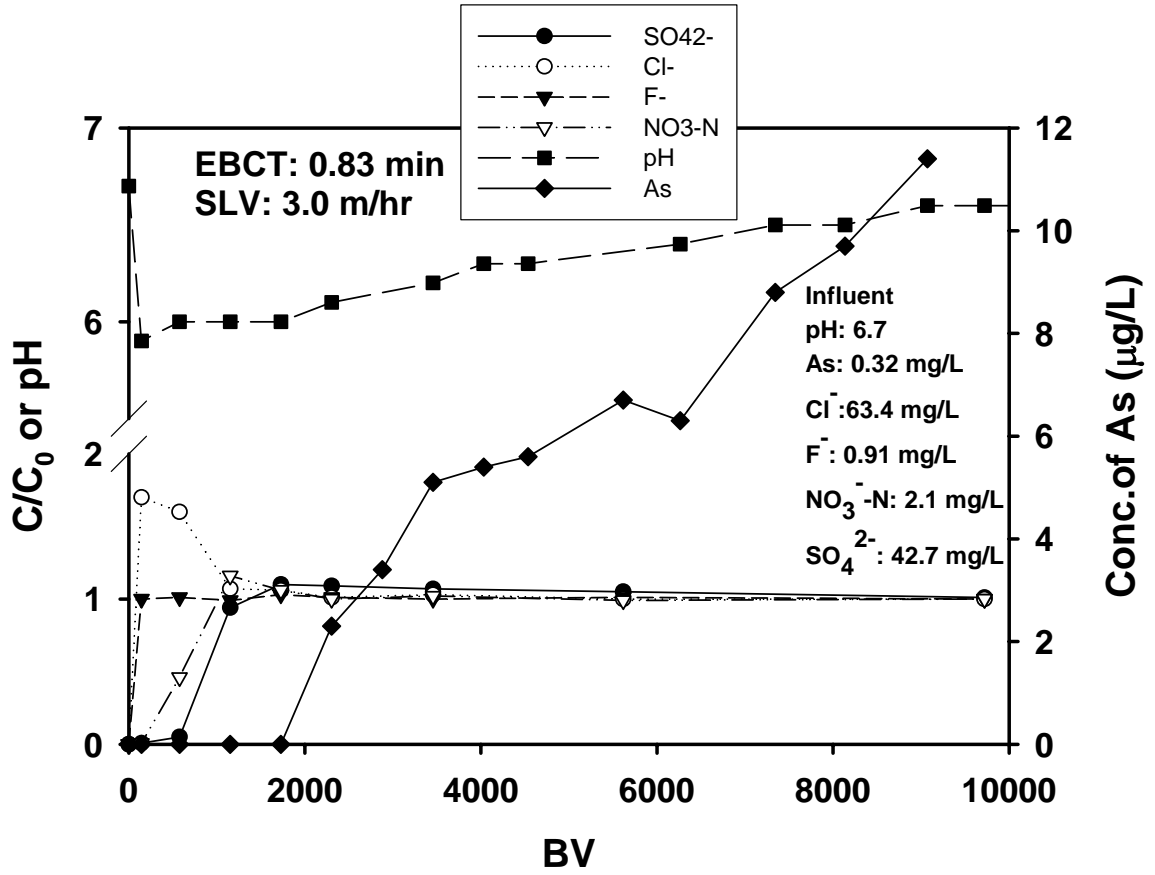


Figure 4.15. Breakthrough histories of arsenate in a multi-component system using a polymeric ligand exchange, XUS 3N-Cu at pH 6.7.

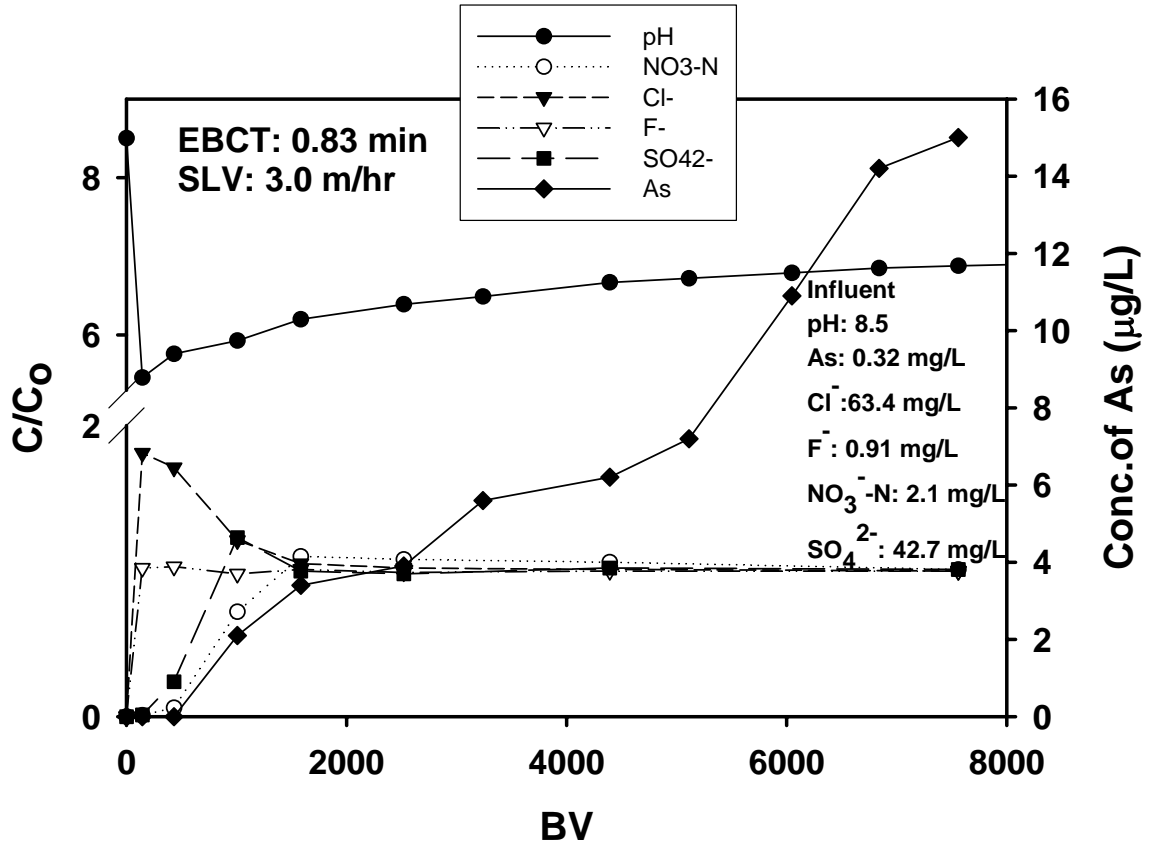


Figure 4.16. Breakthrough histories of arsenate in a multi-component system using a polymeric ligand exchange, XUS 3N-Cu at pH 8.5.

4.3 Effect OF pH

As in any ion exchange process, the PLE's selectivity for various competing ligands can be strongly impacted by solution pH. Solution pH can affect the PLE's arsenic uptake in two different ways. First, solution pH governs the speciation of arsenate, resulting in arsenate species (H_3AsO_4 , H_2AsO_4^- , HAsO_4^{2-} , and AsO_4^{3-}) of different ionic charges and ligand strength. Second, the hydroxyl anions become aggressively formidable competitors for the ligand exchange sites as solution pH goes up.

Figure 4.17 shows the observed arsenate uptake data as a function of the equilibrium solution pH. Note that sulfate at an initial concentration of 86 mg/L was present for all points tested. Also superimposed in Figure 4.17 is the speciation curve of the HAsO_4^{2-} species as a function of solution pH based on the reported pK_a values. Figure 4.17 indicates that the optimal arsenate uptake occurs in the pH range of ~ 6.0 – ~ 8.0 , with the peak uptake being at pH ~ 7.0 . At pH < 4.0 or pH > 11 , there was virtually no uptake of arsenate observed. It is also interesting that As uptake started increasing at pH ~ 4.0 almost in proportion to the increasing formation of the bidentate hydrogen arsenate species (HAsO_4^{2-}). However, the As uptake drops sharply as pH exceeds ~ 8.0 .

The acid dissociation constants (pK_a) for arsenate are $\text{pK}_{a1} = 2.2$, $\text{pK}_{a2} = 6.9$, and $\text{pK}_{a3} = 12$ (Dean, 1979). Based on both ligand strength and ionic charge, the adsorbability of various arsenate species follows the sequence of $\text{H}_3\text{AsO}_4 < \text{H}_2\text{AsO}_4^- < \text{HAsO}_4^{2-} < \text{AsO}_4^{3-}$. At pH < 4.0 , the much less adsorbable H_2AsO_4^- or H_3AsO_4 is the predominant arsenate species, which cannot stand the competition of divalently charged sulfate anions. As a result, no As uptake is likely in the low pH range, as observed in Figure 4.17. The fact that the As uptake appears to be in proportion to the formation of HAsO_4^{2-} in the pH

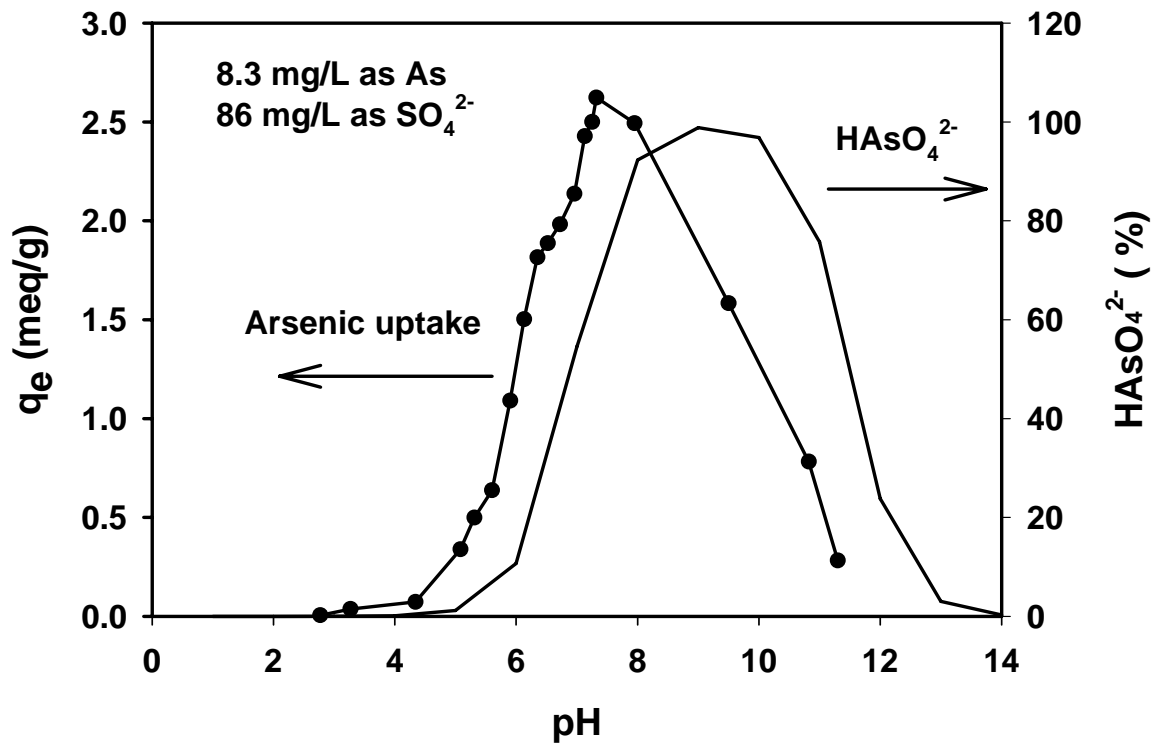


Figure 4.17. Arsenate uptake by DOW 3N-Cu as a function of solution pH.

range of 4.0-7.0 agrees with the notion that to overcome the competition from sulfate, arsenate must be converted to the more adsorbable HAsO_4^{2-} species. However, comparing the As uptake and HAsO_4^{2-} speciation curves, it appears counter-intuitive in the sense that formation of HAsO_4^{2-} and its uptake did not really take place concomitantly; i.e., there appears to be a pH shift (~ 1 pH unit) between the uptake curve and the HAsO_4^{2-} formation curve.

The observed pH shift reveals that the pH at the ligand exchange sites is actually higher than that in the bulk solution phase. This is in accord with the Donnan co-ion exclusion principle (Kunin and Meyers, 1950). The immobilized Cu^{2+} ions in DOW 3N-Cu tend to attract counter-ions including OH^- to the close vicinity of the resin surface, and simultaneously exclude co-ions including H^+ away from the surface. As a result, an excess of OH^- at the resin-solution interface is built up, which promotes the conversion of the H_2AsO_4^- from the bulk solution to HAsO_4^{2-} at the resin surface. This interfacial pH shift was also observed by Zhao and SenGupta (2000) in their study on phosphate uptake by DOW 3N-Cu. At pH above 8.0, although the more adsorbable HAsO_4^{2-} ions are the predominant species, the competition from OH^- ions becomes increasingly fierce, resulting in the increasing reduction in As uptake as pH goes up. From a practical view point, the optimal pH range of 6.0-8.0 is quite novel. Since the pH value for most natural waters falls in this range (Sawyer, 1978), there is no need to adjust source water pH to achieve the PLE's maximal sorption capacity. Figure 4. 18 is for arsenite uptake as a function of pH. At pH 10, the arsenite uptake is the maximum. This is also due to speciation of arsenite. H_2AsO_3^- is predominant in this pH range.

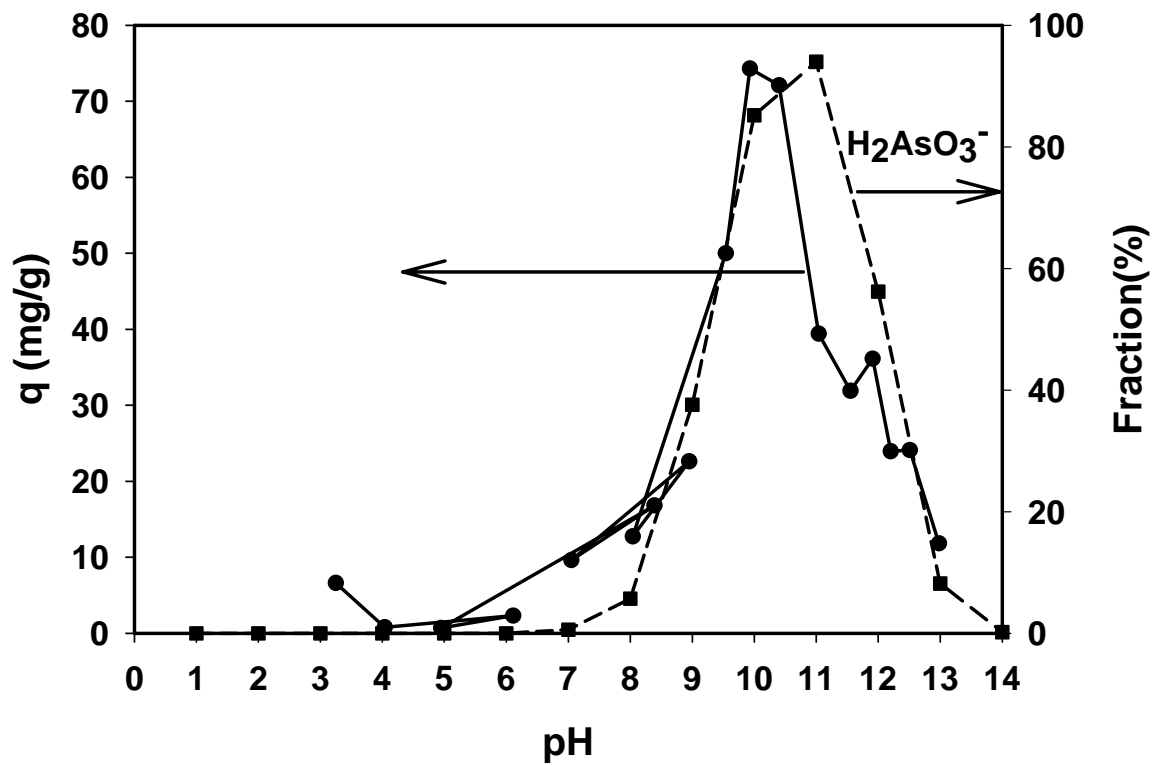


Figure 4.18. Arsenite uptake by DOW 3N-Cu as a function of solution pH.

4.4 KINETIC TEST

In a prior study on phosphate sorption, Zhao and SenGupta (2000) identified that intraparticle diffusion is the rate-limiting step during sorption of phosphate to DOW 3N-Cu. They also determined the effective intraparticle diffusivity for phosphate to be $1.0 \times 10^{-7} \text{ cm}^2/\text{s}$. Given the molecular analog between phosphate and arsenate, the intraparticle diffusivity is determined in a similar manner. Equations 4-8 through 4-11 present the changes in A_s concentration in solution during the transient sorption of A_s by various PLEs in a continuously stirred batch reactor.

For intraparticle-diffusion-controlled process, sorption rates are often modeled based on the Fick's second law. For spherical beads, the governing equation is given as (Crank, 1975; Zhao and SenGupta, 2001)

$$\frac{\partial q}{\partial t} = D \left(\frac{\partial^2 q}{\partial r^2} + \frac{2}{r} \frac{\partial q}{\partial r} \right) \quad (4-8)$$

where r is the radial coordinate and $q(t, r)$ is the solid-phase arsenic concentration at time t . Under the experimental conditions, the following initial and boundary conditions apply

$$q(0) = 0 \quad \text{at} \quad 0 \leq r \leq a \quad (4-9)$$

$$\frac{\partial q}{\partial r} = 0 \quad \text{at} \quad r = 0 \quad (4-10)$$

$$\left(\frac{\partial q}{\partial r} \right) (3D M / a) = -V \left(\frac{\partial C}{\partial t} \right) \quad \text{at} \quad r = a \quad (4-11)$$

where a is the mean radius of the resin beads, which was determined to be $\sim 0.22 \text{ mm}$, M is the mass of the resin added, and V is the solution volume, which is considered constant during the course of the experiment.

The above experimental system conforms to the scenario where diffusion takes place in a well-stirred solution of limited volume (Crank, 1975). The solution given by Crank (1975) as the fractional attainment of equilibrium (F),

$$F = \frac{q(t)}{q_{\infty}} = 1 - \sum_{n=1}^{\infty} \frac{6\alpha(\alpha+1) \exp(-Dq_n^2 t / a^2)}{9 + 9\alpha + q_n^2 \alpha^2} \quad (4-12)$$

where q_{∞} is the arsenate uptake by DOW 3N-Cu at infinite time (i.e. at equilibrium), the parameter α is expressed in terms of the final fractional uptake of arsenate as

$$\frac{Mq_{\infty}}{V_o C_o} = \frac{1}{1 + \alpha} \quad (4-13)$$

where V_o and C_o are initial solution volume and initial arsenate concentration in solution, respectively. The q_n 's are the non-zero roots of

$$\tan q_n = \frac{3q_n}{3 + \alpha q_n^2} \quad (4-14)$$

The form of eqn (4-13) is convenient in bracketing the roots in well-defined intervals as determined by the tan function, which allows for simple root finding using the method of bisection.

The aqueous phase concentration at time t , $C(t)$, was determined using the following mass-balance equation:

$$Mq(t) = V [C_o - C(t)] \quad (4-15)$$

The best fit of the model to the experimental kinetic data in Figure 4.19 and 4.20 was achieved by adjusting the diffusivity value (D) until the sum of the squared error is minimized, which yields a diffusivity value of $1.0 \times 10^{-7} \text{ cm}^2/\text{s}$ for DOW 3N-Cu, $2.0 \times 10^{-6} \text{ cm}^2/\text{s}$ for XAD1180-3N-Cu, $3.0 \times 10^{-6} \text{ cm}^2/\text{s}$ for XAD16-3N-Cu, and $3.0 \times 10^{-6} \text{ cm}^2/\text{s}$ for XAD7HP-3N-Cu. Based on these numbers, the sorption rate of DOW 3N-Cu is quite comparable to that of standard macroporous ion exchange resins, while the XAD-based PLEs demonstrated a more than one order of magnitude faster kinetics. This observation suggests that the arsenate sorption sites of the XAD-based PLEs are much more easily

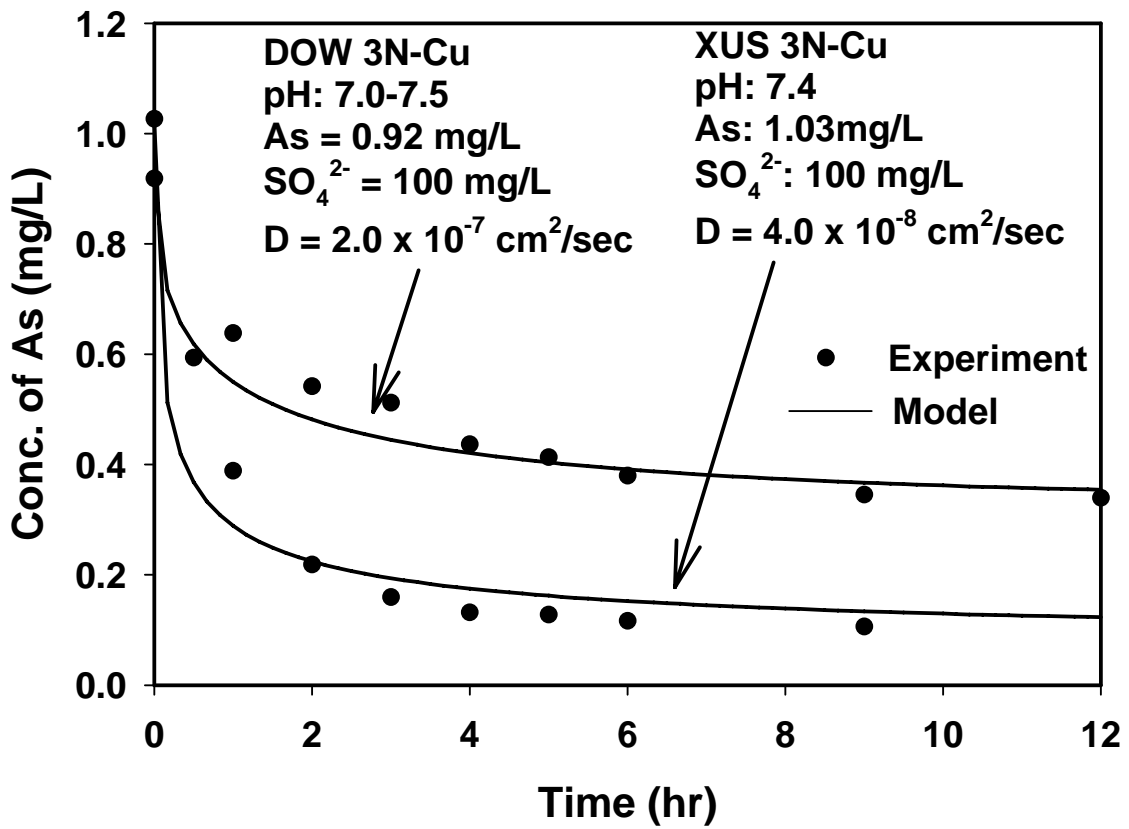


Figure 4.19. Experimental and model-simulated arsenate sorption kinetics of DOW 3N-Cu. (symbols: observed data; line: model simulation)

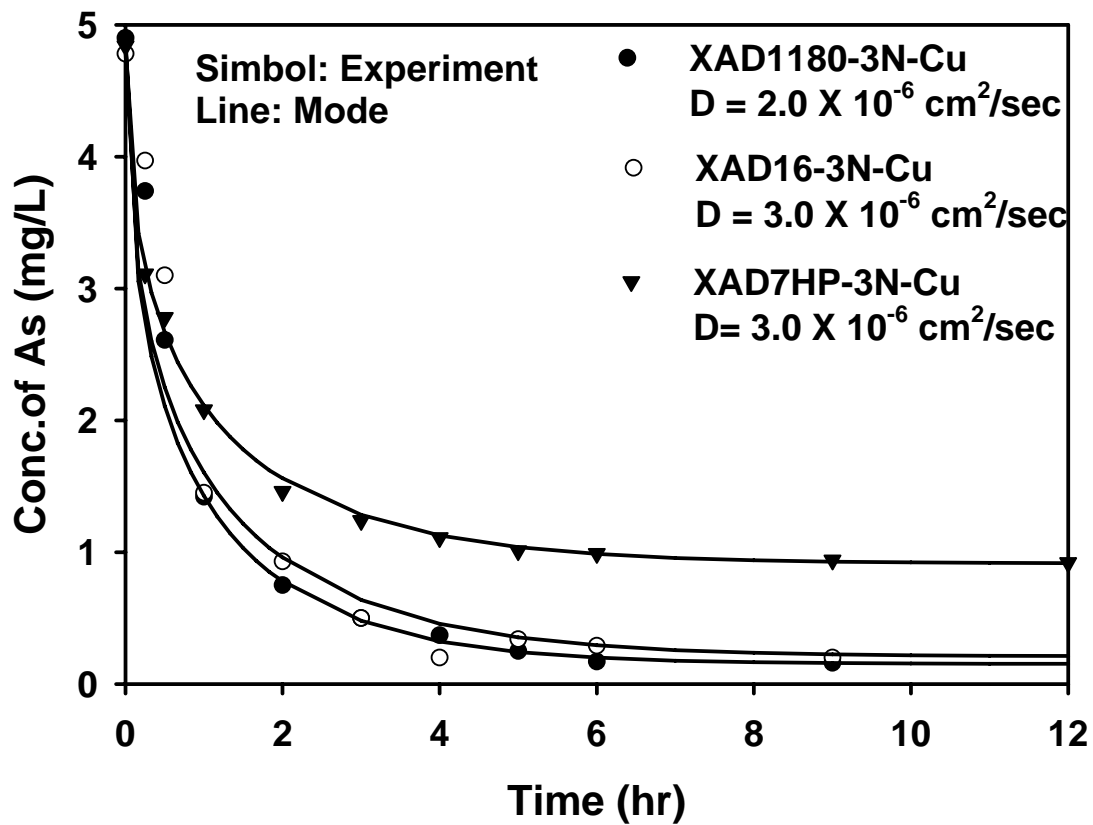


Figure 4.20. Experimental and model-simulated arsenate sorption kinetics of XAD16-3N-Cu (symbols: observed data; line: model simulation)

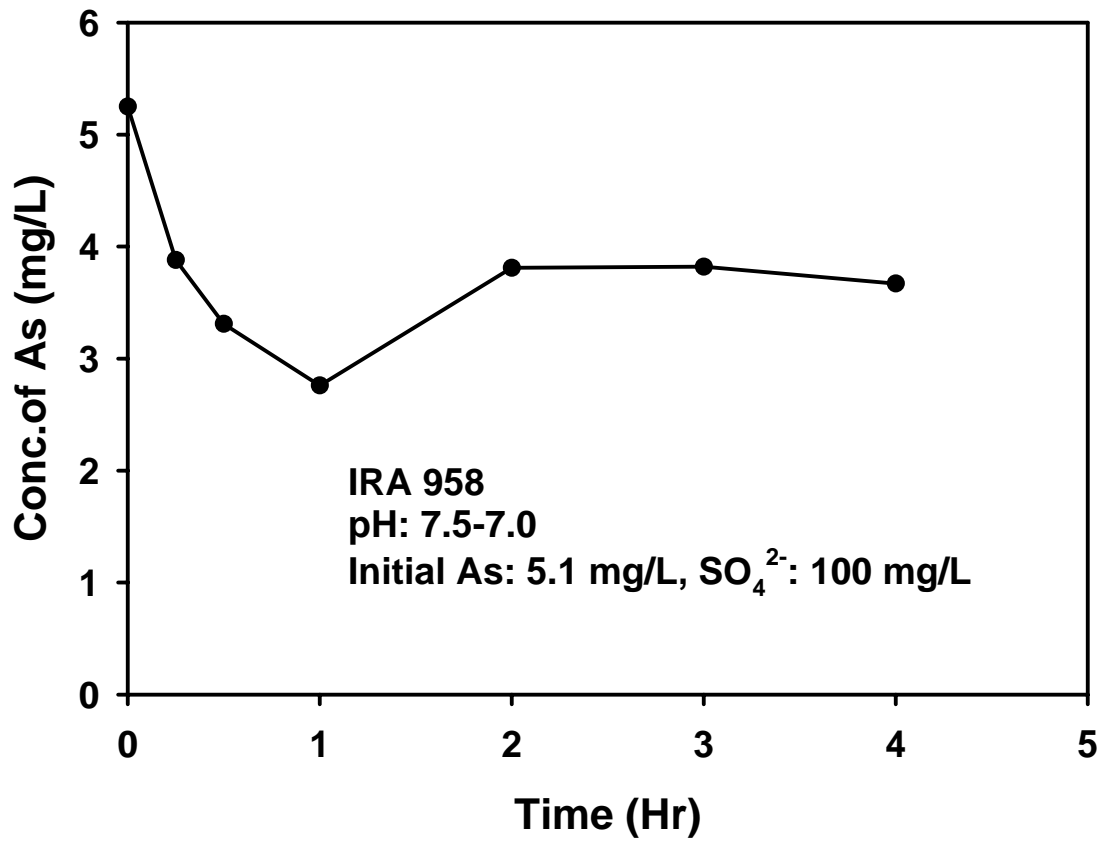


Figure 4.21. Experimental arsenate sorption kinetics of the commercial ion exchange, IRA 958.

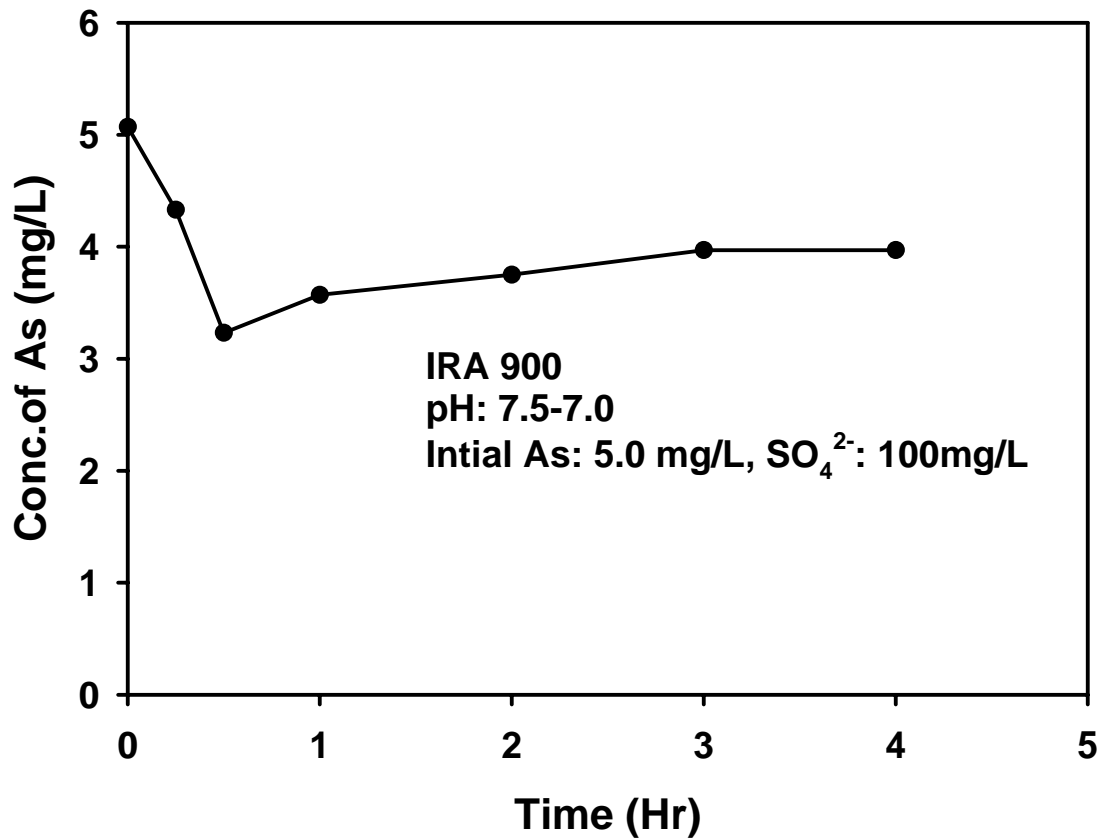


Figure 4.22. Experimental arsenate sorption kinetics of the commercial ion exchange, IRA 900.

accessible. This kinetic advantage adds value to the XAD-based PLEs. For example, these relatively low-capacity PLEs may be more resistant to organic fouling, and thus, may perform better for treating water that contains high strength of dissolved organic matter.

Additional tests were carried out to determine the kinetic of arsenic for currently commercial ion exchange, IRA 958 and IRA 900. The experiment physical and chemical conditions are the same to the kinetic test of XAD resin. Figure 4.21 and Figure 4.22 show the arsenic sorption for IRA 958 and IRA 900, respectively. The arsenic concentration was diminished to 2.7 mg/L at 1hr and increased to 4 mg/L. After 2 hours, for both ion exchangers, the concentration of arsenic is constant to be about 4 mg/L. Based on column test for IX which showed that arsenic breakthrough is earlier than that of sulfate and arsenic chromatography occurred, selectivity of sulfate is higher than that of arsenic. In spite of these reasons, in the beginning time, what arsenic concentration decreased can be explained by arsenic sorption kinetic which is much faster than that of sulfate.

4.5 REGENERATION AND REUSE OF PLES

From the standpoints of both cost-effectiveness and environmental friendliness, it is highly desirable that an ion exchange resin be amenable to efficient regeneration using the cheapest possible regenerant. Furthermore, it is even more beneficial if the spent regenerant can be recycled and reused. Multiple reuses of regenerant brine can further reduce brine needs and cut down the volume of process waste residuals. Minimizing process waste residuals is currently gaining increasing attention in the U.S. due to the much tightened regulations on waste discharge.

For the regeneration of arsenate-saturated DOW 3N-Cu, three kinds of XAD and IRA 900 were tested in the same fixed-bed configuration. Figure 4.23 compares arsenate elution profile and recovery during regeneration using 4% (w/w) NaCl at pH 4.1, 7.0, and 9.1, respectively. As expected from the results on pH effect (Figure 4.17), greater regeneration efficiency was observed at either acidic or alkaline pH than at neutral pH. At pH 9.1, more than 96% of sorbed arsenate was recovered within 22 bed volumes of the regenerant. For comparison, regeneration of *As*-saturated IRA 900 was also tested using 4% NaCl at pH 9.2, and the results showed that under the same conditions, it took ~15 BVs of the regenerant to achieve 95% arsenate recovery.

Figure 4.24 shows that the regeneration efficiency for XAD1180-3N-Cu was only 49% using 4% NaCl at pH 9.0; however, over 90% arsenate capacity was recovered using the concentration of NaCl raised to 6% and pH to 10. Figure 4.25 indicates that, using 4% NaCl at pH 9.0, the regeneration efficiency for XAD16-3N-Cu was 82%, but increased regenerant (6% NaCl) achieved 92% regeneration efficiency. Figure 4.26 shows that for

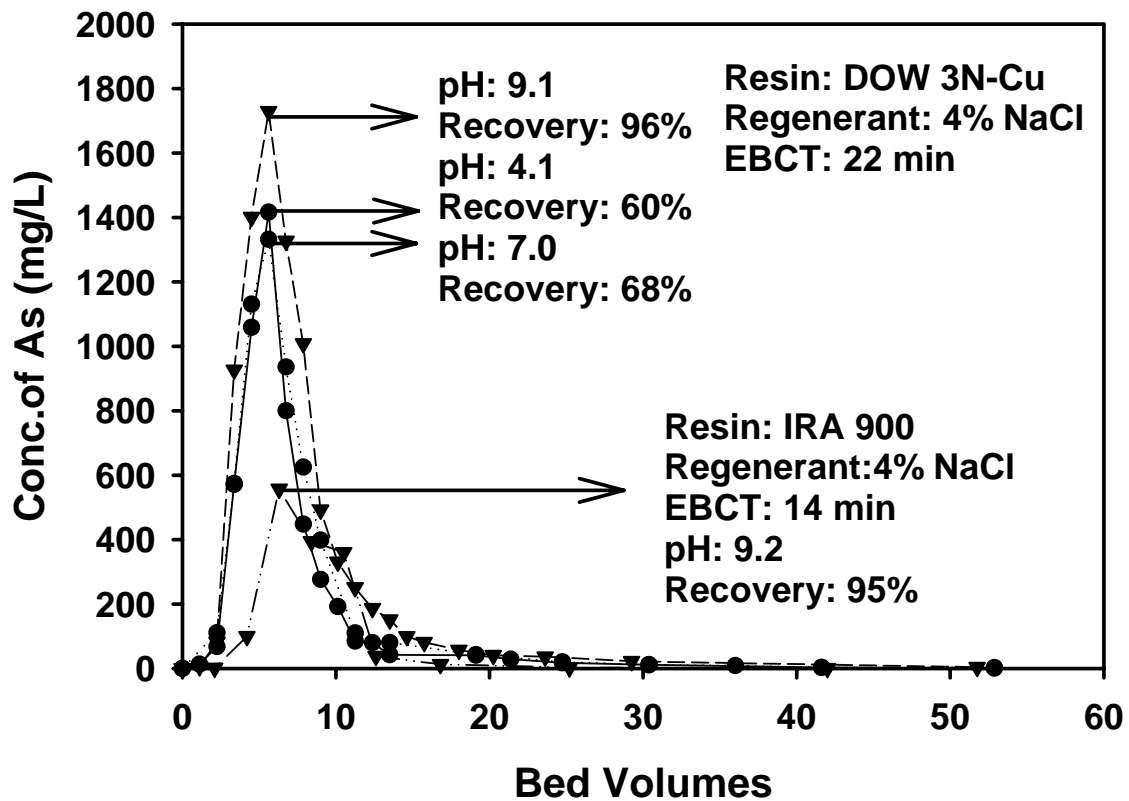


Figure 4.23. Arsenic elution profile during regeneration of saturated DOW 3N-Cu using 4% NaCl (w/w) at pH 4.1, 7.0, and 9.1, respectively, and of saturated IRA 900 using NaCl (w/w) at pH 9.2.

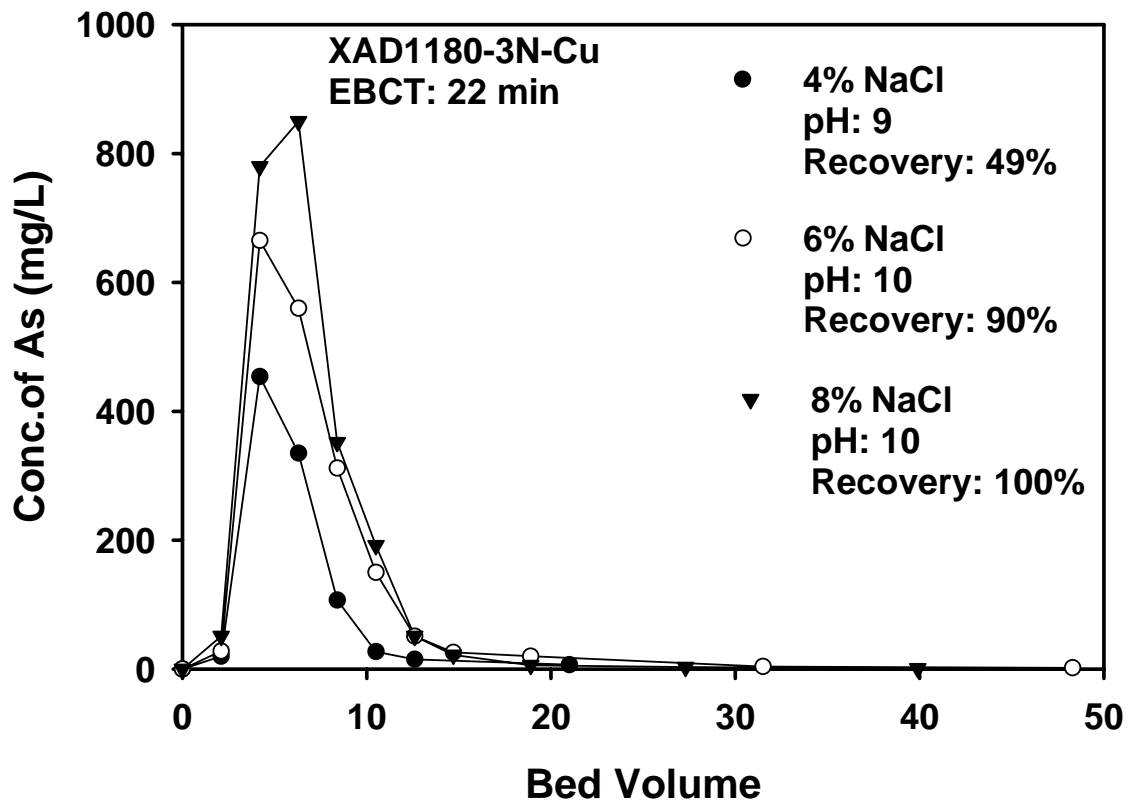


Figure 4.24. Arsenic elution profile during regeneration of saturated XAD1180 -3N-Cu using 4%, 6%, and 8% NaCl (w/w), respectively.

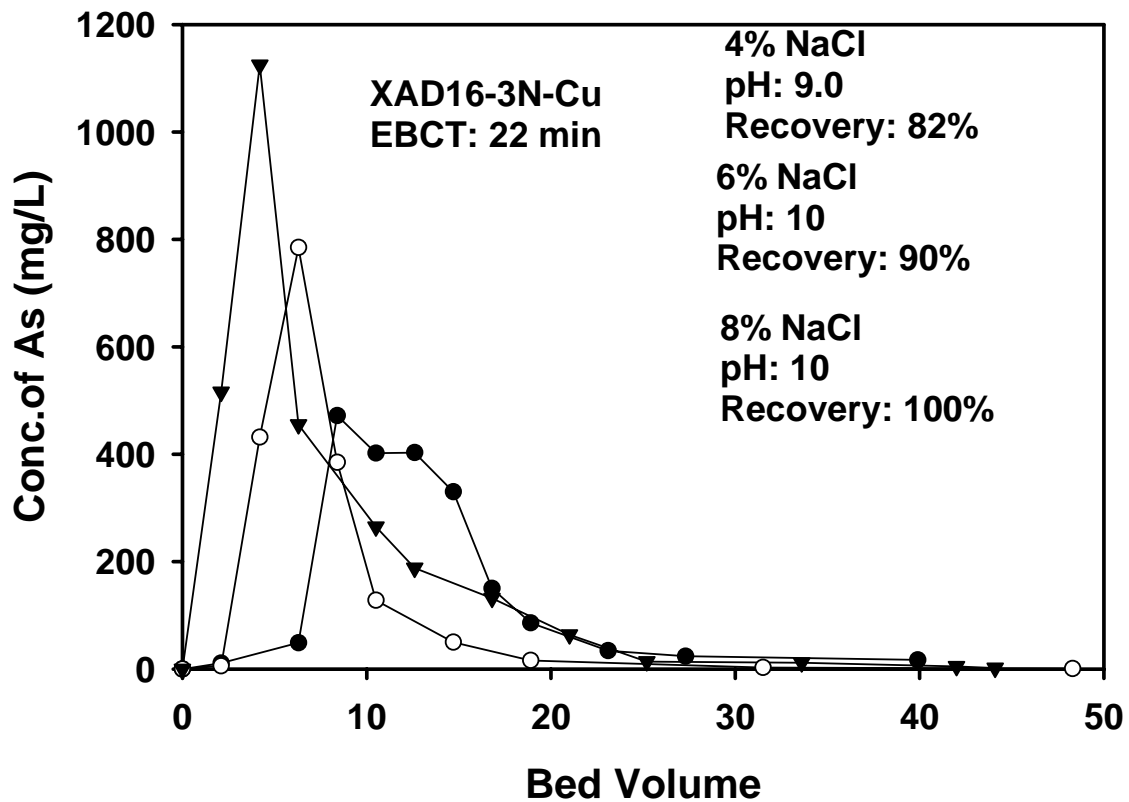


Figure 4.25. Arsenic elution profile during regeneration of saturated XAD16-3N-Cu using 4%, 6%, and 8% NaCl (w/w), respectively.

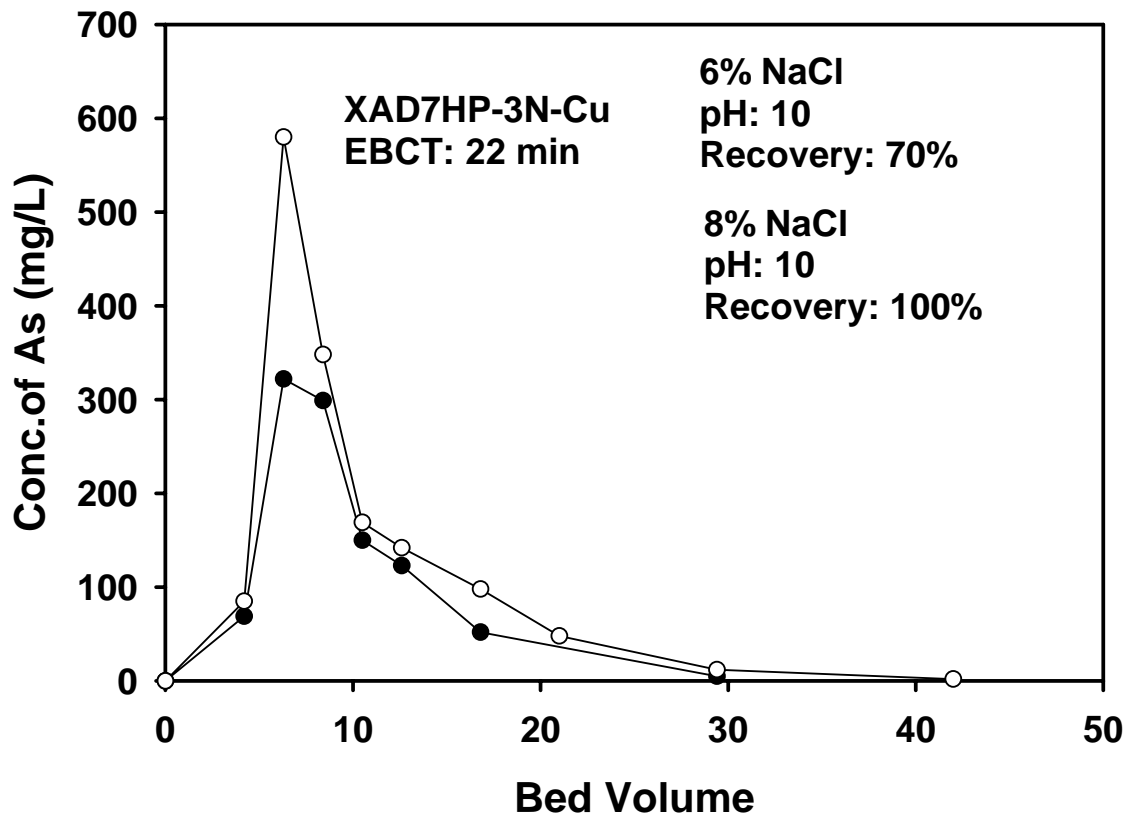


Figure 4.26. Arsenic elution profile during regeneration of saturated XAD7HP-3N-Cu using, 6%, and 8% NaCl (w/w), respectively.

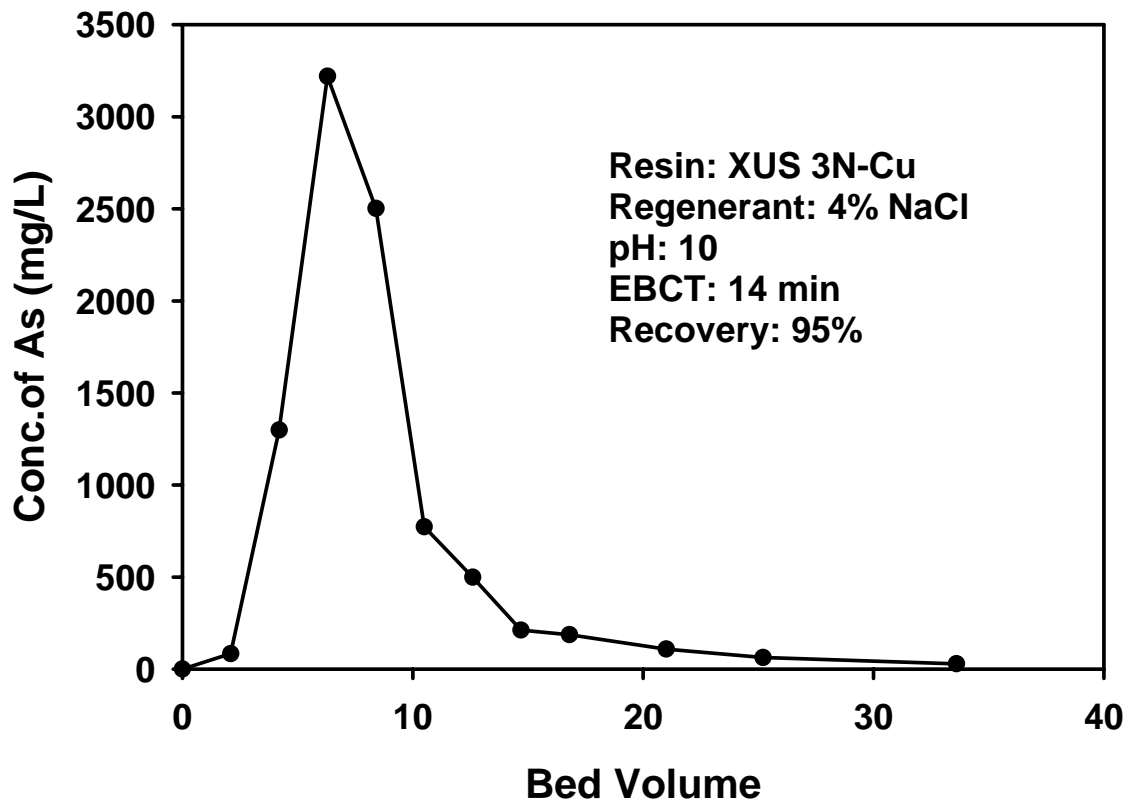
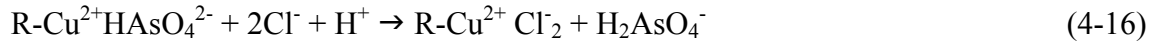


Figure 4. 27. Arsenic elution profile during regeneration of saturated XUS 3N-Cu using 4% NaCl (w/w) at pH 10, respectively.

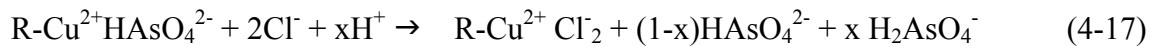
the hydrophilic PLE, XAD7HP-3N-Cu, a higher NaCl concentration (8%) is required to achieve 100% regeneration of the resin. Figure 4.27 is regeneration for the XUS 3N-Cu.

Equations (4-16) through (4-18) illustrate the regeneration reaction stoichiometry at the specified pH:

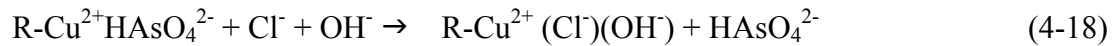
At pH ~4.1



At pH ~7.0



At pH >9.1



Evidently, the participation of OH^- in the ligand exchange reaction at alkaline pH greatly enhances the regeneration efficiency.

To find out the efficiency of reuse of spent regenerant in multiple cycles, the experiments were conducted for DOW 3N-Cu by using different regenerants. In this test, the pH of used regenerant is dropped due to adsorbed OH^- into adsorbent. Thus, spent regenerant is needed to be adjusted to about 10.0 pH. However, there was no treatment for spent regenerant to reuse, e.g., adding more NaCl, or removing containments from spent regenerant. Figure 4.28 shows the recovery of arsenic each time of regenerants used 4% and 10% NaCl. For both fresh regenerants, as mentioned, the recovery of arsenic is over 95%, but in the case of 4% NaCl, the 2nd, 3rd, and 4th time the recovery is 34%, 40%, 0%, respectively. Thus it is impossible to reuse 4% NaCl in regeneration to recover the arsenic. However, when using 10% NaCl, over 90% of arsenic recovery can keep until the 4th run and at the 5th run the recovery is dropped to 50%. Figure 4.29 is the recovery

of arsenic for XUS 3N-Cu using 8% NaCl. By 3 times reuse, the recovery is up to 96 % but at fourth time, the recovery is sharply dropped to ~30%.

For practical viability, the PLE should be amenable to multiple cycles of operation without significant capacity drop. Figure 4.30 and Figure 4.31 compare the equilibrium arsenic sorption capacity of virgin DOW 3N-Cu and XUS 3N-Cu and when it was subjected to up to 8 consecutive operating cycles (a cycle = a saturation run + a regeneration run). The regenerated DOW 3N-Cu and XUS 3N-Cu did not show any significant capacity drop compared to its fresh form. The fact that the arsenic capacity of the PLE was essentially unchanged over multiple cycles indicated that the copper leakage was minimal during both saturation and regeneration runs. Indeed, direct measurement of copper eluted showed that the copper leakage per operation cycle (saturation and regeneration) was less than 0.01% of total copper loaded.

The spent regenerant was repeatedly used for regeneration for seven times with only pH adjustment (pH 9.2-10.0), and more than 95% of recovery was consistently observed. After the regenerant was used for eight times, the recovery was dropped to less than 50%. Earlier, Clifford et al. (2003) reported that spent brine can be reused for three times without chloride makeup for efficient regeneration of a commercial SBA resin.

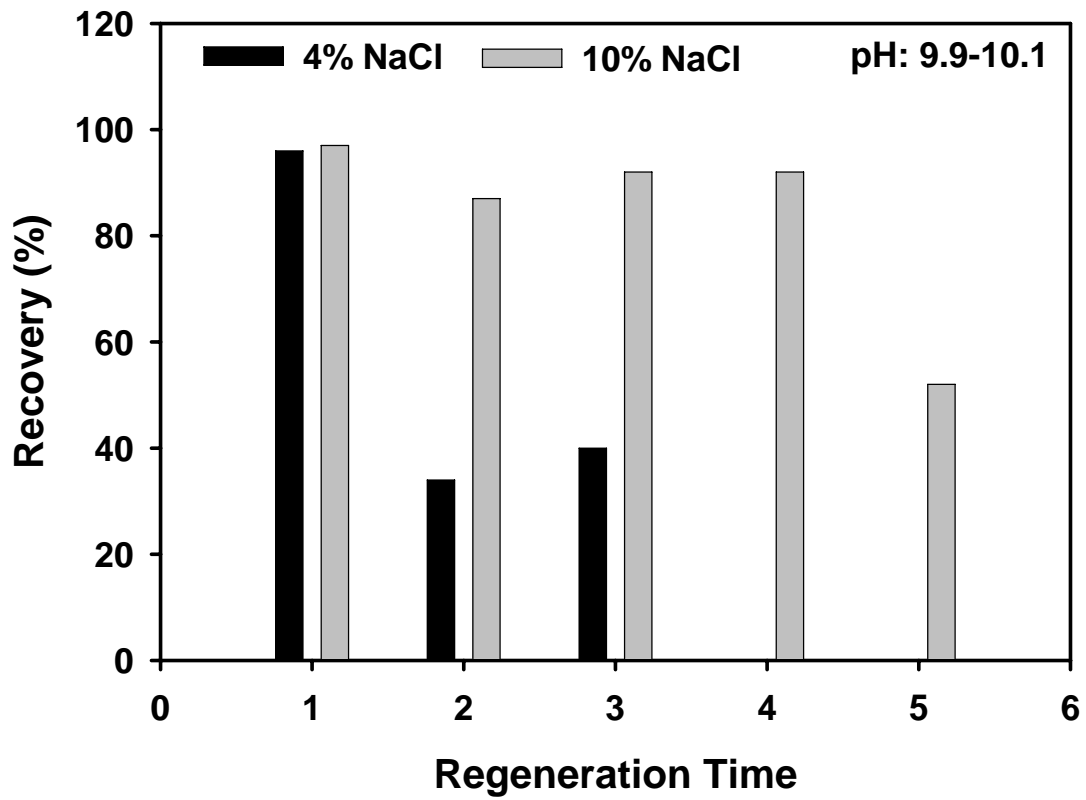


Figure 4.28. Reuse of brine for multiple regeneration cycles for DOW 3N-Cu.

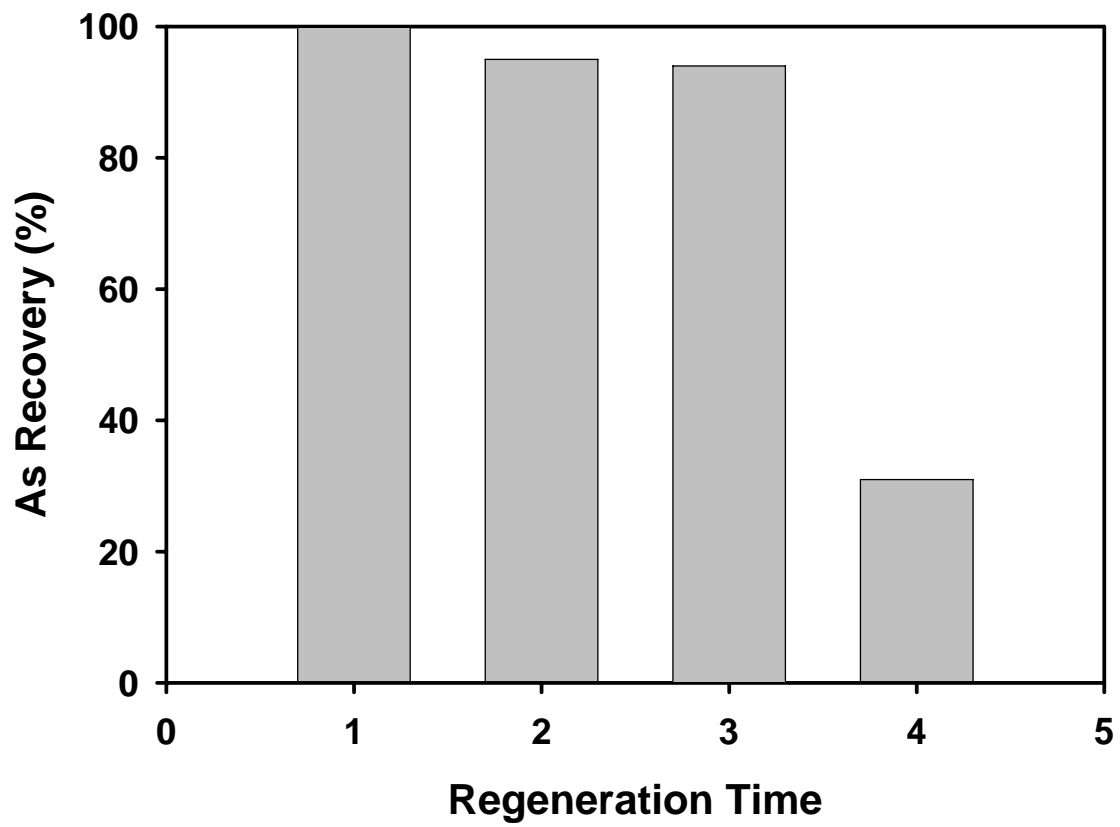


Figure 4.29. Reuse of brine for multiple regeneration cycles for XUS 3N-Cu.

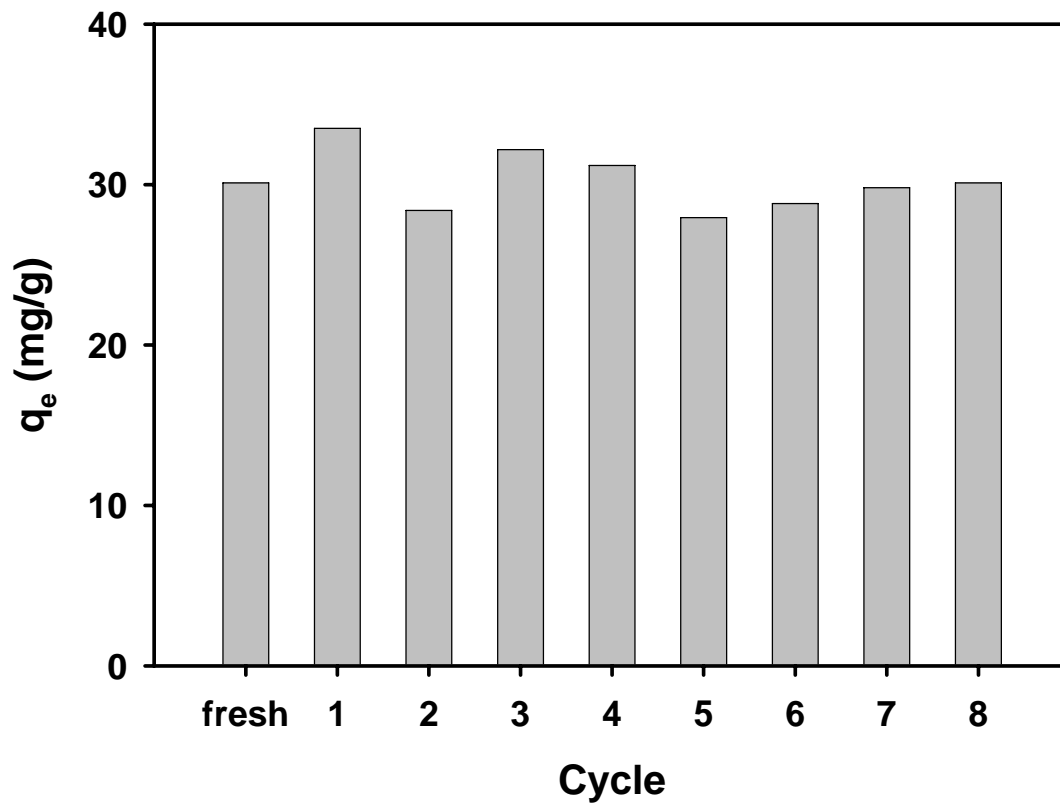


Figure 4.30. Comparing the equilibrium arsenate sorption (q_e) of fresh and regenerated DOW 3N-Cu under otherwise identical conditions. (Note: a. one cycle consists of one saturation run and subsequent regeneration run; b. each point represents mean of duplicates, the maximum standard deviation was 1.60).

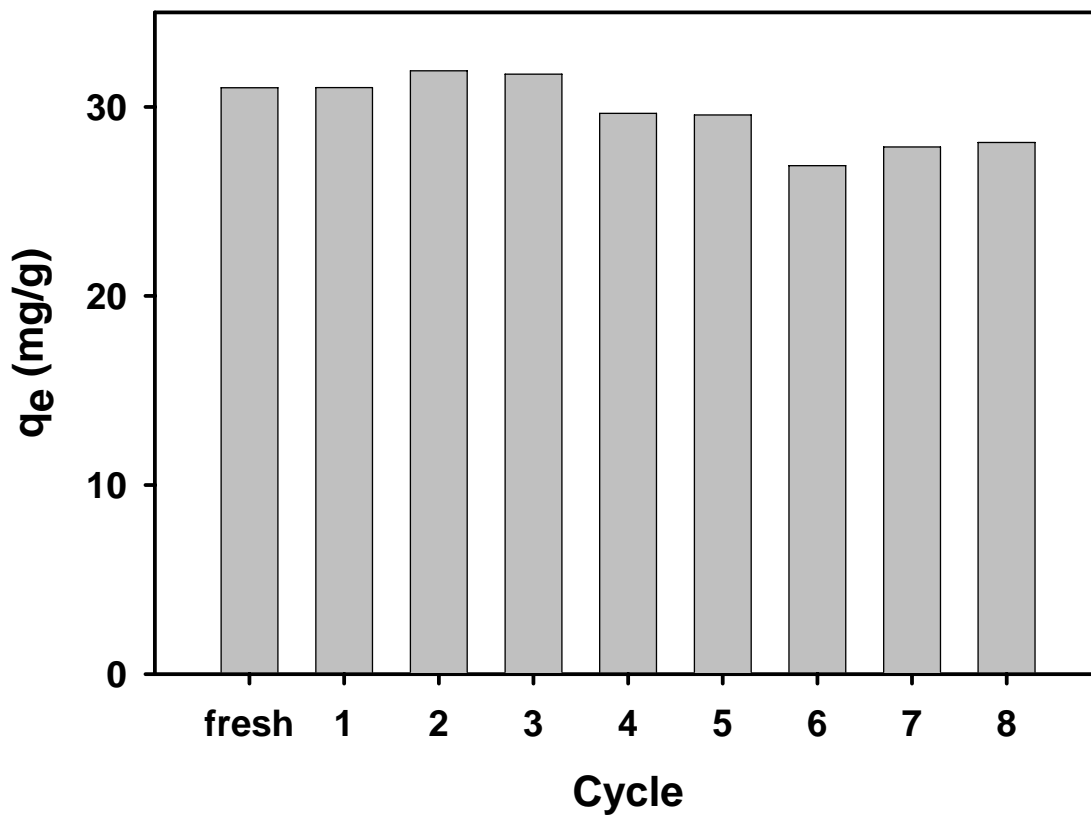


Figure 4.31. Comparing the equilibrium arsenate sorption (q_e) of fresh and regenerated XUS 3N-Cu under otherwise identical conditions. (Note: a. one cycle consists of one saturation run and subsequent regeneration run; b. each point represents mean of duplicates, the maximum standard deviation was 1.60).

4.6 ARSENIC REMOVAL FROM SPENT BRINE

In order to determine the optimal condition at various dosages of AlCl_3 , Batch test were treated at Al/As molar ratio of 2.5, 5, 10, and 20, respectively. During the experiment, the pH of solution was kept constant at 6 using 1N NaOH or 1N HCl. Figure 4.32 shows arsenic removal (% mass removed) at different Al additions. Each batch test sample's initial As concentration is 300 mg/L, and other anion concentration is extremely high. At an Al/As molar ratio of 2.5, the arsenic removal percentage is 98.2%. By increasing Al/As molar ratio to 5 or higher, almost 100% of arsenic is removed from the spent brine despite the presence of high concentrations of salts in the brine.

Another significant effect, pH, on arsenic removal, was determined with batch using a fixed Al/As molar ratio of 5 and 10 in the pH range of 4 – 11. Figure 4.33 shows the percentage arsenic removal as a function of the treatment pH. Between pH 5 and 8, nearly 100% arsenic removal was observed for both cases. However, at pH 8, the arsenic removal percentage for both Al additions begins to be decreased with increasing pH. At a solution pH of ~ 11 , a removal efficiency of just 17 and 40% was observed for Al/As of 5 and 10 Al/As respectively. A sharp decrease in arsenic removal occurs between pH 4 and pH 5. At pH 5, $\sim 100\%$ removal can be achieved at both Al/As of 5 and 10, but if the pH is decreased to 4, only 17 and 60% As is removed. These results indicate an optimal pH range between 5 ~ 8. Over 98% removal can be achieved in this optimal range at both Al/As 5 and 10.

The observed optimal pH range in these experiments agrees with those determined by Hering et al. (1996). These authors reported that this optimal pH range is governed by the solubility of aluminum hydroxide. At alkaline pH ($\text{pH} > 8$), the principal

soluble species present at equilibrium is the monomeric anion Al(OH)_4^- , and the formation of negatively charged surface species becomes unfavorable for arsenate uptake (Dzombak, et al., 1990). At lower pH, the dominant soluble species at equilibrium are cationic monomers, such as Al^{3+} and Al(OH)^{2+} . However, when pH is below 5, the less absorbable H_2AsO_4^- becomes the predominant arsenate species, and competition from other co-ions (e.g. bicarbonate and sulfate) dramatically reduces the removal of arsenic from the brine. The effects of calcium addition on arsenic removal from the spent brine were investigated under the optimal conditions revealed in Figures 4.34. Calcium concentrations of 0, 50, 100, and 200 were added to the treatment process at pH 6 and an Al/As molar ratio of 10. Figure 4.34 shows that there is no appreciable effect of calcium addition on arsenic removal. In all cases including no calcium addition, the arsenic removal was approximately 99.9%. However, the effect of calcium may contribute to the leachability of arsenic, as revealed in a parallel study by our group where ferric iron was used to treat the spent brine (Zhao et al., 2005). When reused for regeneration of arsenic-laden PLEs, the treated brine showed equal regeneration efficiency as freshly prepared brine.

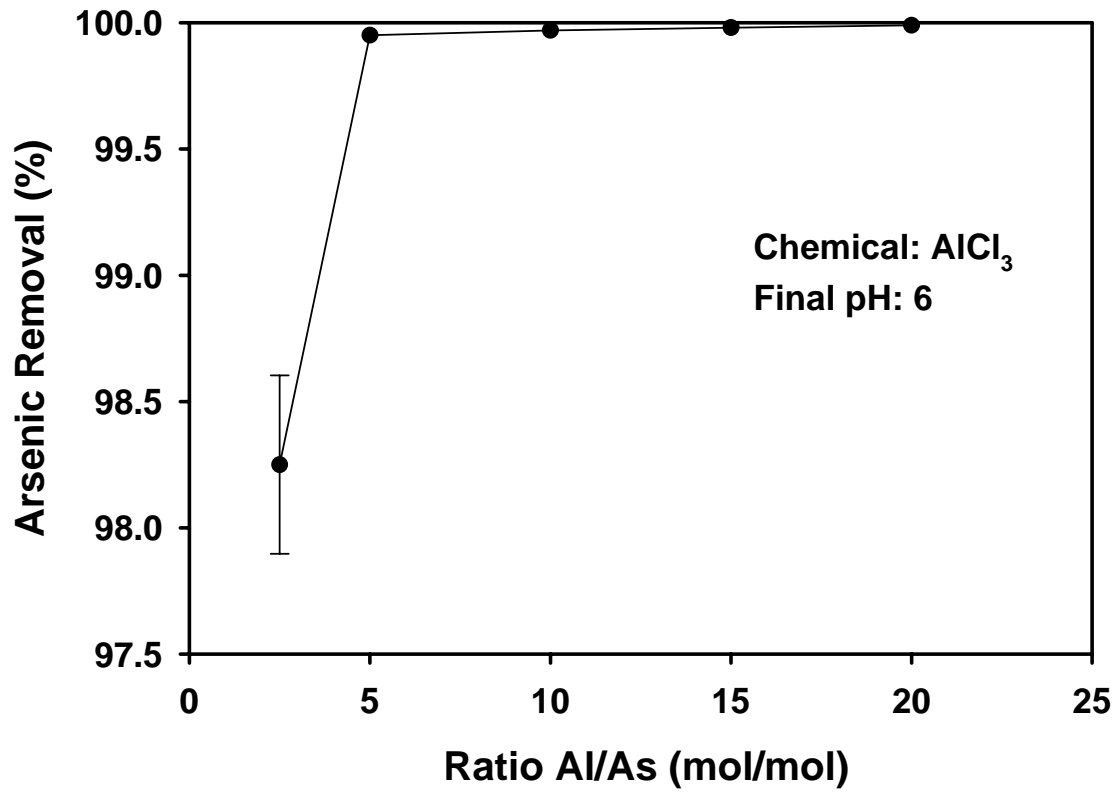


Figure 4.32. Percentage arsenic removed from a simulated regenerant brine as a function of the Al/As molar ratio.

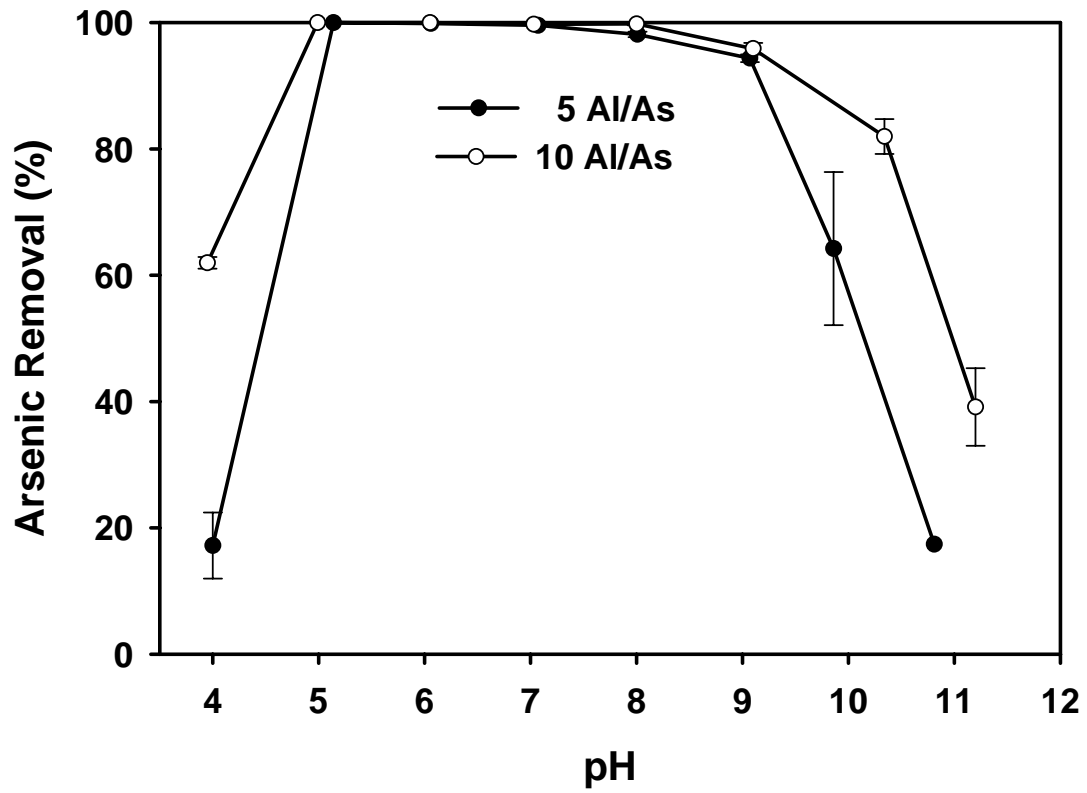


Figure 4.33. Percent of arsenic removed from a simulated regenerant brine as a function of the pH Al/As molar ratio of 5 and 10.

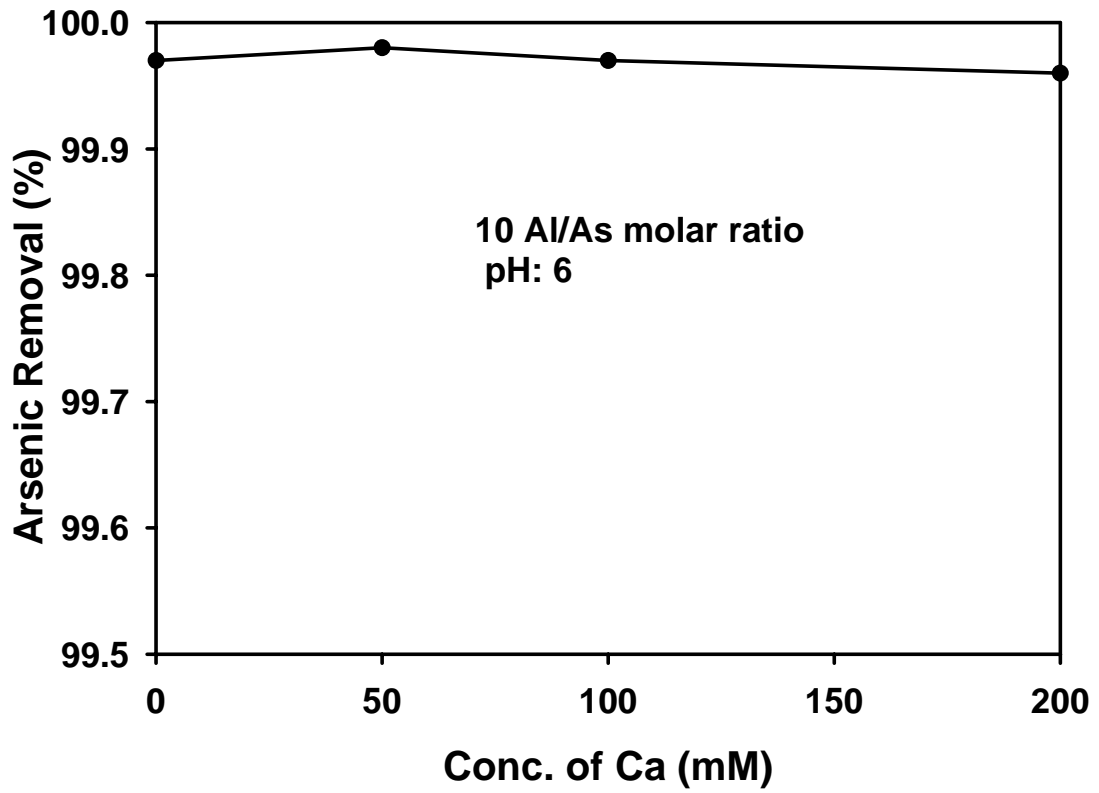


Figure 4.34. Percentage removal of As as a function of calcium dosage.

4.7 STABILIZATION OF ARSENIC-LADEN PROCESS WASTE SLUDGE

To determine arsenic leachability from solid sludge treated under different conditions, including Al/As molar ratio, pH, and aging time (wet and dry), TCLP, by the U.S.EPA, and WET, by California, were used in these experiments. Figure 4.35 presents the arsenic concentration in the extraction fluids for solid samples formed when the spent brine was treated at pH 6 and at an Al/As molar ratio of 5, 10, and 15, respectively. Both leaching tests confirmed that leachable As decreased dramatically with increased Al dosage. In all cases, the TCLP-leachable arsenic in the process waste residuals was well below the 5 mg/L threshold. However, when the WET method was applied to the same sludge, the extractable As concentration was greater than the limit even at an Al/As molar ratio of 15. Obviously, more elevated Al dosage is needed when the much more stringent WET criterion is required. Figures 4.36 and 4.37 show the effects of wet treatment temperature (5, 25, 35, and 50 °C) and wet aging time (2, 30, and 60 days) on arsenic leachability with WET and TCLP, respectively. These experiments were conducted with an Al/As ratio of 10 and pH 6. Figure 4.36 indicates that the effect of wet-aging (from 2 to 60 days) on the WET-extractable As appears insignificant at all temperatures although residuals aged for 60 days at room temperature (25° C) exhibited the lowest extracted As. However, when the wet aging time is extended to 150 days at 25 °C, the extracted arsenic concentration is dropped ~35% (Figure 4.37). O'Reilly et al. (2001), Zhang and Selim (2005) and Lin and Puls (2000), all confirm that As mobility decreases with aging time, suggesting that As anions must develop more stable complexes with the host particles over time. Figure 4.38 exhibits that the TCLP-extractable arsenic dropped, to various extents for different temperatures, with the wet aging time. The results indicate that wet

aging time has less effect on arsenic leaching, while temperature plays a more profound role in arsenic leachability. At 50 °C (the highest temperature in this experiment), the concentration of TCLP-extractable arsenic is at a minimum (Figure 4.38), suggesting that residuals treated and aged at higher temperatures will leach less As when TCLP is applied. However, for WET-extractable arsenic, Figure 4.36 shows that elevated temperatures (>25 °C) resulted in increased arsenic leachability. Extractable As concentration based on TCLP method is a function of treatment temperature and wet aging time. All samples were air-dried for 20 days before the extraction tests.

Many utilities employ heat treatment to their treatment residuals to reduce the waste volume before disposal. To test the effect of heat treatment of the process wastes on arsenic leachability, the sludge residuals were oven dried at 105° C and then subjected to the WET. A fixed Al/As molar ratio of 10 and 20 was employed in these tests. For comparison, a portion of the same residual was air-dried at room temperature (~21 °C) and subjected to the WET to compare As leaching in two different drying environments. Figure 4.39 indicates that at Al/As 20, the WET extractable arsenic concentration is about 50 mg/L for both oven-dried and air-dried residuals. Also, it is evident that at the higher Al addition the extractable arsenic remains nearly constant over the drying time up to 100 days. However, at an Al/As of 10, the concentration of arsenic leached from samples treated at 105 °C is >3.5 times greater than those at room temperature, agreeing with Figure 4.39 that increased temperature has a detrimental effect on the stability of the residuals tested by the WET method. The data at Al/As 10 and at 105 °C also indicate that the leachability reaches its maximum value when the samples are heated for more than 40 days. Apparently, heating the process waste residuals is not a viable practice.

Sorensen et al (2000) explained crystal transformations are occurring in the heated samples thus decreasing surface site densities for bonding and increasing the As extractable by the WET.

The reduced arsenic stability at elevated temperatures (either in wet brine treatment or dry sludge treatment) can be attributed to a number of factors. First, extended heating of the sludge may alter the sludge composition and mineral structure due to dehydration. Therefore, the arsenic affinity or adsorbability is reduced. Second, in general, arsenate sorption is an exothermic process, and high temperature treatment can cause desorption of sorbed ions. As mentioned before (Figure 4.33), the optimal pH range for As removal from brine is 5 – 8. To be practically viable, the optimum pH should optimize both arsenic removal efficiency and minimize arsenic leachability in the resultant sludge. Figure 4.40 shows the effects of brine treatment pH on the WET leachability of arsenic in the resultant sludge. The tests were conducted over a pH range of 5–10, and samples were dry-aged at room temperatures for either 20 days or 40 days before being subjected to the WET. Figure 4.40 indicates that lower treatment pH resulted in more stable solid waste. When the treatment pH was increased from 5 to 10, the arsenic WET leachability was increased by nearly 3 times for both cases. The results also indicate that prolonged dry aging (from 20 days to 40 days) resulted in a WET leachability increase of 50% (at pH 10) and 58% (at pH 5).

Based on the above results, we suggest that for utilities regulated by the WET method, the following conditions should be applied to achieve both optimum brine treatment and minimum arsenic leachability: 1) the Al/As molar ratio ≥ 15 ; pH = 5 – 6, and 2)

appropriate wet-aging at room temperature. Treatment of both brine and the sludge at elevated temperatures will increase the arsenic leachability considerably.

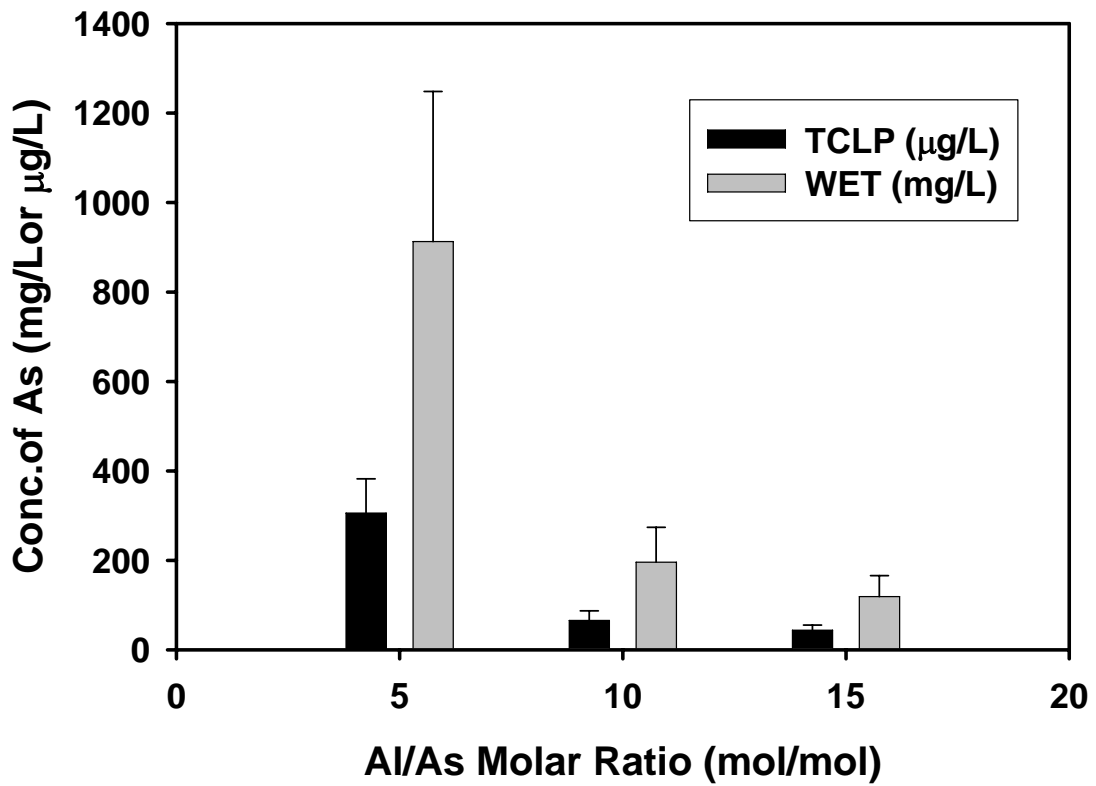


Figure 4.35. Extractable As concentration in TCLP or WET extraction fluid as a function of Al addition. (Note: arsenic is in µg/L in TCLP fluid, but in mg/L in WET fluid).

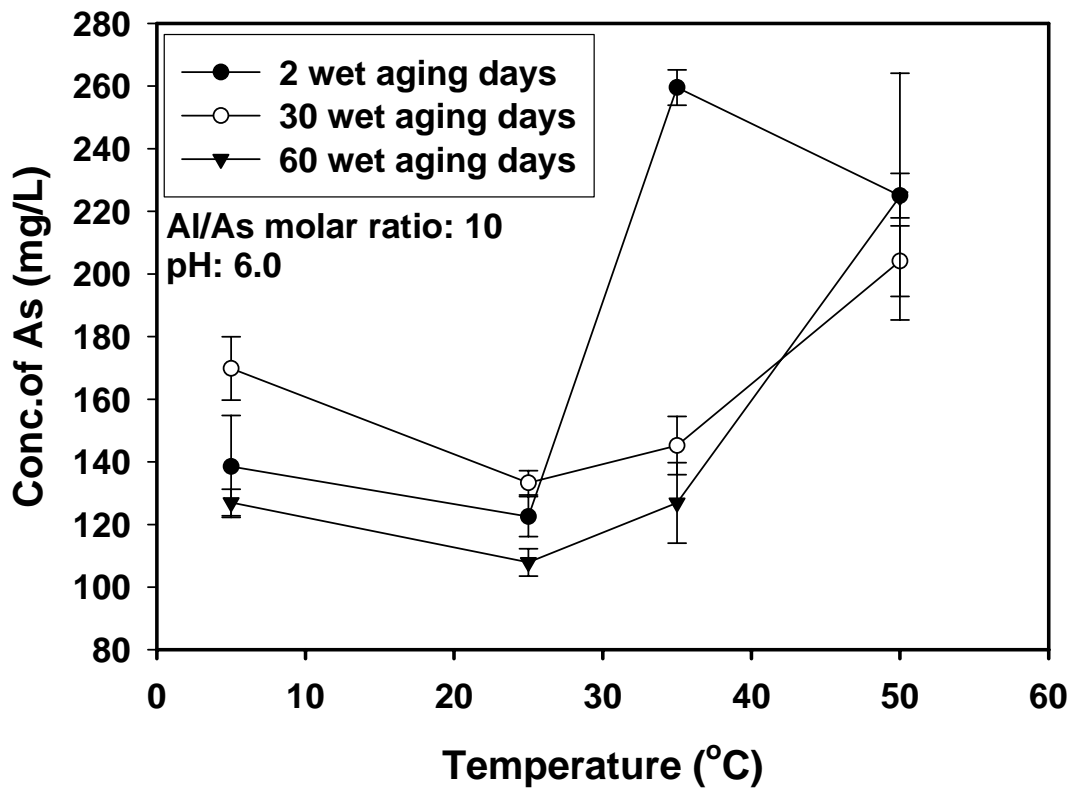


Figure 4.36. Extractable As concentration based on WET method as a function of treatment temperature and wet aging time. All samples were air-dried for 20 days before the extraction tests.

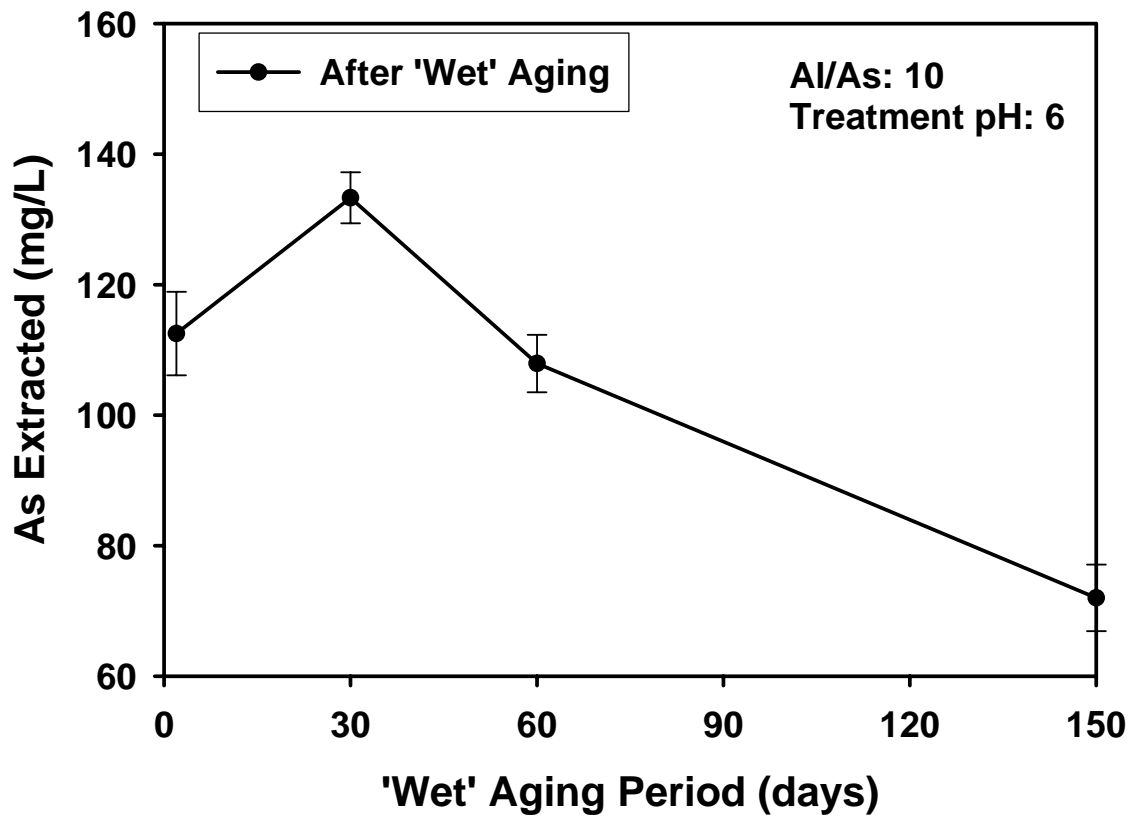


Figure 4.37. Effect of wet aging on extractable As.

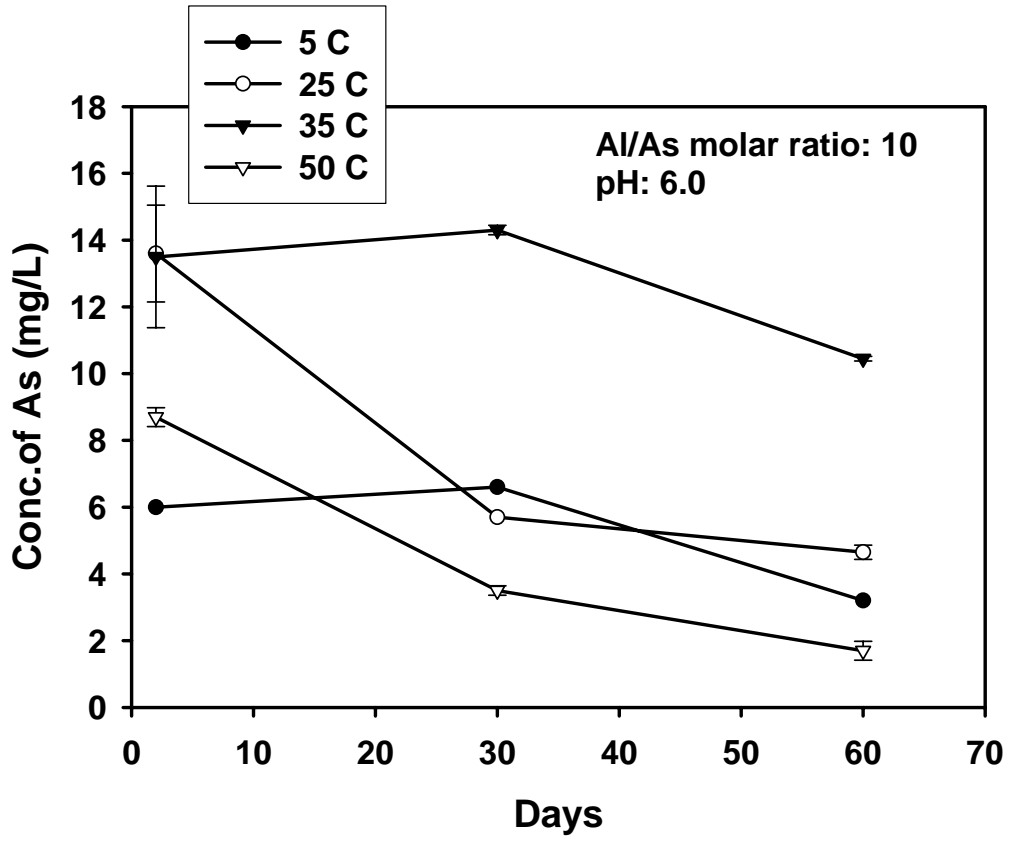


Figure 4.38. Extractable As concentration based on TCLP method as a function of treatment temperature and wet aging time. All samples were air-dried for 20 days before the extraction tests.

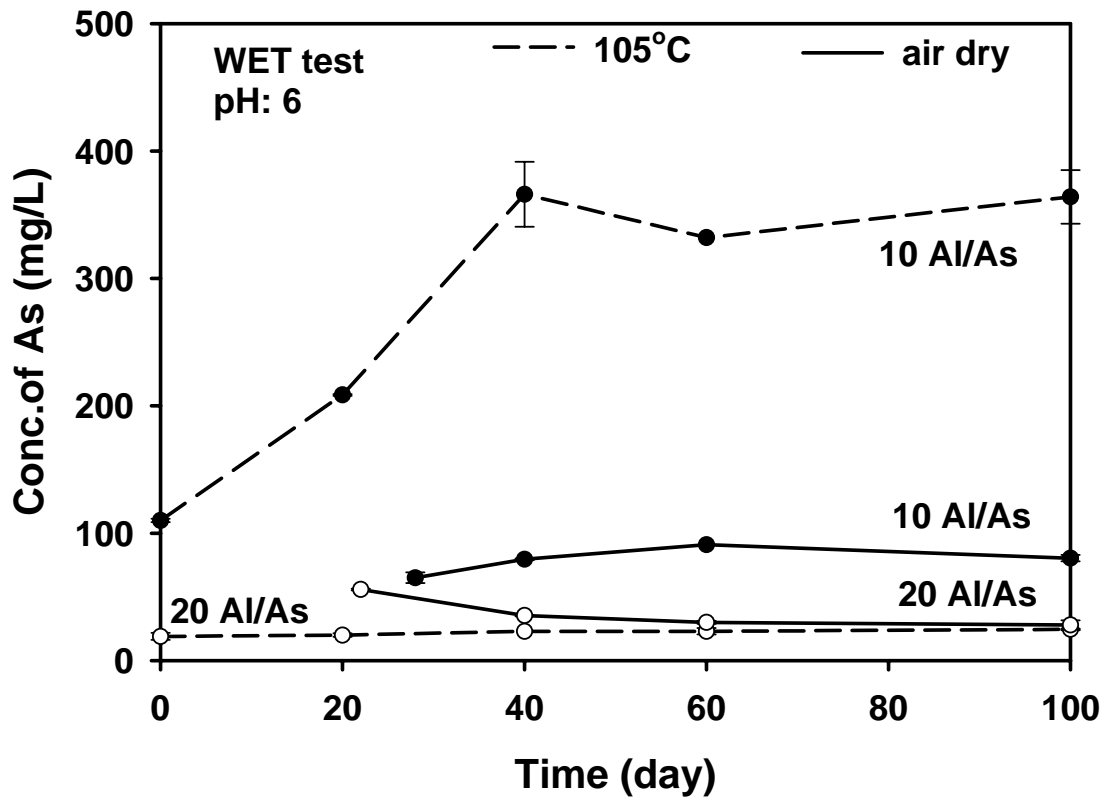


Figure 4.39. Extractable As concentration based on WET method as a function of drying time and temperatures. Tests were carried out at two Al/As molar ratios (10 and 20).

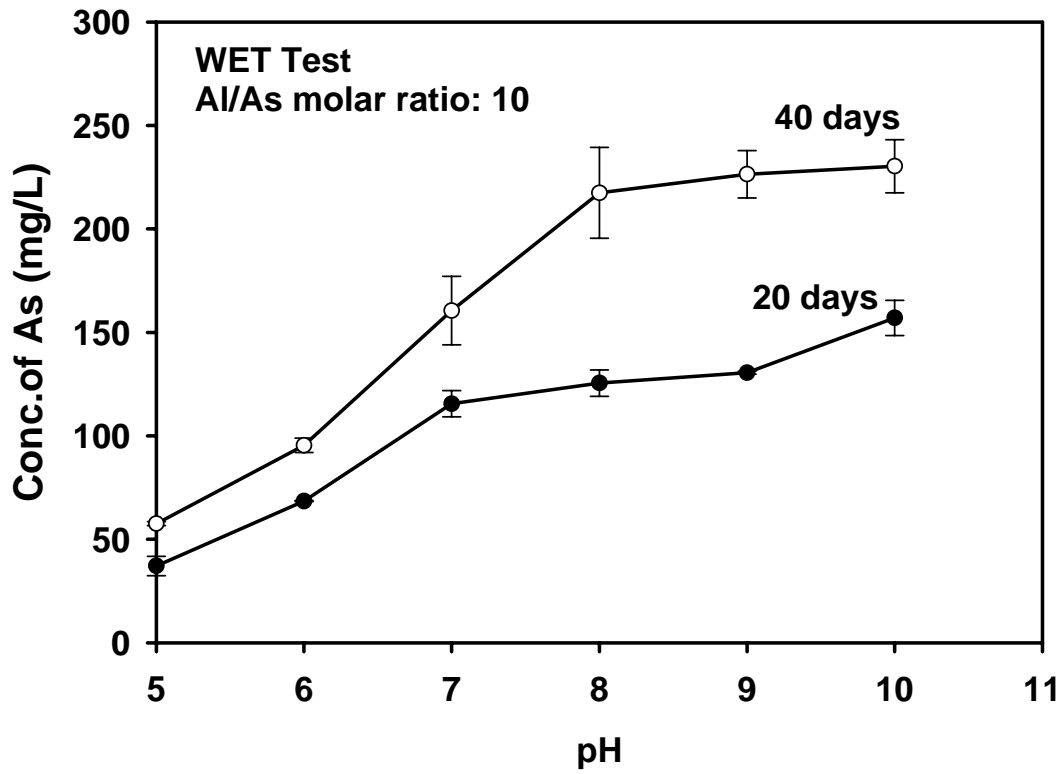


Figure 4.40. Extractable As concentration based on WET method as a function of brine treatment pH and dry aging times.

V. CONCLUSIONS

5.1. CONCLUSIONS

Strong base anion exchanges are currently used to remove arsenic in the drinking water treatment process. The capacity of SBA resins is severely retarded by the presence of competing anion such as sulfate. The newly-developed anion exchange polymeric ligand exchange (PLE) offers a greater selectivity and capacity for the removal of arsenic from drinking water in the presence of strong competing anions, such as chloride, sulfate, bicarbonate, and phosphate. This enhanced arsenic sorption is due to electrostatic ion pairs and Lewis acid-base interactions between arsenate and copper-loaded PLEs.

To determine arsenic selectivity in the presence of sulfate, equilibrium isotherms were constructed. The binary arsenic/sulfate separation factor, $\alpha_{As/S}$, for the PLEs ranged from 4.9 to 12, compared to only 0.1-0.2 for commercially available standard SBA resins (IRA 900 and IRA 958). This separation factor clearly indicates PLEs' high selectivity toward arsenate over sulfate. Fixed-bed column tests confirmed the high arsenic capacity and selectivity of PLEs. While the breakthrough sequence of anions for all SBA resins follows this selectivity order: $SO_4^{2-} > HAsO_4^{2-} > Cl^-$, the selectivity order for DOW 3N-Cu follows: $HAsO_4^{2-} \gg HCO_3^- > SO_4^{2-} > Cl^-$. Another significant indicator is that XUS 3N-Cu can treat over 9000 bed volumes of simulated water, even in the presence of sulfate, bicarbonate, sulfate, and phosphate. This treatment capacity is over 15 times greater than that for a standard SBA which means that the regeneration frequency for the

PLE is only 1/15 that of SBA. Batch kinetic tests were carried out to determine sorption rates of PLEs. The diffusivity value (D) which was determined to be $1.0 \times 10^{-7} \text{ cm}^2/\text{s}$ for DOW 3N-Cu, $2.0 \times 10^{-6} \text{ cm}^2/\text{s}$ for XAD1180-3N-Cu, $3.0 \times 10^{-6} \text{ cm}^2/\text{s}$ for XAD16-3N-Cu, and $3.0 \times 10^{-6} \text{ cm}^2/\text{s}$ for XAD7HP-3N-Cu, $1.0 \times 10^{-6} \text{ cm}^2/\text{s}$ for XAD1180 2N-Cu, $9.0 \times 10^{-7} \text{ cm}^2/\text{s}$ for XAD16 2N-Cu, and $3.0 \times 10^{-6} \text{ cm}^2/\text{s}$ for XAD16 3N-Cu. Based on these diffusivity values, the sorption rate of the PLEs is expected to be better than that of SBA. Optimal arsenic uptake occurs in the pH range of 7.0-8.0. Therefore, there is no need to adjust pH to achieve the optimal arsenic capacity of the resin. All PLEs can be highly efficiently regenerated using NaCl. More than 96% of the adsorbed arsenic for DOW 3N-Cu can be recovered within 20 bed volume using 4% NaCl at pH 9.1, and the regeneration recovery of increased NaCl concentration for all PLEs at pH 9 or 10 is up to 100%. Furthermore, the same regenerant brine can be repeatedly used 4 more times with pH adjustment to 10.

From highly arsenic concentrated spent brine, using AlCl_3 at an Al/As molar ratio of ≥ 2.5 and at pH 6 removes over 98% of arsenic, and at an Al/As molar ratio of 5, in the pH range 5-8, $\sim 100\%$ of arsenic can be removed.

TCLP and WET methods are used to determine the arsenic stability from the resultant sludge. When sludge samples are treated at pH 6 and at an Al/As molar ratio of 5, the extracted arsenic concentration is $\sim 0.3 \text{ mg/L}$ using TCLP and that is $\sim 900 \text{ mg/L}$ using WET. Increasing Al/As molar ratio from 5 to 15 reduces the extractable arsenic concentration using TCLP and WET up to 0.1 mg/L and 100 mg/L , respectively. Treating the sludge at lower pH ($\sim 5-6$) results in lower WET-arsenic leachability.

Lowering the treatment pH from 10 to 5 results in >72% reduction in WET arsenic leachability.

Sludge aging and elevated temperature can affect the arsenic leachability. When wet storage time increases from 2 days to 60 days, the WET leachability of arsenic can be reduced by 20%; whereas increased treatment temperature from 5 to 50 °C increases the WET leachability of arsenic by 100%. Leachability as determined by WET decreases with increased aging time and increases with increased temperature. In contrast to TCLP, increased temperature and aging time decrease the leachability of arsenic. Employing heat treatment at 105 °C dramatically increases leachable As in the WET by up to three times at an Al/As molar ratio 10. But little effect of heat treatment was observed when the increased Al/As molar ratio 20 is used.

REFERENCES

- Agency for Toxic Substances and Disease Registry. 2000. Case Studies in Environmental Medicine: Arsenic Toxicity. ATSDR-HE-CS-2002-0003.
- An, B., Steinwinder, R. T., Zhao, D. 2005. Selective removal of arsenate from drinking water using a polymeric ligand exchanger. *Water Research* 39, 4993-5004
- Badruzzaman, M., Westerhoff, P., Knappe, D.R.U. 2004. Intraparticle diffusion and adsorption of arsenate onto granular ferric hydroxide (GFH). *Water Research* 38, 4002-4012.
- Ballinas, M.L., Rodriguez de San Miguel, E., De Jesus Rodriguez, M.T., Silva, O., Munoz, M., De Gyves, J. 2004. Arsenic(V) removal with polymer inclusion membranes from sulfuric acid media using DBBP as carrier. *Environ. Sci. Technol.* 38 (3), 886-891.
- Baughan, G. T. 1993. Investigation Report CET/LHIR 148: The environmental chemistry and fate of arsenical pesticides in cattle tick dip sites and banana plantations. CSIRO, Division of Coal and Energy Technology, Centre for Advanced Analytical Chemistry, Sydney, Australia.
- Brandhuber, P., Amy, G. 1998. Alternative methods for membrane filtration of arsenic from drinking water. *Desalination* 117 (1-3), 1-10.
- California Department of Health Services. 1990. HML Method 910, California Waste Extraction Test. SOP No. 910.

- Chanda, M., O'Driscoll, K.F., Rempel, G.L. 1988. Ligand exchange sorption of arsenate and arsenite anions by chelating resins in ferric ion form. *Reactive Polymers* 8, 85-95.
- Chwirka, J.D., Colvin, C., Gomez, J.D. 2004. Arsenic removal from drinking water using the coagulation/microfiltration process. *J. AWWA*. 96 (3), 106-114.
- Clifford, D. 1999. Ion exchange and inorganic adsorption. In *Water Quality and Treatment, A Handbook of Community Water Supplies*. American Water Works Association, 9.1-9.91. McGraw Hill, New York.
- Clifford, D.A., Ghurye G., Tripp A.R. 2003. Arsenic removal from drinking water using ion-exchange with spent brine recycling. *J. AWWA* 95(6), 119-130.
- Crank, J. 1975. *The Mathematics of Diffusion*. 2nd Ed. Clarendon Press, Oxford.
- Cullen, R. W. and Reimer, J. K (1989) Arsenic speciation in the environment
Chem. Rev. 89, 713-764
- Dean, J. A., 1979. *Lange's handbook of chemistry*, McGraw-Hill Book Company, Inc. New York, NY.
- Driehaus, W., Jekel, M., Hildebrandt, U. 1998. Granular ferric hydroxide - a new adsorbent for the removal of arsenic from natural water. *J. Water Services Res. & Technol.* 47 (1), 30-35.
- Dzombak, A.D., Morel, M.M.F. *Surface Complexation Modeling: Hydrous Ferric Oxide*. John Wiley & Sons, Inc. New York, NY. 1990.
- United States Environmental Protection Agency. 2001a. Treatment of arsenic residuals from drinking water removal processes. EPA/600/R-01/033. www.epa.gov, Office of Research and Development, Washington, DC.

- United States Environmental Protection Agency. 2001b. Technical Fact Sheet: Final Rule for Arsenic in Drinking Water (EPA 815-F-00-016). Office of Research and development, Washington, D.C.www.epa.gov.
- Fan, M.H., Brown, R.C., Sung, S.W. 2003. Comparisons of polymeric and conventional coagulants in arsenic(V) removal. *Water Environ. Res.* 75 (4), 308-313.
- Frey, M., Chwirka, J.D., Kommineni, S., Chowdhury, Z., Marasimhan, R., 2000. Cost implications of a lower arsenic MCL. AWWA Research Foundation. Denver, CO.
- Focazio, M.J., Welch, A.H., Watkins, S.A., Helsel, D.R., Horn, M.A. 1999. Aretrospective analysis on the occurrence of arsenic in groundwater resources of the United States and limitations in drinking-water-supply characterizations: U.S.Geological Survey Investigation Report 99-4279, p.21.
- Genc-Fuhrman, H., Tjell, J. C., McConchie, D. 2004. Adsorption of arsenic from water using activated neutralized red mud. *Environ. Sci. Technol.* 38 (8), 2428-2434
- German, J., 2001. Arsenic trappers could allay national sticker shock of new EPA standard. Sandia Lab News, 53 (5).
- Ghurye, G., Clifford, D., Tripp, A. 2004. Iron coagulation and direct microfiltration to remove arsenic from groundwater. *J. AWWA.* 96 (4), 143-152.
- Han, B., Zimbron, J., Runnels, T.R., Shen, Z., Wickramasinghe, S.R. 2003. New arsenic standard spurs search for cost-effective removal techniques. *J. AWWA.* 95 (10),109-118.
- Helfferich, F. 1962. Ion Exchange, McGraw-Hill Book Company, Inc. New York, NY.

- Henry, W.D., Zhao, D., Lange, C., SenGupta, A.K. 2004. Preparation and Characterization of a New Class of Polymeric Ligand Exchanges for Selective Removal of Trace Contaminants from Water. *Reactive and Functional Polymer* 60, 109-120.
- Hering, G.J., Elimelech, M. 1996. Arsenic Removal by enhanced coagulation and membrane processes (90706). AWWA Research Foundation. Denver, CO.
- Holm, T.R. 2002. Effect of CO_3^{2-} /bicarbonate, Si, and PO_4^{3-} on arsenic sorption to HFO. *J.AWWA*. 94 (4), 174-181.
- Kim, Y., Kim, C., Choi, I., Rengaraj, S., Yi, J. 2004. Arsenic removal using mesoporous alumina prepared via a templating method. *Environ. Sci. Technol.* 38 (3), 924-931.
- Kunin, R., Meyers, R. 1950. Ion Exchange Resins, John Wiley and Sons, New York.
- Kumar, P.R., Chaudhari, S., Khilar, K.C., Mahajan, S.P. 2004. Removal of arsenic from water by electrocoagulation. *Chemosphere* 55 (9), 1245-1252.
- Lantzy,R.J., Peterson, P.J. (1987) In lead, Mercury, cadmium and arsenic in the environment; Hutchinson, T.C., Meema, K.M., Eds., Wiley, New York, p 279.
- Manna, B.R., Dey, S., Debnath, S., Ghosh, U.C. 2003. Removal of arsenic from groundwater using crystalline hydrous ferric oxide (CHFO). *Water Quality Research Journal of Canada* 38 (1), 193-210.
- McNeill, L.S., Edwards, M. 1997. Predicting As removal during metal hydroxide precipitation. *J. AWWA*. 89 (1), 75-86.

- Mushrak, P. 2000. Arsenic and Old Laws: A Scientific and Public Health Analysis of Arsenic Occurrence in Drinking Water, Its Health Effects, and EPA's Outdated Arsenic Tap Water Standard. NRDC Report.
- National Research Council, 1999. Arsenic in Drinking Water: Washington D.C. National Academy Press.
- National Research Council, 2001. Arsenic in Drinking Water: 2001 Update. Washington D.C. National Academy Press.
- O'Neill, P. 1990. Arsenic. in heavy metals in soils. 2nd Ed. (B. J. Alloway, ed) p.105-121. Blackie, London.
- Ramana, A., SenGupta, A.K. 1992. Removing selenium(IV) and arsenic(V) oxyanions with tailored chelating polymers. *J. Environ. Eng.* 118 (5), 755-775.
- Richmond, W.R., Loan, M., Morton, J., Parkinson, G.M. 2004. Arsenic removal from aqueous solution via ferrihydrite crystallization control. *Environ. Sci. Technol.* 38 (8), 2368-2372.
- Sawyer, C.L., 1978. Chemistry for Environmental engineering, McCraw-Hill Book Company, Inc., New York, NY.
- Scott, K.N. 1995. Arsenic removal by coagulation. *J. AWWA.* 87 (4), 114-126.
- Smith, E., Naidu, R., Alston, A.M. 1998. Arsenic in the soil environment: A review. *Advances in Agronomy*, 64, 149-195.
- Sorensen, M.A., Stackpoole, M.M., Frenkel, A.I., Bordia, R.K., Korshin, G.V., Christensen, T.H. 2000. Aging of Iron(Hydro)oxides by heat treatment and effect on heavy metal binding. *Environ. Sci. Technol.* 34 (18), 3991-4000.

- Sperlich, A., Werner, A., Genz, A., Amy, G., Worch, E., Jekel, M. 2005. Breakthrough behavior of granular ferric hydroxide (GFH) fixed-bed adsorption filters: modeling and experimental approaches. *Water Research* 39, 1190-1198.
- Wang, L., Chen, A.S.C., Sorg, T.J., Fields, K.A. 2002. As removal by IX and AA. *J. AWWA*. 94 (4), 161-173.
- Westerhoff, P., Highfield, D., Badruzzaman, M., Yoon, Y. 2005. Rapid small-scale column tests for arsenate removal in iron oxide packed bed columns. *J. Environ. Eng. ASCE* 131(2), 262-271.
- Zhao, D., 1997. Polymeric ligand exchange: A new approach for enhanced separation of environmental contaminants. Ph.D. Dissertation. Department of Civil and Environmental Engineering, Lehigh University, Bethlehem, PA, USA.
- Zhao, D., SenGupta, A.K. 1998. Ultimate Removal and Recovery of Phosphate from Wastewater Using A New Class of Polymeric Exchangers. *Water Res.* 32 (5),1613-1625.
- Zhao, D., SenGupta, A.K. 2000. Ligand separation with a copper (II)-loaded polymeric ligand exchanger. *Ind. Eng. Chem. Res.* 39, 455-462.
- Zhao, D. and Steinwinder T., An B., Kramer T., and Barnett M (2005) Developing a new class of ion exchangers for selective removal of arsenic and exploring an engineered approach for treatment and reuse of spent regenerant. AwwaRF Final Project Report (in review).